Faculty of Applied Sciences

Robustness of Steel and Concrete Structures

A Comparative Study

Master's Thesis realized by

Nutal Bernard

in order to obtain the Master Degree in Civil Engineering

Members of the Jury:

Demonceau Jean-François (supervisor)
Mihaylov Boyan (co-supervisor)
Caspeele Robby
Taerwe Luc
Demortier Luc

Academic Year 2013 – 2014

"Structural engineering is the art of modelling materials we do not wholly understand, into shapes we cannot precisely analyse so as to withstand forces we cannot properly assess, in such a way that the public at large has no reason to suspect the extent of our ignorance."

– Dr. A.R. Dykes, British Institution of Structural Engineers, 1976.

Tables of Contents

Acknowledgement i

Statement ii

Executive Summary iii

Résumé iv

List of Figures v

Introduction 1
- 1.1 Definitions . . . 1
- 1.2 Importance of Robustness . . . 2
- 1.3 Purpose . . . 4
- 1.4 Method of Procedure . . . 4
- 1.5 Scope and Limitation of the Research . . . 5

2 States of Art – Literature Search 7
- 2.1 Indirect Method to Mitigate Progressive Collapse . . . 7
- 2.2 Direct Method to Mitigate Progressive Collapse . . . 8
  - 2.2.1 Specific Local Resistance or Key Element Design . . . 8
  - 2.2.2 Redundancy or Alternative Load Paths . . . 9
- 2.3 Eurocodes Prescriptions . . . 9

3 Design of Structures 11
- 3.1 Structures Solicitations . . . 11
- 3.2 Description of the Steel Structure . . . 13
- 3.3 Description of the Concrete Structure . . . 14

4 Modelization of Structures 16
- 4.1 Constitutive Laws . . . 17
  - 4.1.1 Steel Behaviour . . . 17
  - 4.1.2 Reinforced Concrete Behaviour . . . 18
- 4.2 Validation of FINELg . . . 20
  - 4.2.1 Case Study . . . 20
  - 4.2.2 Numerical Model . . . 21
  - 4.2.3 Comparison of Results . . . 22
- 4.3 Scenario of Column Loss . . . 29
- 4.4 Simulation of Column Loss . . . 29
  - 4.4.1 Imposed Load Method . . . 29

4.4.2 Imposed Displacement Method 30
4.4.3 Limitations of Simulations 31
4.5 Loading Combinations Investigated 35

5 Results Analysis **37**
5.1 Steel Frame 37
5.1.1 Evolution of Column Loss 37
5.1.2 Parametric Analysis 42
5.1.3 Summarize Results 51
5.2 Reinforced Concrete Frame 52
5.2.1 Evolution of Column Loss 52
5.2.2 Parametric Analysis 59
5.2.3 Summarize Results 67
5.3 Comparison of Steel and Reinforced Concrete Structures 67
5.3.1 Incremental Load Results 67
5.3.2 Incremental Displacement Results 69
5.3.3 Evolution of Catenary Action and Membrane Effects 69
5.3.4 Evolution of Internal Forces in Foundations 73
5.4 Conclusion 77

Conclusion **78**
5.1 Structural Requirements for Future Designs 78
5.2 Perspectives 79

References **ix**

Acknowledgement

The present work embodies five years of study at University of Liège. This paper concludes thereby the basis of my learning in the art of civil engineering. Through those years, the amount of knowledge learned day after day gave me a new vision of the world. This intellectual development has no price.

First of all, I would like to thanks Dr. Jean-François Demonceau, the promoter of this thesis, for his complete availability and the relevance of his remarks. He led me all along of this project by his methodological approach.

The construction of this master's thesis would not have been possible without the intervention of Prof. Boyan Mihaylov. May he find here the expression of my sincere thanks for his valuable advice and his complementary vision brought to this research.

This project is the fruit of a successful collaboration with Ghent University, who understood the importance of this work by giving myself a bit of their time. I wish to express my gratefulness towards Prof. Robby Caspeele, Prof. Dirk Gouverneur and Prof. Luc Taerwe for their contributions, their hospitality within their university and the visit of the Magnel Laboratory.

My acknowledgement go also to Prof. Jean-Pierre Jaspart, who conveyed me his passion for the construction field. The pragmatism of his lectures and his highlighting of the physical understanding made numerous developments more decipherable.

This research was also carried out thanks to the participation of Greisch design office. I want to thank them here for putting their calculation software FINELg at my disposal.

Finally, my gratitude goes to my parents for their boundless support and Sarah for her careful listening in addition to the necessary amount of stress she procured me to accomplish this master's thesis.

Statement

Title: Robustness of Steel and Concrete Structures: A Comparative Study

Eurocodes introduce notions of progressive collapse, structural integrity and robustness in the design of civil engineering structures, in case of exceptional events such as explosion, impacts, localized fire, significant deteriorations ... The aim of such considerations is to obtain structures exhibiting an appropriate behaviour in case of the loss of one structural element, i.e. this localized damage doesn't lead to the progressive collapse of a significant part or of the entire structure.

Many researches are currently emerging in this field. For instance, the University of Liege focuses on the behaviour of frames that are submitted to the loss of one supporting column, involving a team of several researchers. Also, the University of Gent is studying the development of membrane forces in a slab that losses one of its supports.

Until now, the robustness of steel or concrete building structures has been investigated separately, generally by different research units. The objective with this master thesis is to perform a comparative study by investigating the behaviour in case of a column loss of two identical buildings (i.e. with the same geometry and applied loads) but characterized by different construction materials: one would be made of steel and one of concrete.

The first steps of this master thesis will be to establish the geometry of a reference structure, and then the design of the two structures in partnership with the University of Gent. Following the definitions of both structures, different scenarios of column loss (assumed to be static) will be investigated using numerical tools. In order to validate reinforced concrete elements in numerical tools, the numerical simulation of an experimental test, studied by the University of Gent and focusing on membrane forces in a slab, will be performed. The main goal of this master thesis is the identification of structural requirements thanks to the analysis of the so-obtained results.

Members of the Jury:

Dr. Ir. Jean-François DEMONCEAU

Prof. Dr. Ir. Boyan MIHAYLOV

Prof. Dr. Ir. Robby CASPEELE

Prof. Dr. Ir. Luc TAERWE

Ir. Luc DEMORTIER

Executive Summary

Author: Bernard Nutal, in order to obtain the Master Degree in Civil Engineering (Academic year 2013 - 2014)
Title: Robustness of Steel and Concrete Structures: A Comparative Study

The objective of this master's thesis is to performed a comparative study between two identical structures under an accidental event. Both structures, designed according Eurocodes Limit States, differs only by the materials used. One is made of steel profiles while the other is made of reinforced concrete elements.

To conduct this study, a static scenario of column loss is numerically studied thanks to the finite element software FINElg. The scenario investigated is the failure of the central ground floor.

First, the FINELg reinforced concrete elements validation is accomplished by replicating an experimental slab trip test carried out by Ghent University. As many numerical troubles occurred throughout this work, a additional section is devoted to the explanation of the methods implemented in FINELg.

After that, the column loss evolution of each frames is independently discussed. The main goal of this chapter is to provide a physical interpretation of their different behaviour. Following this part, a parametric analyzes is made in order to bring out the major improvements that could be considered to enhance the structural integrity. Finally, we confront the results obtained to quantify and compare the structural response of both frames under the column loss.

From this work, it has been demonstrated in the parametrical investigation that promoting the horizontal ties rather than the vertical tying is more effective to raise the structural integrity. Furthermore, steel frames offer more easily feasible solutions to ameliorate robustness.

Finally, it comes out that both structures collapse if the entire column is removed. Under the assumptions introduced in the research, the initial designs are not robust. In addition, the steel frame performs better during the collapse. The frames fail in the indirectly affected part. The building foundations, turned into plastic hinges, form a panel mechanism in both structures. The challenge is now to prevent the formation of these hinges.

Résumé

Auteur: Bernard Nutal, en vue de l'obtention du grade de Master Ingénieur Civil en Construction (année académique 2013 - 2014)
Titre: Robustesse des structures métaliques et en béton armé : Étude comparée

L'objectif de ce travail de fin d'études est de réaliser une étude comparée de deux structures soumises à une perte inopinée d'un élément structurel. Les deux structures de références, dimensionnées selon les états limites de l'Eurocodes , sont parfaitement identiques si ce n'est par les matériaux employés. L'une d'elles est composée de profilés métalliques tandis que l'autre d'éléments en béton armé.

Afin de mener à bien cette thèse, le scénario accidentel est modélisé au moyen du logiciel d'éléments finis FINELg. Le scénario envisagé est la rupture de la colonne centrale du rez-de-chaussée.

Tout d'abord, la validation des éléments de type béton armé de FINELg est accomplie grâce à la reproduction d'un test de rupture d'un tronçon de dalle effectuée par l'Université de Gand. Au vu du nombre de difficultés numériques rencontrées au travers de ce mémoire, une section supplémentaire est consacrée à l'explication des méthodes de résolution mise en œuvre dans FINELg.

Dans un premier temps, l'évolution de la perte de colonne est discutée dans chaque portique de manière indépendante. Ceci afin de fournir une explication physique quant au comportement différent des structures. Ensuite, une étude paramétrique est opérée dans le but de mettre en évidence les modifications à apporter aux bâtiments pour améliorer leur intégrité structurale. Enfin, les résultats provenant des deux portiques sont confrontés afin de quantifier et comparer la réponse des structures sous le scénario défini. Au travers de cette étude, il a été démontré dans l'analyse paramétrique que, pour favoriser l'intégrité structurale, il est préférable de promouvoir les tirants horizontaux plutôt que les liens verticaux.

Pour terminer, il résulte de ce mémoire que les deux structures s'effondrent avant le retrait complet de la colonne. Sous réserve des hypothèses introduites dans cette recherche, les structures initiales ne sont donc pas robustes. Cependant, la structure en acier présente un meilleur comportement durant l'effondrement. La rupture a lieu dans la partie indirectement affectée. Les fondations, devenues des rotules plastiques, forment un mécanisme de panneau dans les deux structures étudiées. L'enjeu est dorénavant de se prémunir contre l'apparition de ces rotules néfastes.

List of Figures

1.1 Ronan Point Collapse 2
1.2 World Trade Center Collapse 3
1.3 Windsor Tower After Collapse[26] 3
1.4 Perspective Representation of the Structure 6

2.1 Strategies for Accidental Design Situations[4] 9

3.1 Schematic Representation of the Building 11
3.2 Schematic Representation of the Loading considered for Design 12
3.3 Schematic Representation of the Loading considered for Robustness Investigation 13
3.4 Initial Steel Frame Investigated 13
3.5 Initial Reinforced Concrete Frame Investigated 14
3.6 Reinforced Concrete Beams Cross-Section 15
3.7 Reinforced Concrete Columns Cross-Section 15

4.1 Lack of Stiffness in the Elastic Perfectly Plastic Model 17
4.2 Trilinear Steel Profile Law 18
4.3 Uniaxial Concrete Law 18
4.4 Steel Reinforcement Rebars Law 19
4.5 Test set-up [17] 20
4.6 Slabs Strip Cross-Section 20
4.7 Schematic representation of the Test After the Central Support Removal[17] . . . 21
4.8 Support Conditions After the Central Support Removal 21
4.9 Plane Reinforced Concrete Beam Element composed of Three Nodes[13] 22
4.10 Fine Element Discretization of the Slab Strip in FINELg 22
4.11 Load-Deflection Curve in Central Span During Phase 3 [17] 23
4.12 Progression of Crack within the Slab Strip 24
4.13 Progression of Yielding within the Slab Strip 24

4.14 Evolution of Slab Strip Displacement During Phase 3 (Scale Factor x3) 25
4.15 Slab at the End of Test[17] 26
4.16 Evolution of Bending Moment During Phase 3 26
4.17 Evolution of Axial Force During Phase 3 26
4.18 M-N Interaction Diagram at the Inner Support of Slab Strip During Phase 3[17] . 27
4.19 Catenary Action in Slab Strip in function of Central Span Deflection 28
4.20 Central Ground Floor Column Scenario 29
4.21 Evolution of Column Loss by the Imposed Load Method 30
4.22 Vertical Displacement at Missing Column Location according to the Loading . . . 31
4.23 Comparison between Incremental Load and Incremental Displacement Results . . 33
4.24 Example of Numerical Troubles occurring at High Displacement ($\Delta_{\text{dep}} = 2,5$ mm) 33
4.25 Rotation of IPE 360 beam according the Vertical Displacement of Support 34
4.26 Member Classification of IPE 360[16] 35

5.1 Progression of Plastic Hinges in Steel Frame 38
5.2 Steel Yielding at Displacement of 120 cm 38
5.3 Evolution of Displacement in Steel Frame 39
5.4 Steel Frame Deformation at Displacement of 120 cm 39
5.5 Bending Moment [kNm] (left) and Normal Force [kN] (right) with Column in place in Steel Frame 40
5.6 Bending Moment [kNm] (left) and Normal Force [kN] (right) at Displacement of 120 cm in Steel Frame 41
5.7 Addition of Bending Moment coming from the Initial Loading (a) and from the Column Loss (b) [18][19] 42
5.8 Shape Deformation of the Frame under Vertical and Horizontal Loading [19] . . . 42
5.9 Elastic IAP Definition (Grey Elements) 43
5.10 Elastic IAP with Ground Floor able to Yield 43
5.11 Full Development of Membrane Effects with Elastic IAP 43
5.12 Influence of Indirectly Affected Part in Steel Frame 44
5.13 Normal Force Evolution according to Vertical Displacement of Central Support for Different Horizontal Restraints 45
5.14 Normal Force Evolution according to Vertical Displacement of Central Support for Different Column Profiles 46
5.15 Membrane Effects Evolution according Vertical Displacement of Central Support for Column Profiles 47
5.16 Bending Moment [kNm](left) and Normal Force [kN] (right) at Displacement of 120 cm in Steel Frame composed of HEB 450 Columns 47

5.17 Normal Force Evolution according Vertical Displacement of Central Support for Different Steel Grade 48

5.18 Normal Force Evolution according Vertical Displacement of Central Support for Different Beam Profiles 49

5.19 Plastic Hinges Localisation with IPE 360 but without Loading 50

5.20 Plastic Hinges Localization at Displacement of 80 cm according Beam Profile . . 51

5.20 Evolution of Cracks in Reinforced Concrete Frame 54

5.21 Concrete Cracks at Displacement of 90 cm 54

5.22 Concrete Crushing at Displacement of 90 cm 55

5.22 Evolution of Rebars Yieling in Reinforced Concrete Frame 57

5.23 Rebars Yielding at Displacement of 90 cm 57

5.24 Bending Moment [kNm] (left) and Normal Force [kN] (right) with Column in place in RC Frame 58

5.25 Bending Moment [kNm] (left) and Normal Force [kN] (right) at Displacement of 90 cm in RC Frame 59

5.26 Elastic IAP Definition (Grey Elements) 60

5.27 Elastic IAP with Ground Floor able to Crack 60

5.28 Membrane effects with Elastic IAP in RC Frame 60

5.29 Influence of Indirectly Affected Part in Steel Frame 61

5.30 Positive Influence of Elastic Indirectly Affected Part in RC Frame 61

5.31 Basic Principle of Arching Action[35] 62

5.32 Normal Force Evolution according Vertical Displacement of Central Support for Different Horizontal Restraints 62

5.33 Normal Force Evolution according Vertical Displacement of Central Support for Different Concrete Class 63

5.34 Normal Force Evolution according to Vertical Displacement of Central Support for Different Concrete Beam Reinforcements 64

5.35 Normal Force Evolution according to Vertical Displacement of Central Support for Different Concrete Beam Heights 65

5.36 Normal Force Evolution according to Vertical Displacement of Central Support for Different Concrete Column Widths 66

5.37 Normal Force Evolution according to Vertical Displacement of Central Support for Different Concrete Column Reinforcements 66

5.38 Comparison of Catenary action developed according Column Loss with Incremental Load 68

5.39 Comparison of Catenary action developed according Column Loss with Incremental Displacement 69

5.40 Beam Elements investigated 70

5.41 Comparison of Normal Force Evolution according to Vertical Displacement 70
5.42 Comparison of M-N Interaction Diagrams according Vertical Displacement 71
5.43 Comparison of Moment-Rotation Curve according Vertical Displacement 72
5.44 Rotation Evolution at Beams Extremity according Vertical Displacement 72
5.45 Horizontal Displacement Evolution at Beams Extremity according Vertical Displacement 73
5.46 Shear Force Evolution in Foundations according Vertical Displacement 74
5.47 Total Shear Force Evolution in Foundations according Vertical Displacement . . . 74
5.48 Shear Force [kN] in Steel (left) and RC (right) Frames before Collapse 75
5.49 Comparison of M-N Interaction Diagrams in Foundations according Vertical Displacement 76
5.50 Comparison of Bending Moment in Foundations according Vertical Displacement 77

Introduction

A structure has to ensure an appropriate behaviour for all contingencies. While the behaviour of structures under ordinary circumstances is well-known and studied since decades, the behaviour of structures under exceptional loading is still largely undiscovered. In classical design philosophy, the probability of occurrence of exceptional actions is too low to justify their direct coverage. Directly considering those unforeseen actions in the design loads would be too tedious due to the myriad of possible occurrences.

Nevertheless, too many buildings still collapse because conventional approaches are sometimes no longer sufficient. Moreover, terrorist attacks, gas explosions and always higher buildings proved the importance of robustness in building design. Since the terrorist attacks on World Trade Center in 2001, progressive collapse has become a major research subject in order to save lives, reduce the risk for interventions services and limit collateral damages.

Up to now, robustness of steel and concrete building structures has been investigated separately, generally by different research units. This master thesis aims to perform a comparative study by investigating the behaviour in case of a column loss of two identical buildings but characterized by different construction materials. The first one will be made of steel while the second one will be a reinforced concrete frame.

The main goal of this research is to identify adequate structural requirements necessary to maintain the structural integrity of both structures under exceptional loading.

1.1 Definitions

Notions of robustness, progressive collapse and structural integrity are involved in the case of unforeseen accidental actions. Contrary to earthquake or fire, magnitude of unidentifiable accidental actions cannot be precisely determined because of their unpredictability nature. Indeed, local failures, internal explosions or vehicles impacts may result from a wide range of sources.

Several definitions of progressive collapse can be found in literature. General Services Administration defines progressive collapse as a situation in which local failure of a primary structural component leads to the collapse of adjoining members which, in turn, leads to additional collapse.[6] For R. Shankar Nair, progressive collapse is the collapse of all or a large part of a structure precipitated by damage or failure of a relatively small part of it.[22] In all cases, progressive collapse refers to a disproportionate structural response compared to a initial local failure.

Eurocodes integrate the concept of robustness by advocating a structure has to be designed and built in a such a way that the structure should withstand events like fire, explosions, impact or the consequences of human error, without being damaged to an extent disproportionate to the original cause.[4] General Services Administration gives a similar definition of robustness.

In civil engineering, robustness is the ability of a structure or structural components to resist damage without premature and/or brittle failure due to events like explosions, impacts, fire or consequences of human error, due to its vigorous strength and toughness.[6]

Structural integrity is the capacity for a structural system to remain as a whole stable. When focusing on exceptional circumstances, priority is to design a building able to reach a new deformed equilibrium state without the collapse of the entire structure. There is no more control of deformations and displacements. The structure has to withstand even if one of its parts is destroyed.

1.2 Importance of Robustness

Numerous cases can attest to the importance of robustness in structural engineering. The best known example is the infamous Ronan Point collapse. "*Ronan Point was a 22-storey tower block in Newham, East London, which partly collapsed on 16 May 1968 when a gas explosion demolished a load-bearing wall, causing the collapse of one entire corner of the building. Four people were killed in the incident, and 17 were injured. The tower was built using a technique which involves casting large concrete prefabricated sections off-site and bolting them together.*"[34]

(a) High Angle View[27]

(b) Colour View[28]

(c) Explosion Site[29]

Figure 1.1: Ronan Point Collapse

Closer to our time, the most striking example is the World Trade Center. "*On September 11, 2001, World Trade Center buildings 1, 2 and 7 in New York City, collapsed as a result of terrorist attacks and the subsequent fires that followed. After a 3-year investigation by the National Institute of Standards and Technology, it was concluded that fire weakened the steel structure until the long truss bridge-like floor sections began to progressively sag. This sagging converted the downwards pull of the trusses into an inwards pull. This intensifying inwards pull on the walls eventually caused the outer columns of Tower 2, and later the inner columns of Tower 1, to buckle and fold, thus initiating the various progressive collapses. 2,752 people died in the buildings.*"[33][24]

(a) Beginning of Collapse[30]

(b) Middle of Collapse[31]

Figure 1.2: World Trade Center Collapse

"*The last example is the 28 story Windsor Tower in Madrid, which suffered the collapse of the upper 11 floors of the building on February 12, 2005. The tower had a reinforced concrete inner-core surrounded by a traditional webbed steel-frame outer-perimeter. Between floors 16 and 17 was a 2 meter thick, reinforced concrete transfer floor, designed to act as a bulkhead and to support the steel framework of the upper 11 stories. An office fire began on the 21st floor and after 5 hours, the concrete inner-core could no longer support the melting steel outer-framework. The upper 11 stories collapsed down to street level with remnants of the upper 3 floors collapsing down on to the transfer floor. No one was killed. The building was a composite steel-frame and steel-reinforced concrete design.*"[32][33]

Figure 1.3: Windsor Tower After Collapse[26]

Through these features examples, the prominence of robustness in building design becomes obvious. First, avoiding the collapse, and more particularly progressive collapse, can saves a lot of human lives. Then, if the structure meets robustness requirements, fire-fighters and others emergency services will be able to operate inside the building more safely. They will no longer fear a risk of general collapse or structural element fall. In addition, providing more safe time before the collapse is recommended in high buildings for the evacuation. It may takes time for fire-fighters to reach the fire location. Finally, by reducing the damaged area, the reparation costs will be reduced too.

By the way, the Figure 1.3 clearly shows the dual behaviour of steel and reinforced concrete. The reinforced concrete inner-core was still standing while the surrounding steel framework collapsed. Understanding their response in a similar initial configuration will help selecting the appropriate material for future designs.

1.3 Purpose

The aim of this master's thesis is to highlight and compare the behaviour of two frames, one made of steel and one made of reinforced concrete, under accidental loading. In addition to the interest aroused by undiscovered behaviour of frames at large displacement, the investigation will lead to practical impacts for design offices. Thanks a better knowledge of structural behaviour under accidental loading, design office will be able to conceive a structure able to sustain the loss of one of its elements.

1.4 Method of Procedure

This master's thesis is divided into several parts. First of all, a realistic design for both structures according Eurocodes recommendations will be made for a common situation. By example, the location, the shape and the function of the two buildings will be the same. This to ensure that the difference come from the materials employed for the construction. The steel structure will be designed by University of Liège while the reinforced concrete will be designed by Ghent University.

After designing the structures, we will proceed to the modelization of both structures in FINELg, a finite element software. FINELg is a homemade program developed by University of Liège and Greisch design office. Since all the numerical analysis are performed with this software, the validation of the FINELg results is required.

Validation of steel beam elements is omitted because those elements are used since decades by Greisch design office and the University of Liège. Only the behaviour of reinforced concrete beam elements will be validated, mainly for academic purposes. In order to check the satisfactory behaviour of those elements under exceptional loading, we will reproduce an experimental large-scale test for a reinforced concrete slab strip performed by Ghent University.

Following the validation, a numerical investigation of both models will be made. The scenario investigated is the lost of one of the ground columns for whatever reason. To simulate the column loss, two strategies will be implemented in FINELg: the imposed load strategy and the imposed displacement strategy. In this work, we assume an inelastic static analysis.

A static analysis is, of course, less accurate than a dynamics approach, but it is also less time consuming. Several authors as demonstrated that non-linear static analysis are generally close

or slightly more conservative results than a non-linear dynamic analysis. Hence, as argue by Simon Benson & al., an inelastic static analysis is valid for the purposes of progressive collapse analysis. The assumptions inherent in the static method, which neglects the influence of time dependent mass and damping effects, are acceptable for progressive collapse investigation.[10] [20]

In this comparison, we will confront the results such as the displacements at the removed column, the M-N interaction curves in the beams and columns extremity, the magnitude of the catenary actions developed in the element or the rotation required to activate catenary action.

Finally, we will bring out requirements for future design to avoid the appearance of progressive collapse.

1.5 Scope and Limitation of the Research

In order to design a very common structure, we will focus the study on an office building. This building includes 6 floors of $3,5$ m high, 4 spans of 6 m long in the x – z plane and 3 spans also 6 m long in the y – z plane. Figure 1.4 gives a perspective view of the building. The red frame in the x – z plane is the one investigated.

The columns on the ground are assumed to be embedded and the connection are rigid and fully resistant. In addition, there is no bracing system in order to promote the development of nonlinear phenomena.

This building is located in Brussels area, which means in an urban area. In Belgium, the capital is the most probabilistic place where this kind of structure could be built. This choice will have consequences on the design, and specially on the wind and snow loads. Since the forces generated by the wind are much lower than the expected stress under expectational loading, we only consider a simplified wind action. Moreover, wind influence is not the focus of this research. It results that only horizontal wind forces in the x – z plane acting on external walls will be taken into account.

In addition to the snow and the wind, the self-load of the structures and the global imperfections of the elements are taken into account for the design.

Shear is neglected in this thesis so that interaction only happens between bending moment and axial force. To check if this assumption is valid, we will use a common criteria expressed as follows:

$$V_{Ed} \leq 0,5 V_{Pl,Rd} = \frac{1}{2} \frac{A_v \frac{f_y}{\sqrt{3}}}{\gamma_{M0}} \tag{1.1}$$

If this condition is valid, shear forces can be neglected. Otherwise, an analysis has to be performed in order to ensure that the failure occurs first because of a lack of bending moment resistance or axial resistance. If not, shear has to be taken into account by a full interaction analysis.

Only columns and beams will play a role in the resistance. In this thesis, we do not focus on slabs, walls or other non-structural elements that can have some influence in the load carrying.

The investigation of the frame will be performed in the x – z plane. We will focus the analysis on a central frame. However, we consider in the analysis the load coming from the

adjacent frames. Since the analysis is made in the plan, we assume that there is no influence of the transverse frames in the plan y – z.

Moreover, an 2D analysis also implies that there is no lateral buckling or buckling according the weak axis. Therefore, the out-plane instabilities are not taken into account in the verifications. Finally, the structures will be designed according Eurocodes procedures.[1]

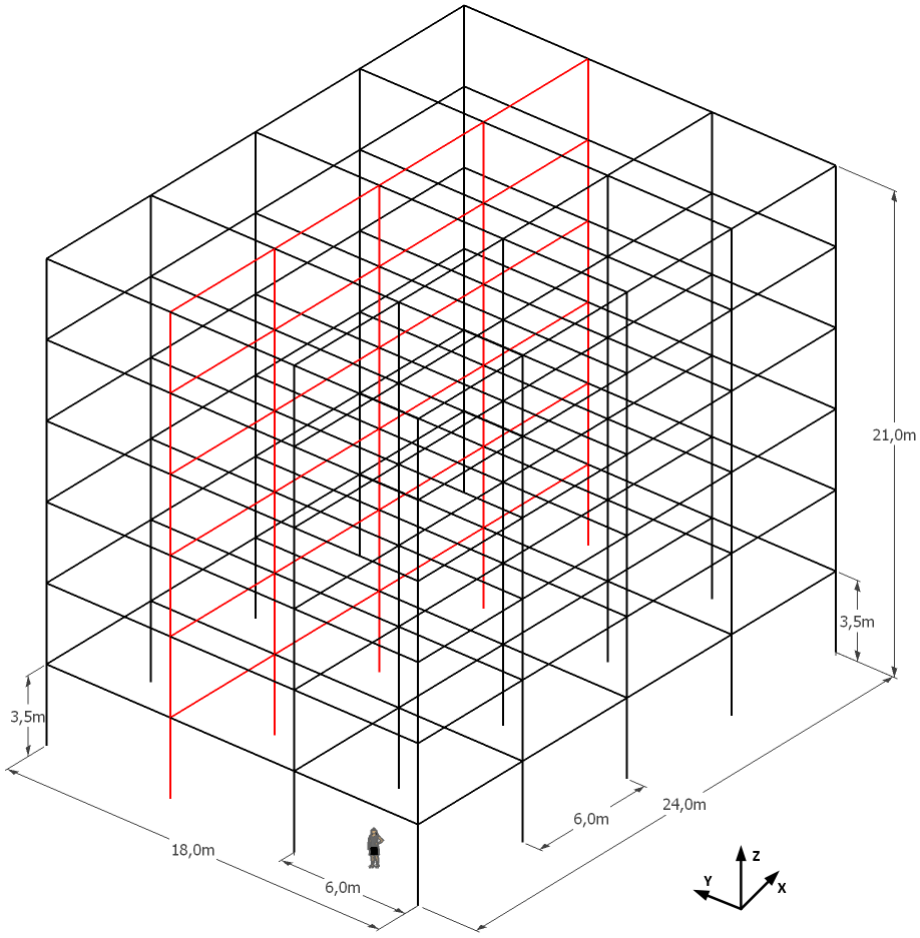

Figure 1.4: Perspective Representation of the Structure

In this paper, the analysis will be focused exclusively on direct methods. To be more precise, this master's thesis fits into the alternative path methods research (see section 2.2.2).

By comparing the performance of the two investigated structures in terms of robustness, we will be able to establish relevant conclusions about the behaviour of the two main materials used in civil engineering.

[1]Eurocode are standards rules for construction design provided by the European Committee for Standardisation (CEN).

Chapter 2

States of Art – Literature Search

This chapter presents the current state of knowledge regarding robustness. Particular attention is given to the prescription rules of Eurocodes for buildings. Indeed, one of the objective of this thesis is to develop practical rules and recommendations that can be applied in design offices.

Nowadays, there are two major strategies to design a building against disproportionate collapse. These strategies depend on the inclusion or not of a specific scenario coming from a risk assessment of vital element loss that could be lost.

If there is no specific scenario against which the structure has to sustain, minimum prescriptions and design rules are applicable to enhance general structural integrity. Those methods are called indirect method because the hazard is not explicitly taken into account in the design.

On the contrary, the general contractor, the design office or the owner may identify a highly likely threat against which the structure has to withstand. In this case, direct methods are used in order to prevent the building collapse for this particular event.

In both cases, a risk evaluation should be undertaken in order to determine the level of risk in terms of human lives, economic losses or social impacts. This assessment should include a tradeoff analysis involving pre-construction and post-construction costs. In parallel, it is recommenced to establish the consequences magnitude according the likelihood of occurrence. Finally, this analysis should be performed in a such way that the benefits from mitigating the risk will be clearly stated.[14]

2.1 Indirect Method to Mitigate Progressive Collapse

As mentioned by Dusenberry & al., indirect design approaches the problem by identifying and incorporating into a building several systems that are known to enhance robustness, without specific consideration of events.[14] This approach is well suit for low risk of progressive collapse.

The indirect method is the easiest approach to apply and provide a uniformity of compliance. Furthermore, little additional analysis is required by design office.[23]

Trough the years, researchers and engineers developed several techniques and prescriptions to increase the general structural integrity and activating higher structural elements capacity. Those methods rely on interconnections of components, redundancy and strong ties between elements. Moreover, promote general strength and continuity in the structure will widen the number of alternative load paths. Ductility connections are also an effective mean to absorb energy during earthquake or vehicle impacts.

One of the most common method of achieving structural integrity is through a proper plan layout of the building that will foster the general stability. As an example, reduce spans or appropriate locations of walls will provide more stability. For large structures, compartmentalizations will create independent substructures that will lead to arrest the disproportionate collapse.[14]

Several authors recommend detailed connections to ensure minimum joint resistance and inter-member ties reinforcement. For instance, top and bottom reinforcements in concrete floor slabs must extend into beams and columns to improve capability to withstands load reversals. Moreover, the connections should be able to develop the resistance of the weakest connected elements.[14]

Non-structural equipment such as shock absorbers or exterior walls can also help to reduce the effect of an abnormal load and prevent the progressive collapse.

As a last example, changing direction of span of floor slabs if one of the supported walls is removed is an effective way to mitigate progressive collapse too. To do so, reinforcements in both directions have to be planned during the design.

2.2 Direct Method to Mitigate Progressive Collapse

At the opposite, direct methods rely on heavily structural analysis and detailed calculations to demonstrate that the remaining load paths are sufficient to confine the collapse under postulated abnormal loads. Including the damage in the design becomes a part of the process. The direct method suits for high occurrence probability of local failure.[14][23]

However, general integrity for normal design should always be considered as a beginning step. So that a judicious combination of both strategies can be obtained.[23]

Conceptually, one can obviously understand that only two approaches are possible. Either the element is designed to sustain the abnormal load, or else the remaining structure is able to outlive the loss of one of its elements. The first solution is named the key element method while the second one is called the alternative load paths method.

2.2.1 Specific Local Resistance or Key Element Design

In this strategy, the designer explicitly redesigns the building to resist the abnormal load. The first step is to identify key elements without which the consequences for the structure are unacceptable. These individual members are locally hardened and detailed to withstand the specific threat. As recalled by National Institute of Standards and Technology (NIST), this approach develop the full resistance of the key members.[23]

One easy way to include the threat in the design is to increase the load factors on the normal loads. Nevertheless, this could cause the failure mode to change since stiffness attract stress. Indeed, modifying the relative stiffness of elements will results in a change of the stress distribution within the structure. Hence, this method is often an iterative process.

The key element method is often the most suitable option when retrofitting an existing building into compliance. It allows to strengthen key elements, such as exterior columns, at a reasonable cost and in a practical way.[23]

Note that to count on local resistance solution, connections or supporting members framing to key elements must be designed to develop the full capacity of the latter.[23]

2.2.2 Redundancy or Alternative Load Paths

National Institute of Standards and Technology (NIST) gives an accurate definition of the alternate load path method. In this method, the structure is designed to carry loads by means of alternate path in the event of a bearing component loss.[23]

According U.S General Services Administration (GSA), this method has been selected as the preferred approach for providing resistance to progressive collapse when required ties capacities cannot be obtained in low level of protection by the indirect method.[23] Moreover, in his review of guidelines and provisions, Dusenberry & al. also argue that first investigations should be focused on alternative loads path.

Techniques currently employed in alternative load path method are, by example, ensuring beam action for walls or arching action in masonry construction to redistribute load of floor slabs. In steel construction, catenary action of restrained beams have similar effects of continuous horizontal ties. For reinforced concrete beams, catenary action can also be activated thanks to the reinforcement. In concrete structure, compressive membrane actions, equivalent to arching action, can reduce the risk of a progressive collapse too.

2.3 Eurocodes Prescriptions

The part in Eurocodes devoted to progressive collapse is the Eurocode EN 1991-1-7. As indicated at the beginning of the norm, this code provides strategies and rules for safeguarding buildings against identifiable and unidentifiable accidental actions. The recommended strategies range from provision of measures to prevent or reduces the accidental action to that of designing the structure to sustain the action.[4]

The following Figure 2.1, found in the Eurocodes, offers a concise diagram on strategies that can be adopted in accidental design situations.

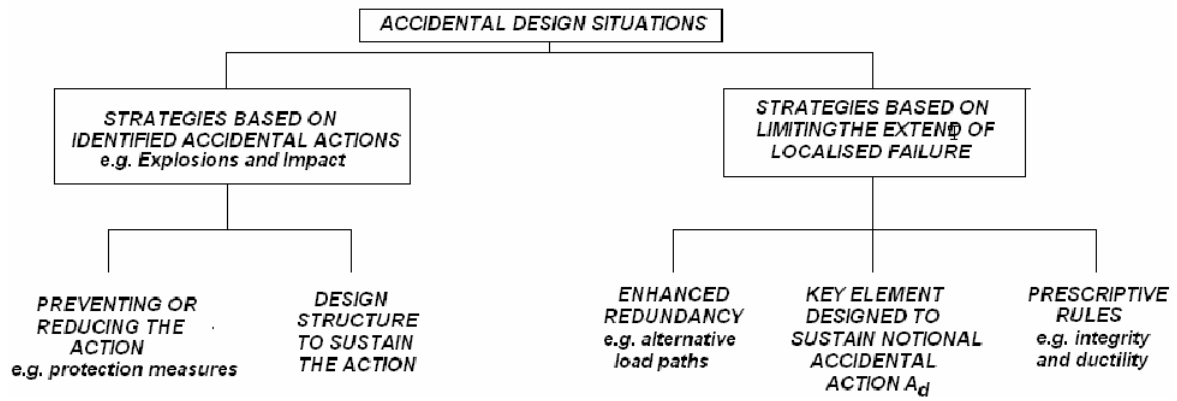

Figure 2.1: Strategies for Accidental Design Situations[4]

Several sections of Eurocodes are focused on defining accidental action and their modelling such as internal explosions or impact.

For building structure, Eurocodes introduces 4 consequence classes or CC (1, 2 Lower Risk, 2 Upper Risk and 3). Hence, appropriate strategies can be undertaken to mitigate the occurrence of disproportional collapse and grant a sufficient level of robustness.

For the lowest class, Eurocodes claims that no specific consideration is needed regarding accidental actions. If a structure is CC2 Lower Group, indirect methods are sufficient. For a building in CC2 Upper Group, both indirect and direct strategies should be apply. For the highest class, a full risk assessment analysis is required to take into account all the normal and abnormal hazards.

Nonetheless, there are almost no performance criteria to certify that the structure meets robustness requirements. Contrary to the others Eurocodes, EN 1991-1-7 contains mainly guidelines and qualitative recommendations. There is no complete step by step methods to follow in order to reach an adequate accidental design to trust with reliability.

In the light of this non exhaustive summarize about the robustness state of art, one can infer that the current knowledge regarding progressive collapse is limited to qualitative recommendations. For the time being, researchers are working on developing quantitative methods applicable and replicable in most situations.

Chapter 3

Design of Structures

In this chapter, we will describe the procedure leading to the dimensions of the two structures. We will discuss about the assumptions and simplifications made. To get a realistic design, we choose common values for the load, span, localisation and so on. Moreover, all elements can be found on market. The design is made in order to respect Eurocodes serviceability and ultimate limit states.

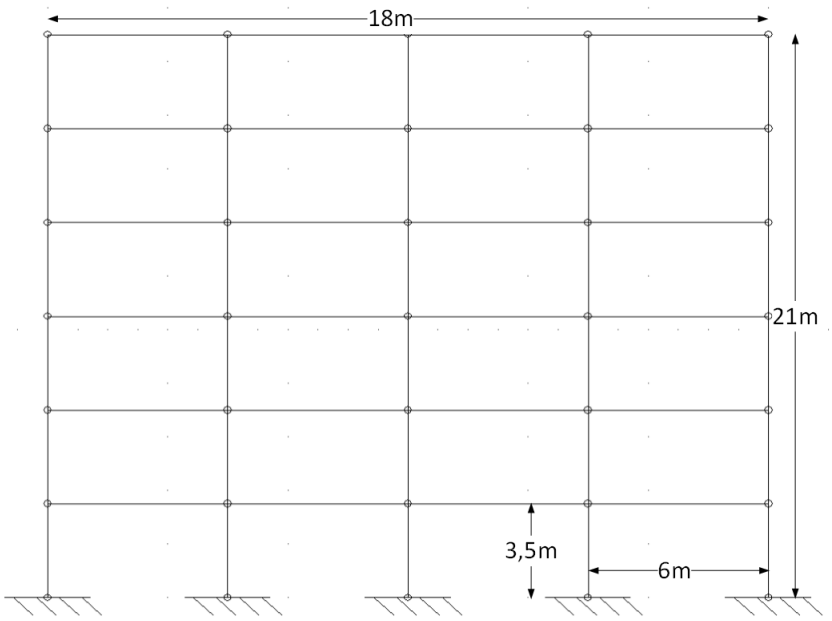

Figure 3.1: Schematic Representation of the Building

3.1 Structures Solicitations

The floor is composed of two ways carrying concrete slabs whose height is equal to 25 cm. Therefore the dead-load will have a triangular distribution. We assume a concrete specific weight of $\gamma_c = 25$ kN/m^3. Moreover, a finishing layer of $1,5$ kN/m^2 is taken into account consider a topping height to 8 cm instead of 5 cm. Therefore, the total self weight of the floor is:

$$q_{fl} = 2\frac{6\,(1,5 + 0,25\gamma_c)}{2} = 46,5 \text{ kN/m} \tag{3.1}$$

The live load of this office building is fixed at 3 kN/m^2.[2] Since the span is 6 m, the characteristic triangularly distributed load capacity becomes:

$$q_k = 2\frac{3 \cdot 6}{2} = 18 \text{ kN/m} \tag{3.2}$$

A roof cladding whose weight is equal to $16,5$ kN/m is employed.[9] The outer shell of the building is composed of steel siding whose weight is $16,5$ kg/m^2.[8] If we assumed the siding is anchored at each corner, it results that the vertical weight on each floor is 4 kN (2 kN on the roof). This is valid for both external sides of the frame.

Since Brussels area altitude, around 15 m, is less than 100 m, the Belgian national annex recommends a characteristic value of snow load $s_k = 0,5$ kN/m^2, which becomes in this case a triangular load of $s_k = 3,5$ kN/m because of the span.[7]

According to Eurocode, Brussels area belongs to the terrain category IV[1] and the average wind speed is 25 m/s. Knowing the dimensions of the office building, we obtained the average pressure acting on external walls. On the windward walls, the pushing pressure is equal to 442 Pa while on the leeward wall, the suction pressure is 272 Pa. Hence, the total pressure acting on the building is 714 Pa. Because the wind is acting on the structure through the steel siding, it results the horizontal pressure on each floor is equal to $P_{k,w} = 15$ kN ($7,5$ kN for the roof).[3]

Figure 3.2 describes a schematic representation of the design load. The self-load of elements is not represented and the roof cladding loading is too low to be noticeable. In this configuration, the design will lead to lighter beam profile than a uniformly distributed load since less load is carrying by the beams.

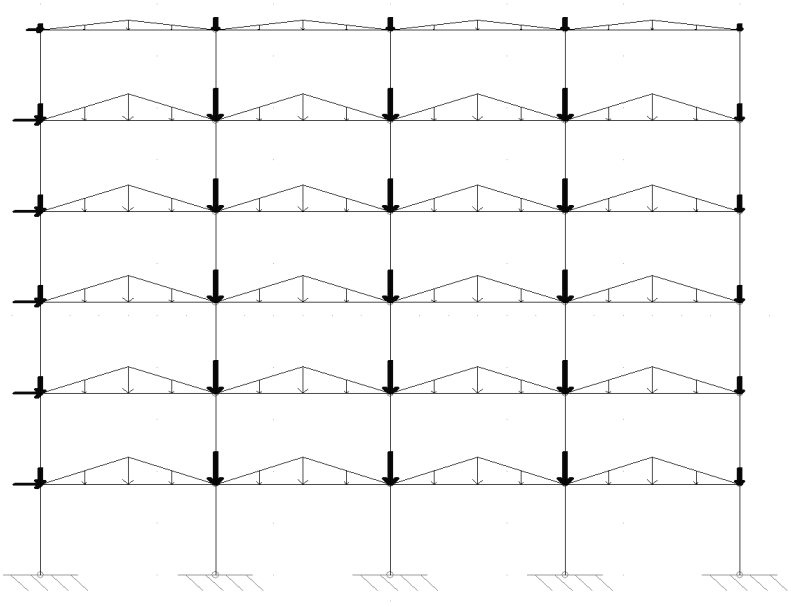

Figure 3.2: Schematic Representation of the Loading considered for Design

Both initial designs consider triangular loads to be consistent with designed made by Ghent University. On the contrary, the investigation under accidental event assumes uniformly distributed load since. Indeed, it is much more easier to implement this type of loading in FINELg.

[1] At least 15% of the surface is covered with building and their average height exceeds 15 m.[3]

Moreover the results can be compared in future investigations to the analytical model developed at University of Liège.

So too light profiles have been set up compared to the investigation. The spans are more loading in the investigation than in the design. If the design was made with uniformly distributed load, IPE 450 beams would have been necessary for steel frame. This will have some consequences in the plastic mechanism formation (see section 5.1.2) and in the shear force influence (see section 5.3.4).

The main difference between the ALS and ULS combination, expected load intensity, is the unsymmetrical situation due to wind load.

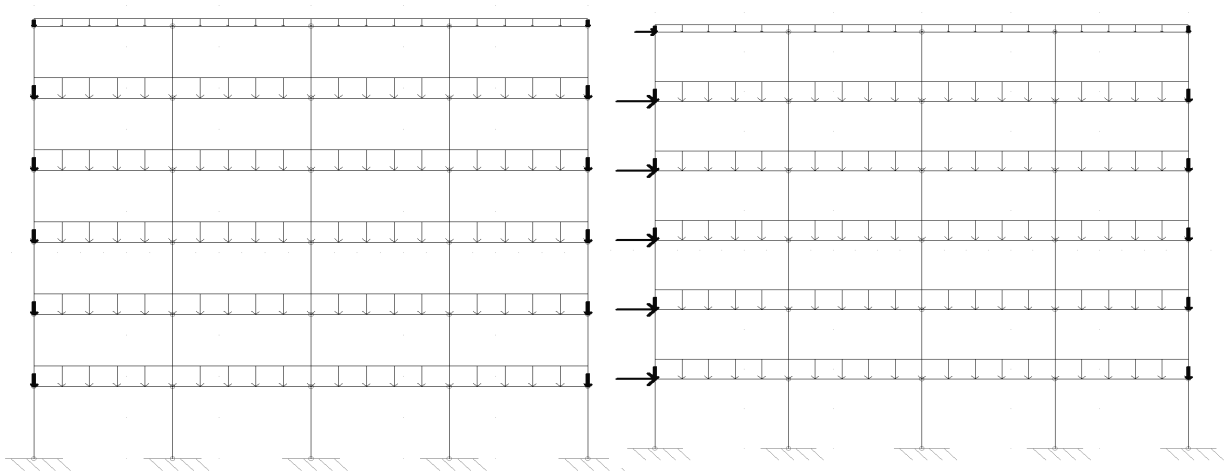

(a) Under ALS Combination

(b) Under ULS Combination

Figure 3.3: Schematic Representation of the Loading considered for Robustness Investigation

3.2 Description of the Steel Structure

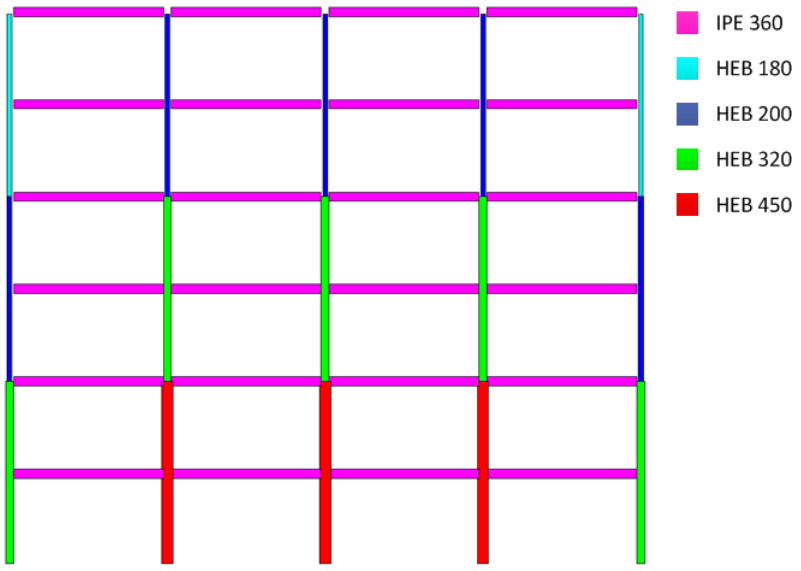

Figure 3.4: Initial Steel Frame Investigated

Figure 3.4 represents the initial steel structure. All the beams are IPE 360 profiles since they carry the same loads. On the contrary, four kinds of columns are defined for realistic purposes. In addition, different columns were designed for internal and external columns For the internal columns, the first two floors are made of HEB 450. The following two stages are composed of HEB 320 while HEB 200 was necessary for the upper floors. The external columns are successively composed of HEB 320, HEB 200 and HEB 180. Finally, all profiles are bent according their strong axis.

3.3 Description of the Concrete Structure

The concrete structure design can be found on Figure 3.5 hereafter. To performed this design, Ghent University choose the quality of concrete C30/37 and reinforcement rebars whose yield strength is equal to $f_{y,k} = 500$ MPa. The nominal concrete cover for all the elements was set at $c_{nom} = 30$ mm. while the stirrups diameter is 10 mm. Note that the stirrups will not be model since the shear force is neglected.

As for the steel structure, one type of beam have been designed in the frame plane as depict on Figure 3.6 (*Beam 1*). To simplify the modelization, the reinforcement rebars are placed all along the beams. The diameter of the reinforcement rebars is equal to 20 mm. The design of the perpendicular frame beams is shown in Figure 3.6 (*Beam 2*) for information purpose only.

To match with a realistic design, all the column have the same width in the frame plane, i.e a width of 35 cm. Only the height and the reinforcement are changing. Four kinds of columns have been designed. For the external columns (*Column 1 and 2*), the diameter of the reinforcement rebars is equal to 16 mm. The internal columns are made with reinforcement rebars of diameter equal to 16 mm. The upper columns (*Column 1 and 3*) have a square shape contrary to the lower column (*Column 2 and 4* which have a depth of 45 cm.

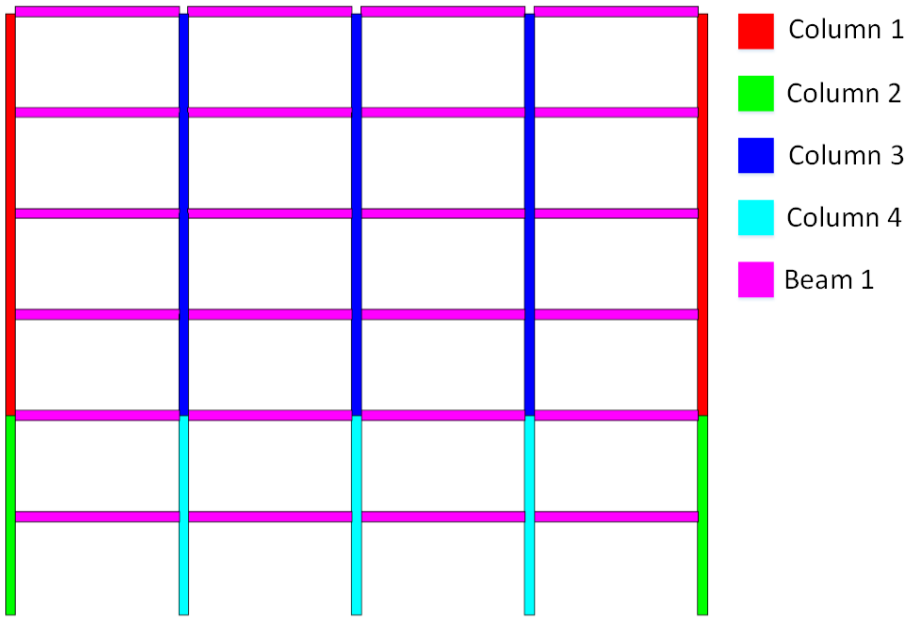

Figure 3.5: Initial Reinforced Concrete Frame Investigated

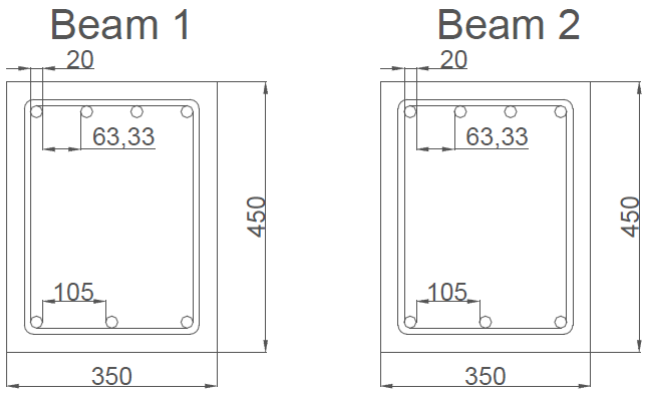

Figure 3.6: Reinforced Concrete Beams Cross-Section

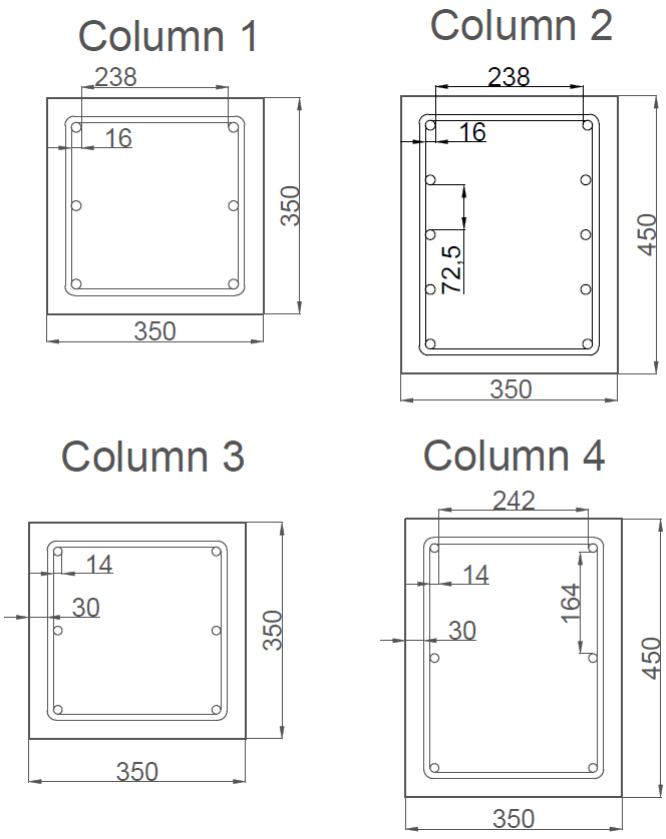

Figure 3.7: Reinforced Concrete Columns Cross-Section

Chapter 4

Modelization of Structures

The present chapter focuses on the numerical modelization of both structures. Among other things, we will present the constitutive law of materials computed, then validate the results coming from FINELg and finally describes the strategy adopted to simulate the column loss.

The computer program FINELg is a homemade finite element software developed since 1974 by University of Liège (Argenco Department) and at Greisch design office (Liège, Belqium). This software allows to solve, inter alia, geometrically and materially non-linear structural problems under static dead loads. Geometrical non-linearity covers large displacements (i.e. large rotations) and material non-linearity covers classical elasto-plasticity theory. The numerical technique available in FINELg enables to follow the behaviour of a structure under an increasing external loading or displacement up to collapse or instability, and even beyond.[12][13]

The iterative procedure uses Newton-Raphson steps taking into account the residual of the previous step. This method is recommended when convergence towards equilibrium states is slow and near collapse. The main increment strategy is the imposed displacement method. In this case, we manually increase the displacement increment by progressively move down the column. In FINELg, this column will be modelled by a support.

Contrary to the load increment, the displacement increment provides a better control of the collapse. Because of the retaining given by the support, it prevents the frame from drifting apart suddenly. With the load increment, it may appear close to the collapse that a small increase in the load level results in a large displacement of the frame. However if the gap between the two steps is too large, the software will not be able to converge to a new equilibrium state and intersect the loading path.

As an example, this numerical trouble was encountered right after the cracking of the entire concrete cross-section. The cracks lead to a brittle failure and the beams fell down instantaneously of several centimetres before all the reinforcements of the cross-section start to be in tension and provide stiffness again. This phenomena was caused by the behaviour transition in the reinforced concrete beams between the compressive arch action and membrane effects. Even by using a very small load incremental step, the gap was to large for the software and FINELg was not able to reach the next step. As a consequence, the load incremental method is not really suitable to focus on catenary action with concrete elements because of the material brittle nature.

Nevertheless, the manually load increment strategy were sometimes used to provide further information and another point of view about the structural integrity.

4.1 Constitutive Laws

This section describes the constitutive law for steel and concrete materials computed in FINELg. In order to accurately describe the behaviour of frames at large deformations, high vigilance is required in materials modelling. Moreover correctly represent the behaviour will leverage the maximum benefit from the materials, especially when seeking for robustness.

4.1.1 Steel Behaviour

In a first approach, an elastic perfectly plastic model was introduced for its simplicity and its good precision. However, this model leads to instability in the investigated frame such as buckling or panel mechanisms. Indeed, because of the number of plastic hinges appearing in the structure, the structure has no more rigidity and therefore collapse because of plastic hinges formation. On the Figure 4.1, one can see that because of infinite ductility capacity, the central columns are no longer hold by the surrounding beams because the latter have no more stiffening. It results that the all the central column suddenly fell down.

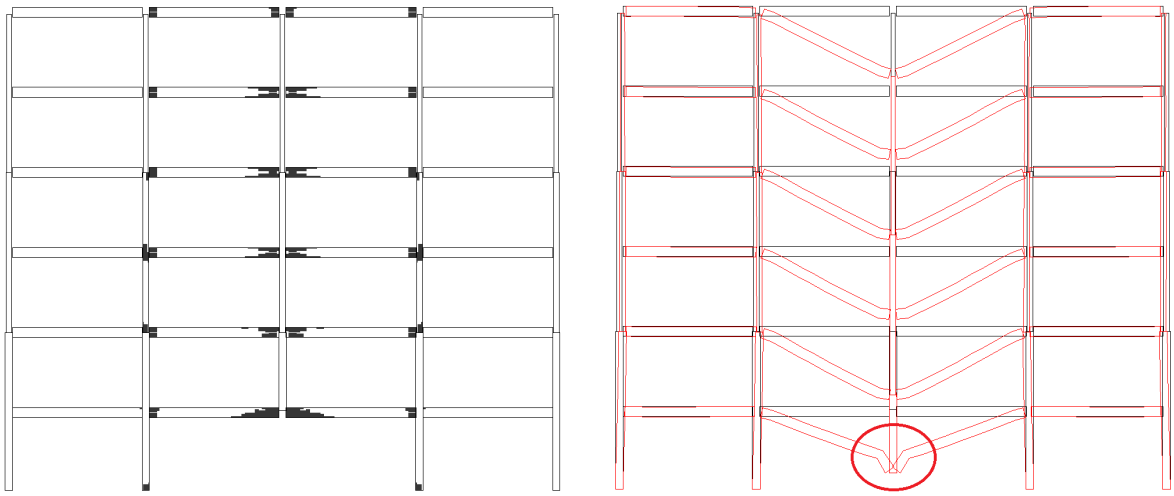

(a) Plastic Hinges (b) Deformation

Figure 4.1: Lack of Stiffness in the Elastic Perfectly Plastic Model

In consequence, we decided to introduce work hardening in the model. It results that we are now able to compute further in the loading path. Nevertheless, readers can see on Figure 4.2 that the stress can increase indefinitely because of the work hardening. The simulation ending will come from a too large displacement, instability or inherent numerical errors. To reflect an exact behaviour, the tangent modulus of work hardening E_t is set at 1500 MPa. In addition, work hardening appears only when strain reaches $\epsilon_h = 2$ ‰.

Otherwise, classical value of Young modulus corresponding to mild steel is chosen, i.e $E = 210000$ MPa. As we designed the steel structure with steel grade S235, the yielding strength is fixed at $f_y = 235$ MPa.

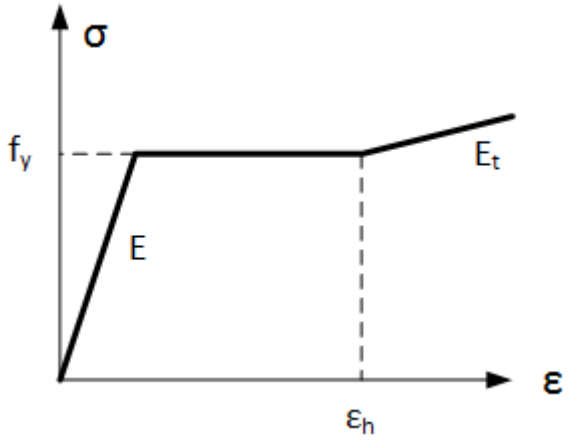

Figure 4.2: Trilinear Steel Profile Law

4.1.2 Reinforced Concrete Behaviour

Reinforced concrete behaviour can be divided into its two components. The first one is the steel reinforcement rebars while the second component is the concrete itself.

Concrete

The concrete constitutive law is represented on Figure 4.3. This is a parabolic law in compression with no post peak reduction so that the concrete reach a plateau at high compression. In tension, the resistance in traction of the concrete is modelled but the tension stiffening is not taken into account. When f_{ct} is reached, the concrete has no more resistance in traction. At this stage, it means that the concrete is cracked. Properties of concrete modelling come from the data base from FINELg.

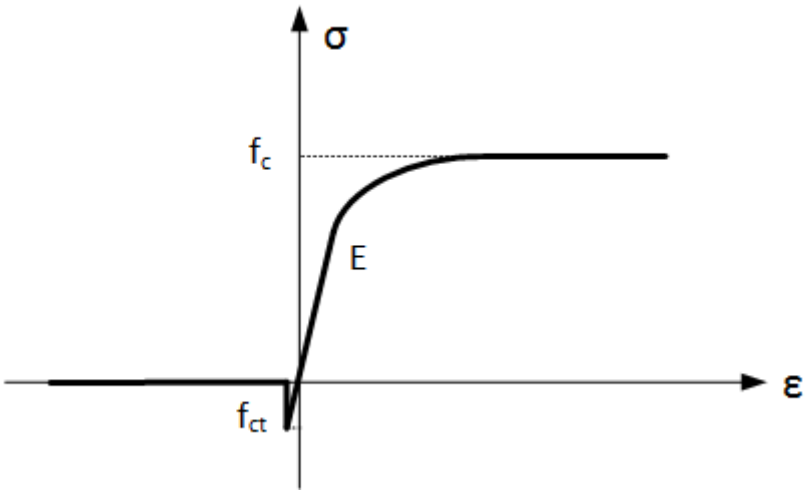

Figure 4.3: Uniaxial Concrete Law

Steel Rebars

The steel rebars constitutive law is depicted on Figure 4.4a. It may surprise to introduce a different work hardening law from that of the steel frame. The reason is to always confer to the frame some stiffness to avoid the apparition of sudden too large displacement as discuss at the beginning of this chapter 4.

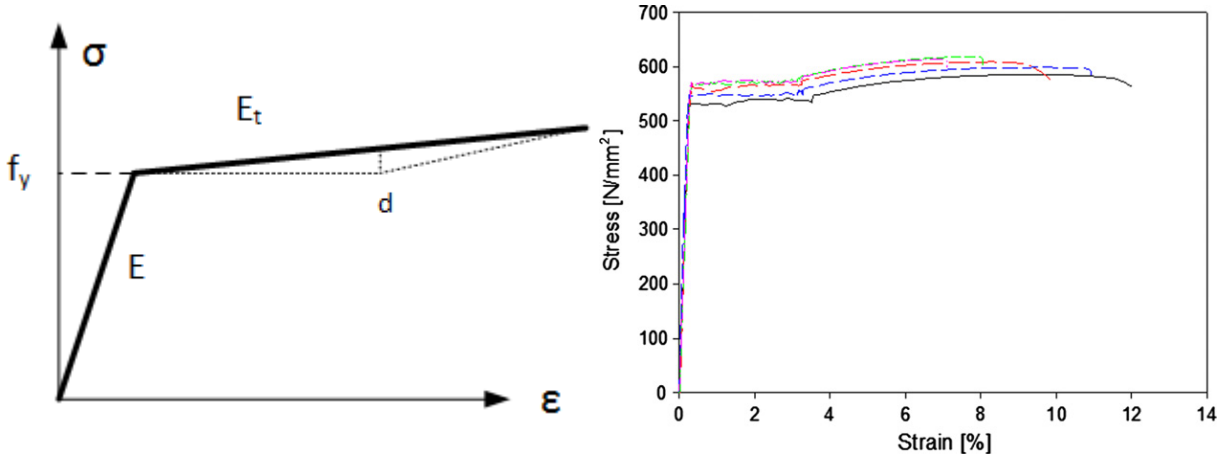

(a) Bilinear Steel Rebars Law

(b) Experimental stress-strain curves of reinforcing bars[17]

Figure 4.4: Steel Reinforcement Rebars Law

In fact, the two steel laws provide close behaviour. To give an estimation of the difference, experimental stress-strain curves of reinforcing rebars performed by Ghent University are employed. The results of this experimental test are provided on Figure 4.4b. The test was performed as a part of a slab strip test focusing on robustness (see section 4.2).

The maximal difference d between the two laws is situated at the end of the plastic stage of the trilinear law, as shown on Figure 4.4a. According to the test, the strains at the beginning of the plastic stage and at the ultimate strength are respectively $\epsilon_y = 0,269$ % and $\epsilon_h = 3,2$ %. Measuring from the test that the tangent Modulus is $E_t = 1275$ MPa and knowing that mean value of yield strength is $f_y = 555$ MPa, the difference d can be easily determined :

$$d = 1275\frac{3,2 - 0.269}{100} = 37,4 \text{ MPa} \tag{4.1}$$

Hence, the maximal error e made by using the bilinear law comparing the trilinear law will be:

$$e = \frac{37,4}{555 + 37,4} \simeq 0,063 = 6,3\ \% \tag{4.2}$$

At the opposite, the difference for mild steel ($f_y = 235$ MPa) would be $13,7$ %, which becomes clearly no more acceptable.

4.2 Validation of FINELg

In this section, we will numerically reproduce a slab strip test performed by Ghent University to validate the results from FINELg for reinforced concrete elements at large deflections. The aim is to bring out the development of catenary action in the slab.

4.2.1 Case Study

The experimental test will be here briefly summarize, however the complete investigation can be found in this article : "*Experimental investigation of the load-displacement behaviour under catenary action in a restrained reinforced concrete slab strip*, by Dirk Gouverneur, Robby Caspeele and Luc Taerwe, 2013".

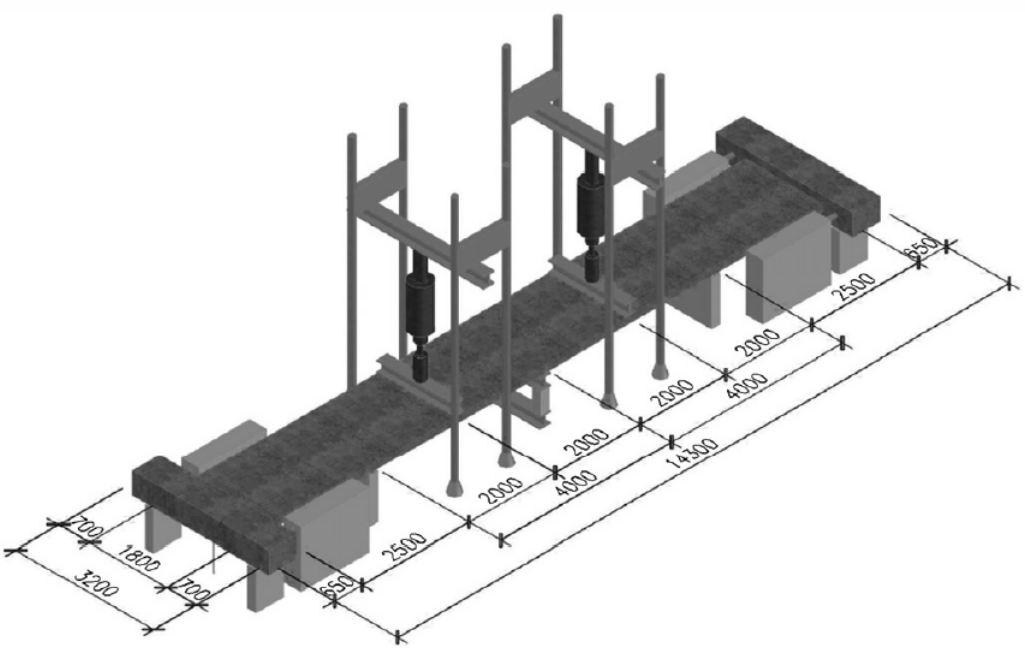

Figure 4.5: Test set-up [17]

A schematic view of the test is shown on Figure 4.5. As described in the article : "*The test set-up consists of a* 160 mm *thick and* 1800 mm *wide reinforced concrete slab strip specimen. The total length of the specimen is* 14,3 m. *The distance between the inner supports and the central support is* 4 m, *changing to one span of* 8 m *between the inner supports after the controlled removal of the central support, which simulates an accidental action.*".

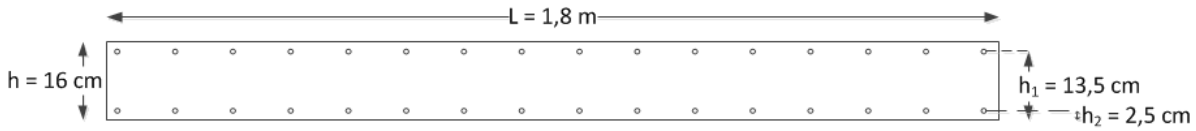

Figure 4.6: Slabs Strip Cross-Section

Concrete with mechanical properties C30/37 was ordered. The longitudinal reinforcement consists of 16 bars for both bottom and top reinforcement layers. The nominal diameter was

equal to 10 mm.

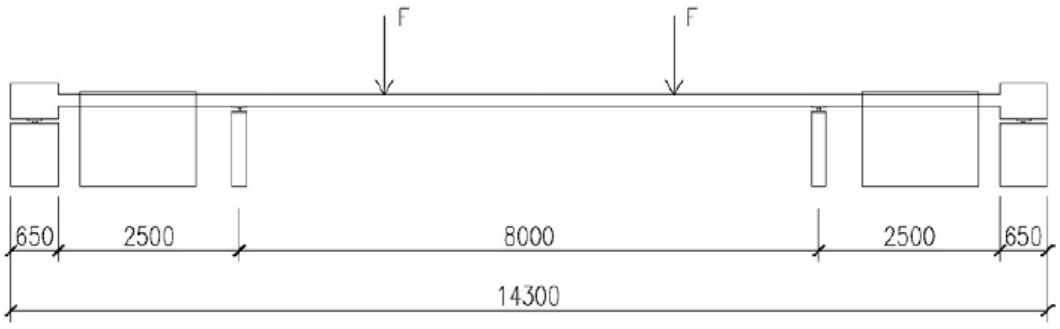

Figure 4.7: Schematic representation of the Test After the Central Support Removal[17]

Thanks to heavy reinforced outer edges and roller bearings, the slab can be seen as a slabs resting on 4 pinned supports after the central hydraulic jack is removed. In consequence, the test set-up is defined as a four point bending test.

The experimental test was divided into three phases. The first phase consisted of loading and unloading the slabs with the central support to simulate the service loading. Then, the central support was slowly removed until the distance changed from 2 spans of 4 m to a unique span of 8 m. Finally, the third phase comprised the application of two line loads pushing on the slab strip until the collapse of the specimen. The two line loads F can be seen on Figure 4.7.

4.2.2 Numerical Model

Since the situation is symmetrical, only a half of the slab strip will be modelled. The support conditions are described in the Figure 4.8. In this numerical model, a 2D simulation is chosen. Through this test, the goal is to prove that finite reinforced concrete elements in FINELg are able to reproduce catenary action. Therefore, a 2D analysis is enough to catch this effect even if it is possible to obtain slightly different results from the experimental test.

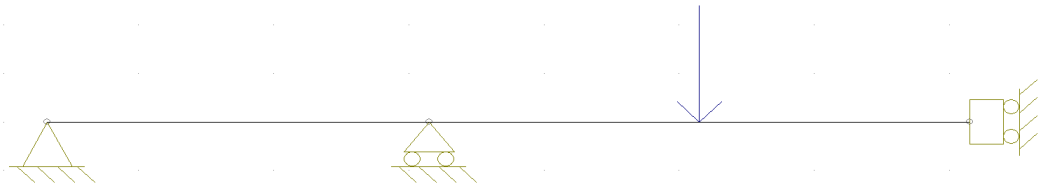

Figure 4.8: Support Conditions After the Central Support Removal

Most of material properties can be found in the article as Ghent University realised several characterisation tests on sample. The others parameters needed come from usual values used for reinforcement steel and C30/37 concrete in conformity with Eurocodes recommendations.

The elements used are modelled with plane beam element defined by three nodes. Each external node has three degree of freedom (2 translations and 1 rotation) while the central node only presents one degree of freedom in translation along the beam element axis.

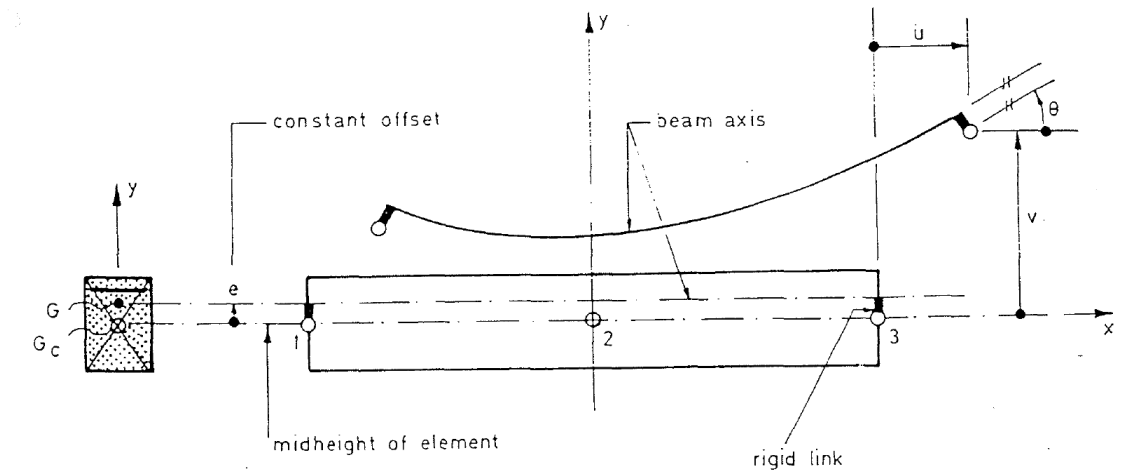

Figure 4.9: Plane Reinforced Concrete Beam Element composed of Three Nodes[13]

The Figure 4.10 provides a representation of the 135 elements composing the slab strip. Each element is 5 cm long.

Figure 4.10: Fine Element Discretization of the Slab Strip in FINELg

This simplify numerical simulation will consists of two phases. During the first phase, the self-weight of the slabs will be apply. To prevent deflection at midspan during this phase, the self-weight vertical reaction will be applied and gradually increase in parallel with the self-weight loading. The determination of this vertical reaction comes from a analysis performed with OSSA2D, a linear elastic software. Then, the value was calibrated in order to take into account non linearity such as cracks.

4.2.3 Comparison of Results

The Figure 4.11 depicts the deflection at midspan according the load applied by the jacks. As described by the article, this load-deflection curve can be decomposed in three parts. Note that the displacement does not start at zero since the slab is already resting under the dead load when starting pushing down the slab with the jack.

The first part of this curve is an elastic response of the cracked reinforced concrete as evidenced by the stiffness of the cracked section. Then, an yielding plateau occurs because of the plastic hinges formation at the internal supports. The third part represents the catenary stage. The top and bottom reinforcements both become subjected to tension. This provide an increase in the load carrying capacity. At the end of the experimental test, the top reinforcement break following by the bottom reinforcement a bit after.

From Figure 4.11, readers can observe that results from FINELg simulation match the experimental curve expected for the last part. This difference is explained by the fact that FINELg

assumes that the heavy reinforced outer edges are fixed nodes and therefore cannot more horizontally. Despite the fact that slab strip was properly anchored and maintain by horizontal jacks during the test, there will always be a small displacement. During the test, Ghent University measured a total inward movement of less than 10 mm.

Because of the modelization of the extremity by a fixed support, the slab strip cannot move in direction of the center of the slabs. If the slab is completely restrained at the extremity, the reinforcement rebars can immediately lean on the extremity when the concrete is fully crack. Thus the slab starts developing catenary action at a lower deflection as described by the red curve. This effect is evidenced by the Figure 4.13c which shows that the bottom reinforcement (and to a lesser degree the top reinforcement) is yielded at the left extremity of the slab strip.

In addition, reader can see on Figure 4.12 the evolution of cracks apparition in the slab strip. The darker the blue is, the wider the crack in the finite element is. At the failure of top reinforcement, each finite element composing the slab strip has cracks, which means that there is at least a crack every 5 cm.

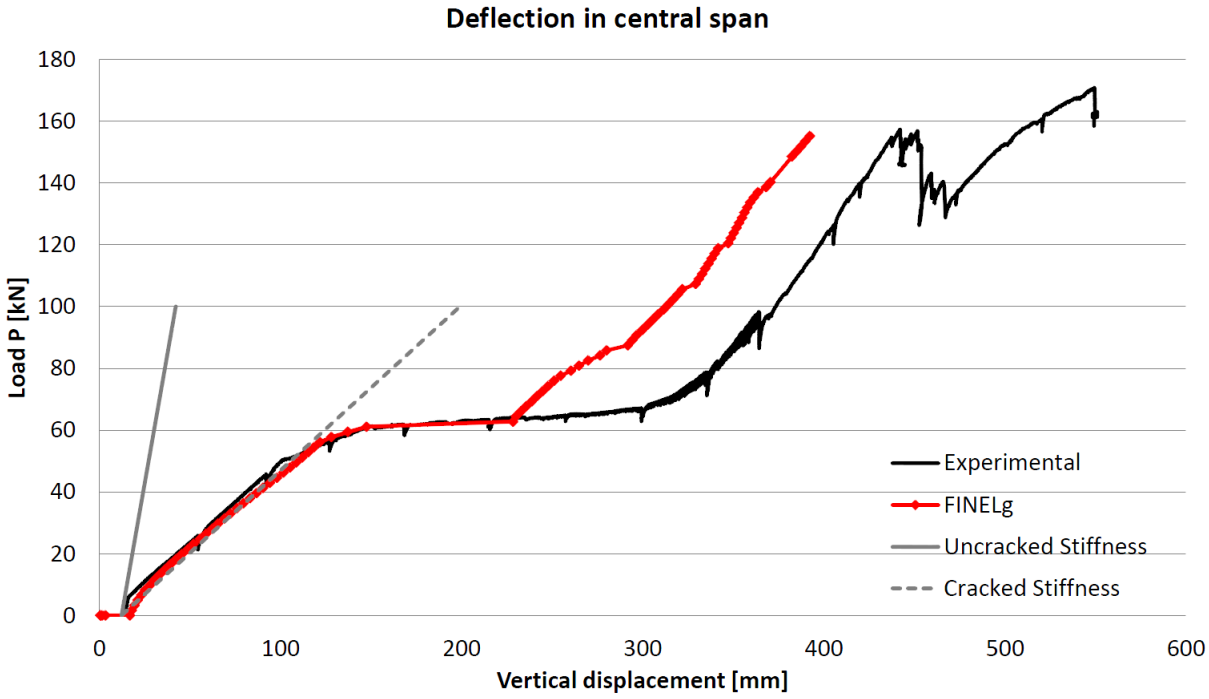

Figure 4.11: Load-Deflection Curve in Central Span During Phase 3 [17]

From the numerical point of view, the second phase of the red curve, which range more or less from 150 mm to 220 mm illustrates well the importance of the strategy to adopt in the numerical simulation as discuss at the beginning of this chapter. In this simulation, the incremental load strategy turned out to be the easiest way to model the action of the jacks. Nevertheless, as can be seen Figure 4.11, there is a large gap between the two steps even if work hardening was introduced in the model. It is due to the transition between the compressive membrane action and the catenary action inside the slab strip.

Up to know, none of the attempts made with the imposed displacement succeeded. Similarly, introducing a spring ($K_h = 838399.2352$ kN/m) instead of the fixed node did not work with the imposed load. It would have been interesting to compare those results from the slab with the

imposed displacement strategy in order to control the plastic phases and also introduce a spring at the outer edge in order to perfectly represents the experimental test.

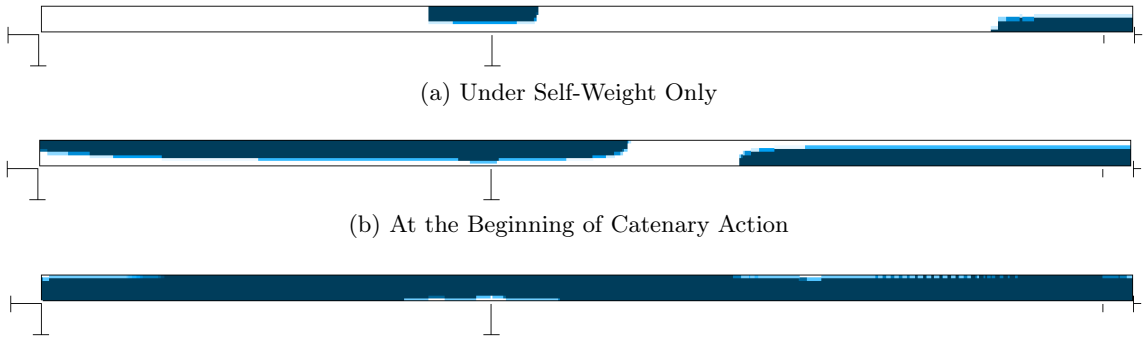

(a) Under Self-Weight Only

(b) At the Beginning of Catenary Action

(c) Before Failure of Top Reinforcement

Figure 4.12: Progression of Crack within the Slab Strip

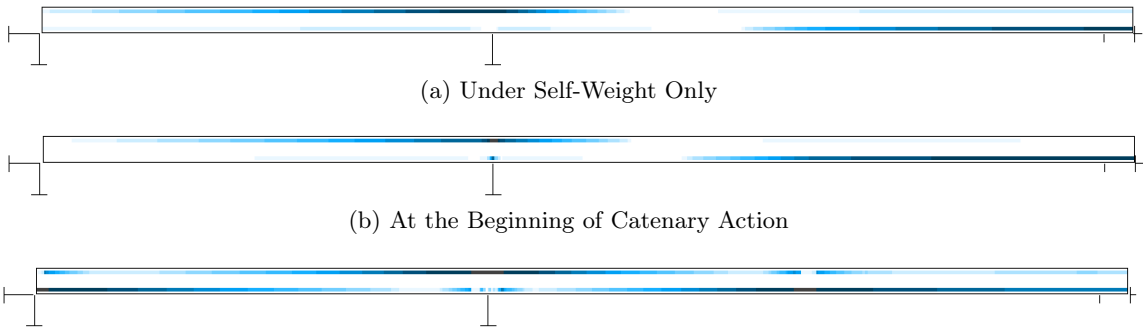

(a) Under Self-Weight Only

(b) At the Beginning of Catenary Action

(c) Before Failure of Top Reinforcement

Figure 4.13: Progression of Yielding within the Slab Strip

Analytical Stiffness

The following equations describe the establishment of the uncracked and cracked stiffness of the slab strip. On Figure 4.6, the dimension of the cross-section can be found. For the uncracked cross-section, the inertia is:

$$A_s = n_b \pi \frac{\phi^2}{4} = 16\pi \frac{10^2}{4} = 1257 \text{ mm} \tag{4.3}$$

$$n = \frac{E_s}{E_c} = \frac{207900}{31970} = 6,503 \text{ mm}^{-1} \tag{4.4}$$

$$I_{uncr} = \frac{Lh^3}{12} + nA_s \left(h_1 - \frac{h}{2}\right)^2 + nA_s \left(\frac{h}{2} - h_2\right)^2 \tag{4.5}$$

$$\begin{aligned} I_{uncr} &= \frac{Lh^3}{12} + 2nA_s \left(h_1 - \frac{h}{2}\right)^2 \\ &= \frac{1800 \cdot 160^3}{12} + 2 \cdot 6,501 \cdot 1257 \cdot 55^2 \\ &= 614 \times 10^6 + 49,45 \times 10^6 \\ &= 663,5 \times 10^6 \text{ mm}^4 \end{aligned}$$

while the cracked inertia is given by:

$$B = \frac{L}{nA_s} = \frac{1800}{6,503 \cdot 1257} = 0,220 \tag{4.6}$$

$$\Gamma = \frac{(n-1)\,A_s}{nA_s} = \frac{n-1}{n} = 0,846 \tag{4.7}$$

$$\begin{aligned} k_d &= \frac{1}{B}\sqrt{2h_2\left(1+\Gamma\frac{h_1}{h_2}\right)B+(1+\Gamma)^2}-(1+\Gamma) \\ &= \frac{1}{0,220}\sqrt{2\cdot 135\left(1+0,846\frac{25}{135}\right)B+(1+0,846)^2}-(1+0,846) \\ &= 30,2 \text{ mm} \end{aligned} \tag{4.8}$$

$$\begin{aligned} I_{cr} &= \frac{Lk_d^3}{3}+nA_s\left(h_2-k_d\right)^2+(n-1)\,A_s\left(k_d-h_1\right)^2 \\ &= \frac{1800\cdot 30,2^3}{3}+6,501\cdot 1257\left(135-30,2\right)^2+5,503\cdot 1257\left(30,2-25\right)^2 \\ &= 106\times 10^6 \text{ mm}^4 \end{aligned} \tag{4.9}$$

(4.10)

Once the inertia is known, we can analytically determine the stiffness of the slab strip or introducing this inertia in OSSA2D, a 2D linear elastic software. The latter will directly give the elastic deflection corresponding to the slab test.

Description of FINELg Results

By comparing Figure 4.14 and 4.15, it can be observed that the deformation of the simulation with the deformation of the experimental test are quite similar. The model represents well the cracks at the inner supports as proved by the discontinuity in the deformed shape.

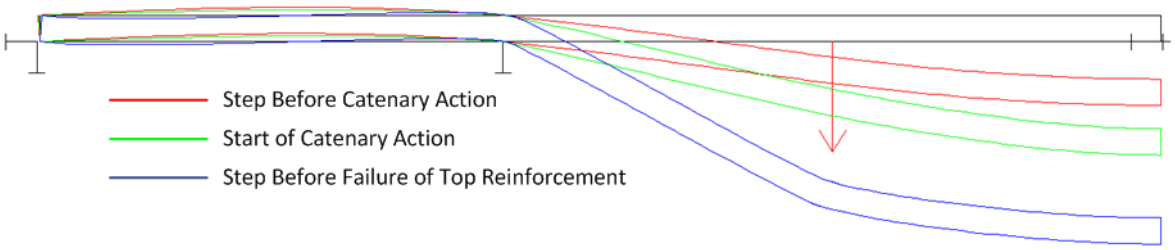

Figure 4.14: Evolution of Slab Strip Displacement During Phase 3 (Scale Factor x3)

However the deformation where the load is applied is more discontinuous than the experimental test. This observation becomes visible at the step before the failure of top reinforcement (blue line on Figure 4.14). The reason comes from the fact that the load in the model is punctually applied while there is a steel profile in the experimental test to spread the jack pressure. This results in a more cracked concrete and a more yielded steel than the experimental test.

Figure 4.15: Slab at the End of Test[17]

The Figure 4.16 and 4.17 depict the evolution of the bending moment and the normal force inside the slab strip. The complete M-N interaction curve at the inner support is plotted on Figure 4.18.

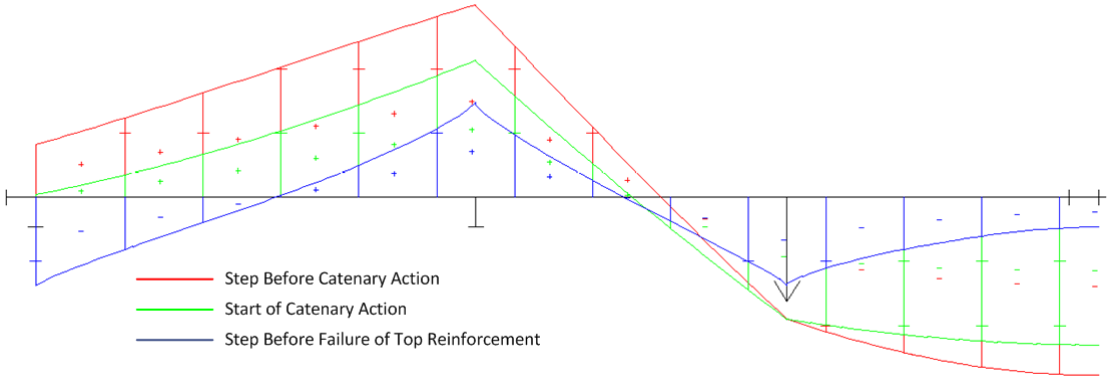

Figure 4.16: Evolution of Bending Moment During Phase 3

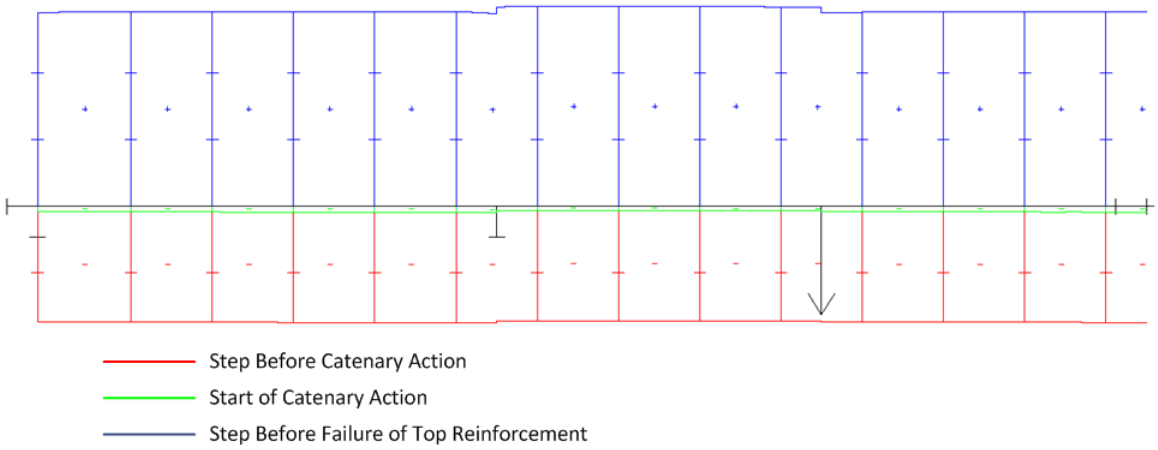

Figure 4.17: Evolution of Axial Force During Phase 3

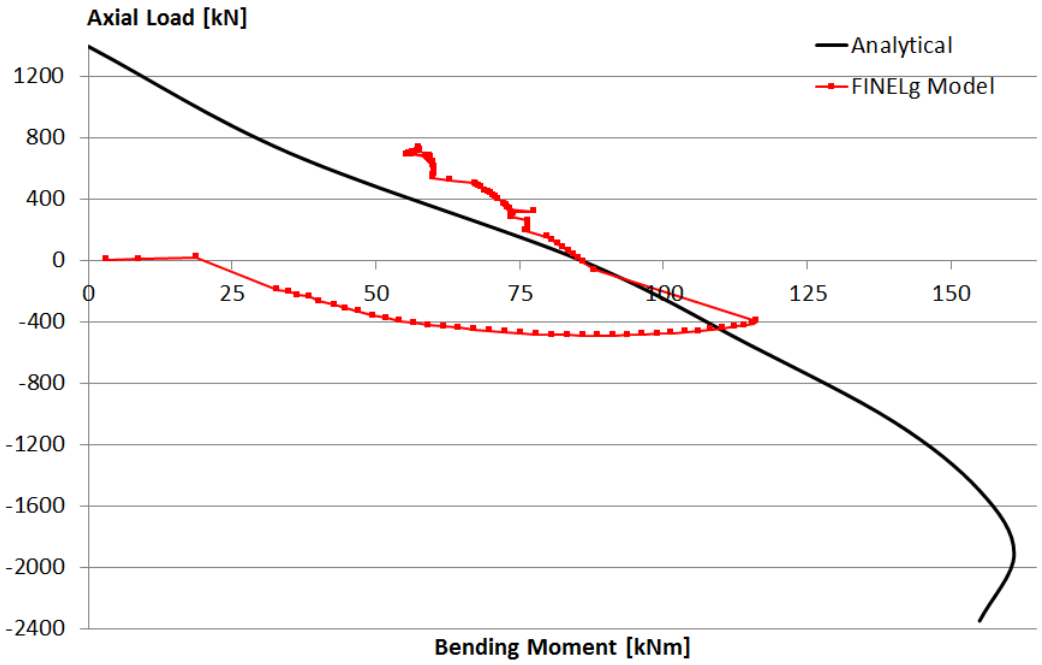

Figure 4.18: M-N Interaction Diagram at the Inner Support of Slab Strip During Phase 3[17]

Before the development of catenary action, the slab strip is in compression because of compressive membrane action. It does not occur in the experimental test because of the ability to move horizontally. About the numerical results, the bending moment in the slab at this stage has not yet significantly decreased. As we enhance the pressure of the jacks, tension occurs in the slabs and the bending moment starts to decrease since a part of the steel is now solicited to absorb traction.

The reduction of bending moment according the augmentation of tension force can be explained as the following. Under bending moment only, the compressed portion of concrete is equilibrated by the traction in the rebars in order to cover the flexural stress. If axial tension is added to the previous situation, this equilibrium will change. The area of concrete in compression will adjust itself and decrease since there is less compressive stress. On the contrary, tensile stress in rebars will increase, but for a constant area of steel. Therefore, a part of the total area of steel rebars has to be allocated to absorb the axial traction. Because less steel remains available to bear flexural stress, the bending moment capacity of the reinforced concrete cross-section will fall down. Furthermore, if the axial tension is so high that the entire cross-section is cracked, all the reinforcement rebars begins to be tense and no more concrete is available to take the compressive stress. Reducing even more the bending moment capacity of the cross section.

The same reasoning can be applied to explain the augmentation of bending moment with the axial compression force. The compression force will reduce the tensile stress in the steel area. This lower level of stress will provide a reserve that can be used to absorb more flexural stress and thus increase the bending capacity of the cross-section.

The explanation here above is valid only if the quantity of steel determines the rupture. In other words, it means that the concrete is superabundant and the strain distributions in the cross-section belongs to the domain 1b (pivot A) in the ultimate limit state. To check this assumption is valid, we need to determine the coefficient μ of the cross-section. In the article from Ghent University, the geometric reinforcement ratio $\rho = 0,5\ \%$. So the mechanical coefficient reinforcement ω is equals to:

$$\omega = \rho\frac{f_{yd}}{f_{cd}} = 0,005\frac{500/1,15}{30/1,5} = 0,121 \tag{4.11}$$

which leads to the coefficient μ,

$$\mu = \frac{\omega - 0,052}{1,09} + 0,052 = 0,115 \leq \mu_{rat} = 0,187 \tag{4.12}$$

Since the coefficient μ is smaller than the rational value, the justification is valid.

On the analytical curve from Figure 4.18, one can see that the bending moment is decreasing as the axial traction force is increasing. At the opposite, the bending moment is increasing with the axial compression force. However after -1800 kN, the concrete starts to crush leading to a reduction of the bending moment capacity. About the FINELg results, the bending moment capacity of the cross-section is higher than the analytical prediction, specially when the cross-section is in tension. The explanation lies in the definition of work-hardening in the constitutive law of reinforcements (see Figure 4.4a). For the same axial load, the cross-section is able to sustain a higher bending moment because stress in steel can be higher due to work-hardening.

The Figure 4.19 represents the evolution of catenary action in the slab strip. Contrary to the experimental curve, the FINELg model develop a compressive arch stage. In the experimental test, the slab strip was able to move expand outwards. It is not the case in the model because of the fixed end. However, after this stage, the membrane effects takes place. As can be seen, the magnitude of the catenary action activated are close to the ones measured during the experimental test. Note that the catenary action occurs sooner again because of the fixed end.

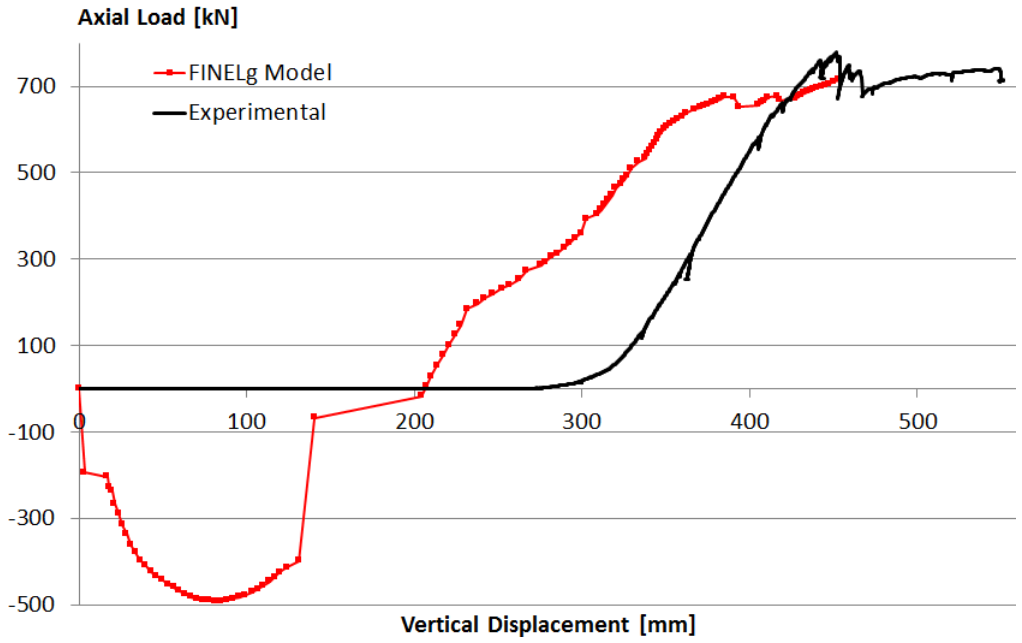

Figure 4.19: Catenary Action in Slab Strip in function of Central Span Deflection

Conclusion

Even if there are still some difference between the model and the experimental test, we were able to describe their origins. It was mainly due to too approximate modelization of the boundary condition. If we ignore this issue, we can conclude that an 2D analysis provide good results.

Thanks to this simulation, it has been demonstrated that the plane reinforced concrete beam elements defined in FINELg are able to represents the compressive membrane action and the membrane effects occurring in the slab strip.

4.3 Scenario of Column Loss

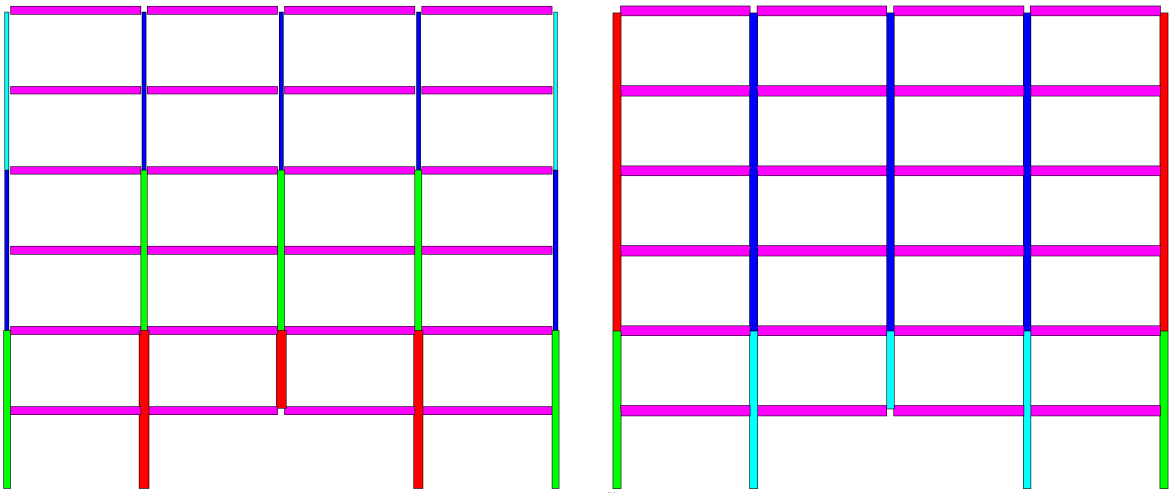

(a) Steel Frame (b) Reinforced Frame

Figure 4.20: Central Ground Floor Column Scenario

The scenario under investigation is the situation in which the central column of the ground floor has disappeared as shown on Figure 4.20. The origin of the loss is undefined but we assume that the column is statically removed. This assumption leads to lay aside the dynamical effects.

The position of the column to be suppressed is led by looking for symmetry, which facilitates the investigation. Furthermore, the ground floor is the most probabilistic floor that can be hit by vehicles. In addition, as the ground floor sustains all the others and is the most loaded, it is the most interesting case to discuss about structural integrity and robustness.

4.4 Simulation of Column Loss

Since two numerical techniques are available in FINELg to follow the behaviour of a structure (incremental loading or displacement), specific strategies were defined in order to simulate the column loss as accurately as possible.

4.4.1 Imposed Load Method

To reproduce the column failure, the first step is to solve the initial structure under the loading investigated. When all the loads are applied on the frame, internal efforts at the top of the column that will be removed are introduced in the model instead of the column itself as shown on Figure 4.21a. During the initial loading of the building, the internal reactions increase proportionally with the loading applied. Hence, these reactions have the same effect on the frame than the missing column during the loading.

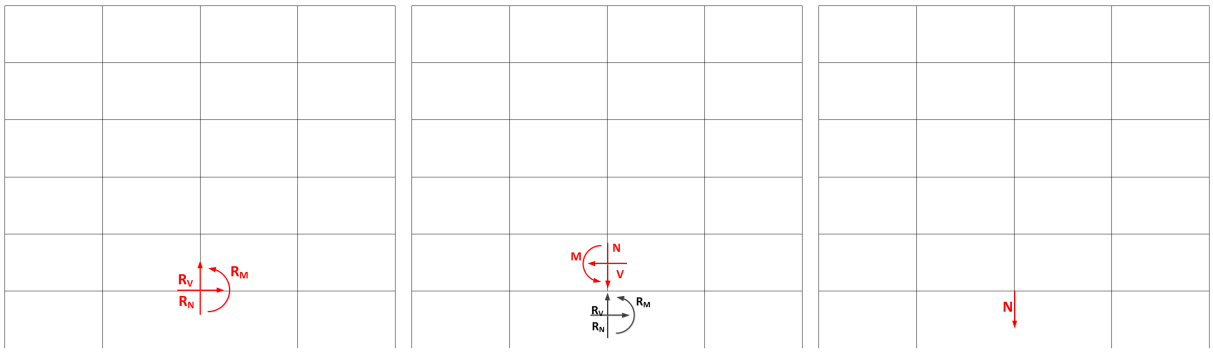

(a) Simulation of Column Presence (b) Simulation of Column Loss (c) Simulation for Further Investigation

Figure 4.21: Evolution of Column Loss by the Imposed Load Method

Then, we progressively counteract these reactions by increasing their respective opposite forces as represented on Figure 4.21b. This lead to slowly reduced the bearing capacity of the column until it completely disappears.

If the structure do not collapse when all the reactions are cancelled, the structure will be considered as being robust (with respect to the assumptions introduced) since the frame can still support the loading. Otherwise, it means that the frame failed to sustain the loading and therefore, and is qualified of non robust structure.

In the event the structure is robust, it is interesting to determine how much reserve in terms of resistance the frame has. In order to determine this reserve before collapse, we will continue to increase only the vertical load until collapse at the node corresponding to the missing column. This situation is depicted on Figure 4.21c.

4.4.2 Imposed Displacement Method

Simulating the column loss by an imposed displacement is an easier technique to implement. Practically, it consists of adding a vertical support instead of the column. Then imposing the vertical displacement of this support will simulate the column failure.

At the beginning of the simulation, the vertical reaction at the support will be a pushing up force since the support is bearing a part of the frame. As we move down the support, the load initially sustained by the column will take an alternative path, and therefore the pushing force will decrease. If we carry on the displacement, the pushing force will become zero and then will turn into a pulling force. When the pushing force is equal to zero, it means the frame no longer needs the support (i.e the column) to sustain the load. At this point, the structure is considered to be robust with respect to our hypothesis. For further investigations, we will keep going to move down the support, which will results in an increase of the pulling down force, in order to estimate the level of safety of the frame before collapse.

Moreover, instead of being interesting in the vertical force at the support, we will focus on its reaction. Focusing on the reaction means following the evolution of the compression force in the column above the support, which is perfectly equivalent. So as we move down the support, the compression in the upper column will decrease until reaching zero (if the frame is robust), and then switch to tension.

4.4.3 Limitations of Simulations

Imposed Load

The first limitation of this simulation method comes from the third graph of the Figure 4.7 in which we increase only vertical loading after the column loss. This approach is convenient but not very realistic. In a real building, the load will not increase punctually. Nevertheless, don't forget that the objective is to determine either or not the structure is robust according our hypothesis. This conclusion can be made before the introduction of the virtual vertical force.

The Figure 4.22 shows that the imposed load approach can perfectly simulate the presence of the column. Figure 4.22 represents the vertical displacement according the fraction of the loading acting on the frame. When fraction is $= 0,5$, half of the load is acting on the building. When the fraction reaches 1, 100% of the load is applied. When all the load is applied, there is vertical shortening of the column of $2,7$ mm. The black line depicts the vertical displacement with the column in place, while the red curve represents the vertical displacement with the implemented reaction simulating the column.

Readers can see that for a fraction ≤ 1, the vertical displacement in presence of the column completely matches the vertical displacement with the equivalent reactions implemented. Moreover, in both case the structure remains in the elastic field since the displacements are directly proportional to the loading.

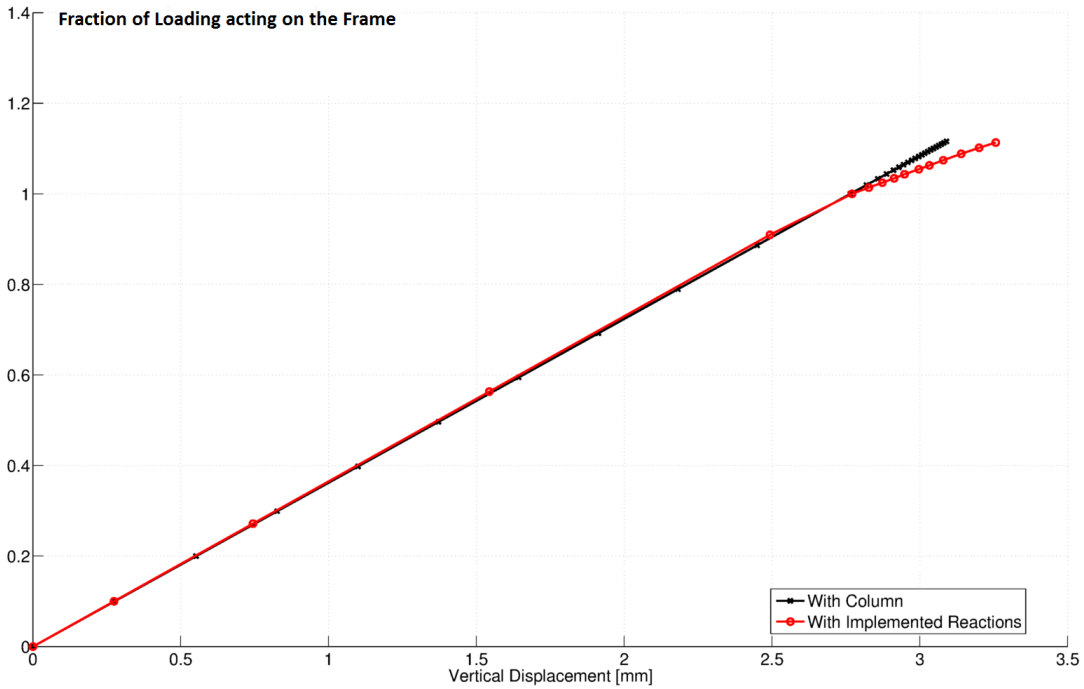

Figure 4.22: Vertical Displacement at Missing Column Location according to the Loading

Beyond fraction $= 1$, divergent behaviours occur. When the loading increases in presence of the column, the displacements remain elastic since the black curve is still a line. The column is still in place and has still some bearing capacity. The column is able to support more loads than designed. On the contrary, the red curve shows the apparition of non-linear effect. At fraction $= 1$, 100% of the reaction forces are counterbalanced. So if we carry on the loading, nothing

can counteract this supplementary loads since the reactions have been defined for this particular level of loading. Hence, the displacement starts to increase disproportionately because of the apparition of non linear effects. It is like the column suddenly disappears. There is no more bearing capacity when exceeding the reaction forces implemented.

Imposed Displacement

The limitations of the imposed displacement method lies in the introduction of the vertical support. Introducing the support will not allow the vertical displacement of the column during the loading. However, from the Figure 4.22 we learned that this error on the displacement is about $2 - 3$ mm.

The second limitation is more restrictive. As we are only imposing the vertical displacement during the collapse, it implies that there is no horizontal displacement of the frame. Otherwise, it would have become necessary to control the horizontal displacement during the failure too. This considerably increase the complexity of the model since the displacement at the top of the column needs to be known in advance to reproduce it in the model. It results that only perfectly symmetrical case can be accurately modelled with this method. In this research, it means that only the ALS combination will be investigated with the imposed displacement strategy because there is no horizontal load such as wind in this combination. Furthermore, only central columns can be investigated. Indeed, the centre of the frame is ensure not to move horizontally by symmetry.

Equivalence of the two Methods

As can be seen through the ALS combination example on Figure 4.23, the two load-displacement curve overlap each others until a displacement of 140 cm. For the imposed load, the ordinate axis represents the ratio between the reactions simulating the columns and the counteracting forces applies. For the imposed displacement, the ordinate axis is 1 minus the ratio between the forces at the support at the current step and the force at the support with the column in place, or well:

$$\text{Ratio}_{\text{dep}} = 1 - \frac{\text{Reaction}_{\text{step}}}{\text{Reaction}_{\text{init}}} \tag{4.13}$$

So the lower the reaction at the support is, the bigger is the ratio.

The automatic strategy were used for the imposed load method. During the simulation, the average incremental load was about $0,34$ % of the reactions and ranges from 6×10^{-5} % to $3,2$ %. On the other hand, the imposed displacement strategy in this simulation were made first with a constant incremental displacement of 1 cm until 80 cm and then of 1 mm because higher steps lead to numerical troubles.

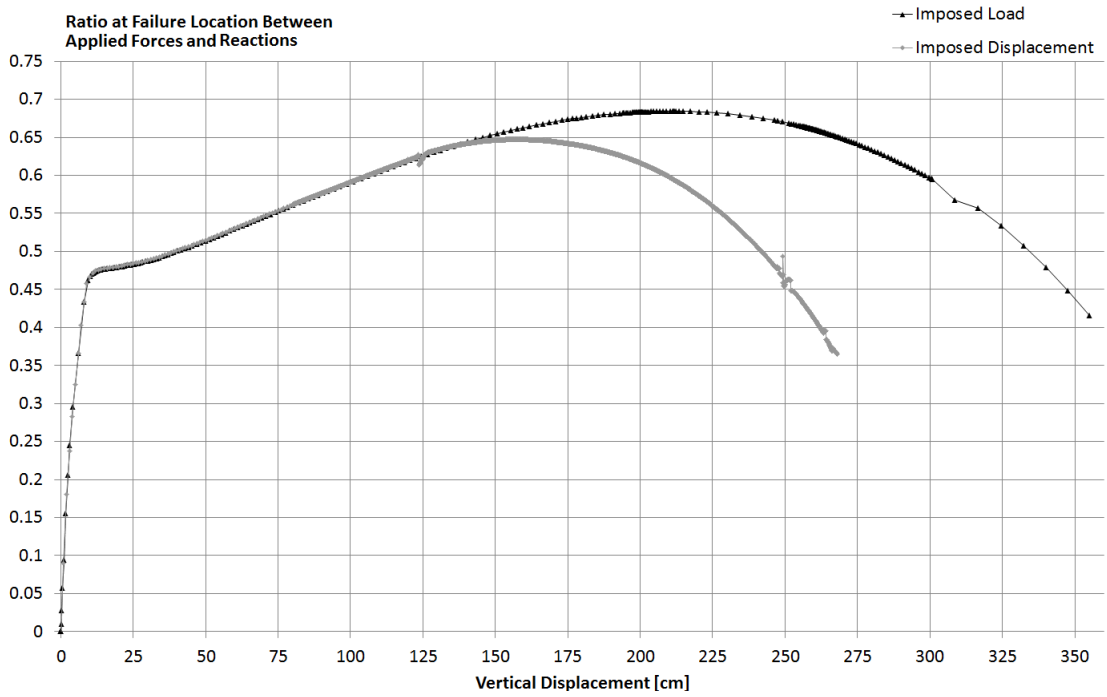

Figure 4.23: Comparison between Incremental Load and Incremental Displacement Results

Nevertheless, after a displacement of 140 cm, the two curves start to have a divergent behaviour. In the case of the imposed displacement, the structure collapse with a lower ratio of 5 %. Presently, the explanation is still unknown. From a conservative point of view, the imposed displacement strategy should be consider since the frame can sustain less load.

In addition, numerical troubles arises at the end of most simulations performed with the incremental displacement. As an example, Figure 4.24 shows the apparition of an erratic behaviour when displacement is greater than 120 mm. For others simulations, the computation breaks sharply around $120 - 140$ cm.

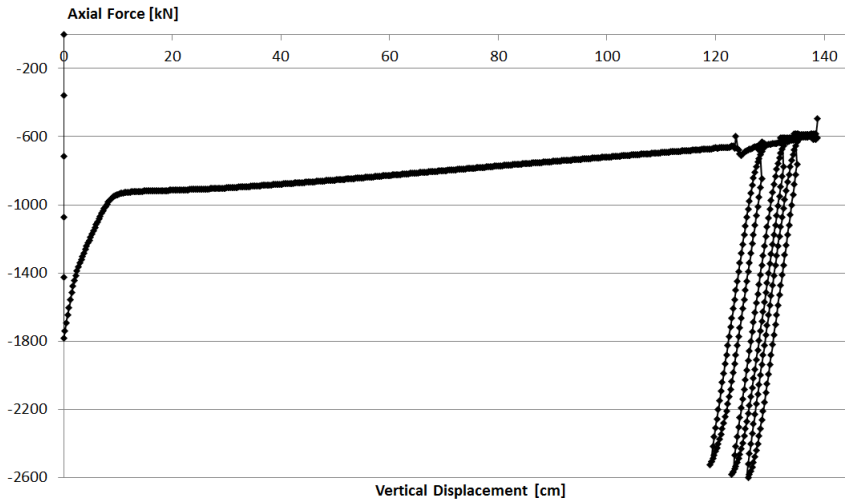

Figure 4.24: Example of Numerical Troubles occurring at High Displacement ($\Delta_{\text{dep}} = 2,5$ mm)

In consequence, the steel data will be limited to in the chapter 5 devoted to the results anal-

ysis. Only the results obtained before this irregular behaviour will be plotted and investigated.

However, the section hereafter try to provide an explanation to this phenomena by estimating the available rotation capacity of IPE 360 beam.

Member Ductility of Steel Beams

One of the explanation to the previous phenomena could be the available member ductility or the rotation ductility. In the best simulation (Figure 4.24), the IPE beam can rotate until 120 mrad. However, in reality the beams may not be able to provide so much ductility regarding the rotation capacity. Local buckling in the flange or the web could appear, impeding the development and the maintaining of the beam bearing capacity.

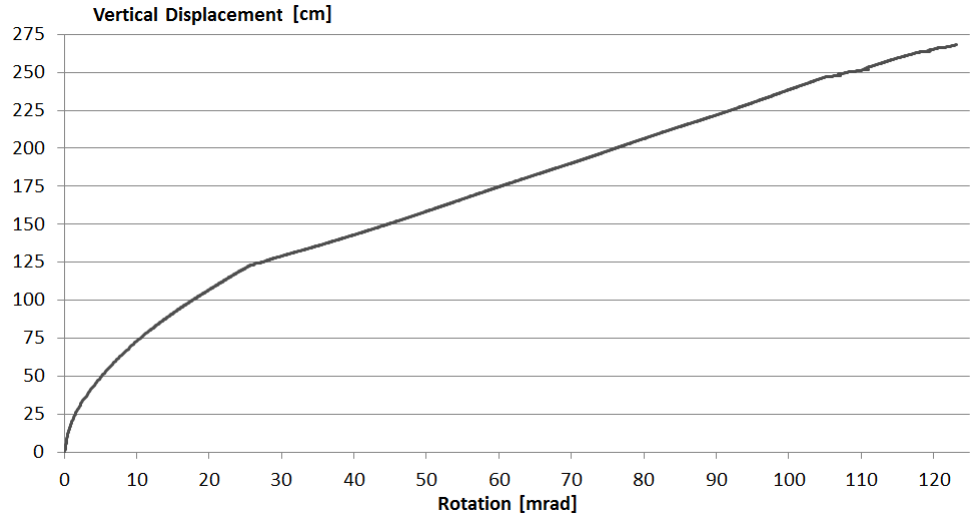

Figure 4.25: Rotation of IPE 360 beam according the Vertical Displacement of Support

The articles wrote by Anastasiadis and al. about the prediction of the available rotation capacity can estimate the rotation capacity of the IPE 360 profile in this situation. According to their work on Figure 4.26, the IPE 360 member is classified at maximum in medium ductility (MD) class and can develop moderate plastic rotations. ($f_y = 235$ MPa and $L = 12\text{ m} \geq 5\text{ m}$) [15][16]

Regarding the MD class definition, the rotation capacity parameter R, expressing the ratio between the plastic rotation at collapse and the elastic limit one, is comprised between $4,5 \leq R \leq 7,5$. Knowing the elastic deformation θ_y thanks to OSSA2D, it comes that the ultimate rotation ranges between : [15][16]

$$\theta_u = \theta_p + \theta_y = R\theta_y + \theta_y = \theta_y\,(1+R) = 3,49\,(\mathrm{R}+1)\ \text{mrad} \tag{4.14}$$

Hence the ultimate rotation varies between $19,2$ mrad and $29,7$ mrad. On Figure 4.25 it means that it is not necessary to consider the results at a higher displacement than 125 cm. It will confer more robustness that what could be really expected. Moreover, this displacement has the same magnitude order as the displacement at the beginning of the numerical troubles. Note on Figure 4.23 that both methods are still equal at this vertical displacement level.

Steel section	Buckling mode	L = 2000mm		L = 3000mm		L = 4000mm		L = 5000mm	
		S235	S355	S235	S355	S235	S355	S235	S355
IPE 300	IP	HD	HD	HD	MD	---	---	---	---
IPE 330	IP	HD	HD	HD	MD	HD	MD	---	---
IPE 360	IP	HD	HD	HD	HD	HD	MD	MD	LD
IPE 400	IP	HD	HD	HD	HD	HD	MD	MD	LD
IPE 450	IP	---	---	HD	HD	HD	MD	MD	MD
IPE 500	IP	---	---	HD	HD	HD	MD	MD	MD
IPE 550	IP	---	---	---	---	HD	HD	HD	MD
IPE 600	IP	---	---	---	---	---	---	HD	MD

IP – In plane post elastic buckling mechanism obtained with measures to increase the torsional rigidity of nodes.
– – Sizing of the member would be other than ductility limit state. For instance serviceability limit state would be the predominant criteria for member sizing.

Figure 4.26: Member Classification of IPE 360[16]

4.5 Loading Combinations Investigated

To discuss and compare robustness capacity of both structures, three load combinations will be investigated. The first loading studied is the ALS combination. This is the recommended loading by the Eurocodes. The second load combination is the ULS combination. This will provide information about the frame bearing capacity under a heavy loading.

Finally, the last combination we will focus on is a combination the we called *Robust Limit State* (RLS). It is the combination in which the building starts to collapse exactly for this particular loading. In this situation, there is no reserve in this combination. This is the maximal loading that the frame can support right before the collapse. It is expressed as a percentage of the ULS combination.

Contrary to the design situation where variable loads could act one span in two, this scenario only considers spans equally loaded. This assumptions is made because it simplifies the study and because it is the only case discuss in the Eurocodes 1-7 focusing on accidental actions.

Accidental Limit State

When focusing on infrequent events, Eurocodes recommends to employ ALS (Accidental Limit State) combination in order to depict a realistic situation.[1] Contrary to a classical design on which wind, snow and crowd can simultaneously act, the probability of encountering a column loss while the building is highly stressed is very low. This low probability allows to reduce the combination factors. Therefore, the effect of design loads acting on this frame is expressed by the following equation:

$$E_d = \sum_i G_{k,i} + \Psi_{1,1} Q_{k,1} + \sum_{i>1} \Psi_{2,i} Q_{k,i} \tag{4.15}$$

$$= \sum_i G_{k,i} + \Psi_{1,1} Q_{k,1} \tag{4.16}$$

This equation means that permanent loads G_i are weighted with an unitary factor. The main variable load $Q_{k,1}$, i.e. the load capacity of 3 kN/m^2, is weighted with a coefficient $\Psi_{1,1} = 0,5$. Moreover, all $\Psi_{2,i} = 0$ in this case because the only others variable loads are wind and snow.

It results that the structure and the loading perfectly symmetrical for the ALS combination. Hence, with respect to the discussion made in section 4.4.3, it will be the combination investigated by the imposed displacement strategy.

Ultimate Limit State

Investigating on ULS combination is an interesting case for two reasons. First, it gives a upper bound for the loading that can acting on the building at the time of the failure. Indeed, the loading has still some probability to range between the ALS and ULS combinations. The other reason is the appearance of a non-symmetrical loading due to wind forces acting only on one side of the building.

As a recall and to compare with the ALS combination, the following equation describing the effect of ULS design loads is presented.

$$E_d = \sum_i \gamma_{G,i} G_{k,i} + \gamma_{Q,1} Q_{k,1} + \sum_{i>1} \gamma_{Q,i} \Psi_{0,i} Q_{k,i} \tag{4.17}$$

This combination will only be model by the imposed load strategy.

Robustness Limit State

Finally, a third load case called “Robustness Limit State” will be studied. This combination is defined as the lowest possible loads acting on the frame that still lead to the collapse of the frame. It is expressed as a percentage of the ULS combination through the coefficient γ_R.

$$E_d = \gamma_R \left(\sum_i \gamma_{G,i} G_{k,i} + \gamma_{Q,1} Q_{k,1} + \sum_{i>1} \gamma_{Q,i} \Psi_{0,i} Q_{k,i} \right) \tag{4.18}$$

This case will give information about the level of safety before collapse or, on the contrary, on the level of excess load acting on the frame compared to the ULS situation. Like the ULS combination, this combination will only be model by the imposed load strategy.

Chapter 5

Results Analysis

In this chapter, we will describe the scenario of column loss investigated. The aim is to determine the evolution of the structural integrity in the case of a missing structural element. First, we will explain the physical behaviour of both structures under column loss emphasizing the origin of their divergent response. After that, a parametric analysis including the major specifications modifiable by design offices will be discuss. Finally, a comparative analysis will be performed in order to confront the results obtained for both structures. Hence, appropriate mitigations could be established for future designs.

5.1 Steel Frame

This section is devoted to the steel frame investigation. The study of the column loss and the parametric analysis will provide interesting information about the steel structure behaviour and more particularly the indirectly affected part. This section will bring out the main characteristics ruling the steel frame structural behaviour.

5.1.1 Evolution of Column Loss

The situation describes in this section is the ALS combination because this symmetrical case is an easier case to understand the appearance of the membrane effects. This section only explains the process of the column loss and the activation of the catenary action. A deeper analysis will be made in the section 5.1.2 and 5.3 respectively dedicated to the parametric and the comparison analyses.

The column failure is computed in the software by gradually moving down the central support introduced to simulate the column presence. As we increase the vertical displacement, which means as the column is slowly failing, the central beams starts to form plastic hinges as depicted on Figure 5.1a.

The plastic hinges are first occurring at the outdoor extremity of the central beams. Afterwards, the inner end of the beams starts also to yield but not exactly at the extremity. The reason comes from a too low plastic moment of IPE 360 as evidenced by the Figure 5.20 and the complete explanation in section 5.1.2.

At a displacement of 50 cm, only the directly affected part (DAP) is subjected to yielding. As the column failure goes on, the indirectly affected part (IAP) starts to yield too. On Figure

5.1b, a displacement of 1 m formed plastic hinges at the bottom of the columns and inside the external beams of the first floor.

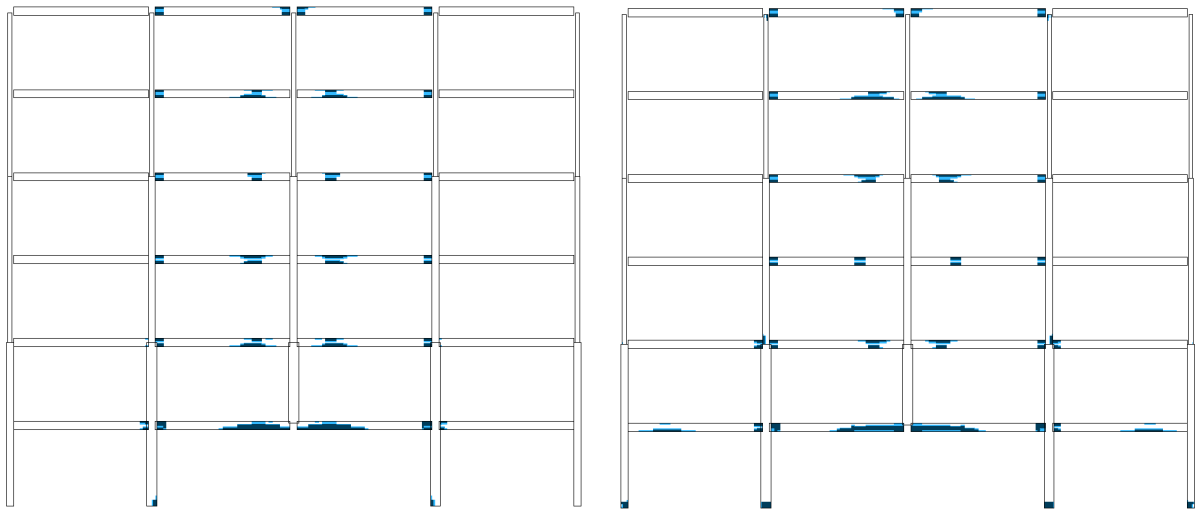

(a) Steel Yielding at Displacement of 50 cm

(b) Steel Yielding at Displacement of 100 cm

Figure 5.1: Progression of Plastic Hinges in Steel Frame

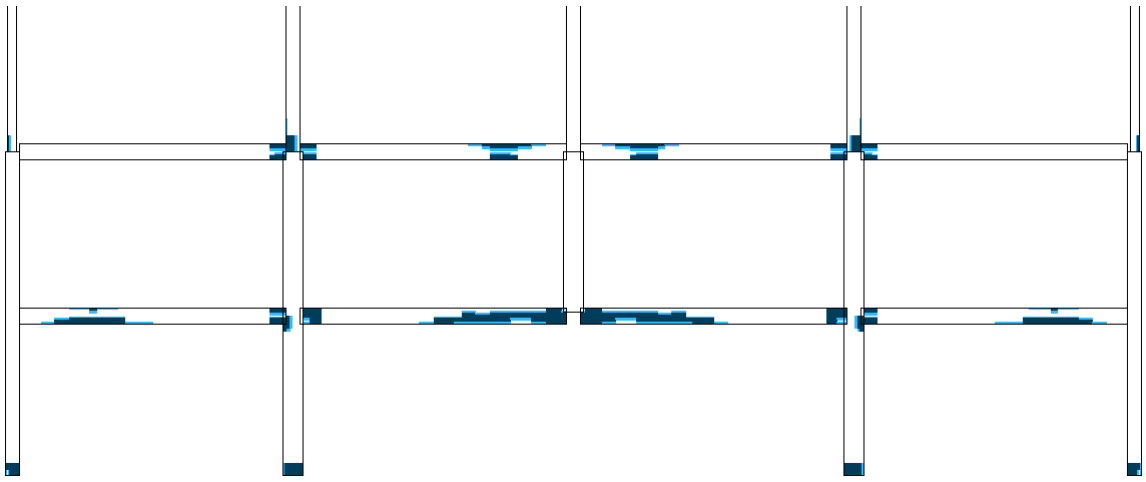

Figure 5.2: Steel Yielding at Displacement of 120 cm

The plastic hinges formation reflects the evolution of the collapse. As the central spans are falling down, a beam mechanism takes place in the middle of the frame. The central column having disappeared, the central frame can only be supported by the outer frames. Hence, the DAP is horizontally pulling on the IAP. The IAP is attracted into the inside of the frame, but the IAP is anchored. It results in a stress concentration in the foundations leading to the plastic hinges formation at this location. At the end, a panel mechanism begins to be established. On Figure 5.4, it can be seen that the IAP is moving inwardly because of the horizontal pulling force. However, on Figure 5.3b, the upper part of the IAP is almost not deformed. The upper part is only shifted inward because of the plastic mechanism occurring in the lower part.

On Figure 5.1 and Figure 5.2, the bottom part of the catenary beams is more yielded than the top part because of the bending moment. The bottom flange is submitted to tension due to

catenary action but also to bending moment due to the uniformly distributed load. While on the top flange, the tension due to membrane effects is diminished by the compression coming from to initial bending moment. Furthermore on Figure 5.2, the web of the central beams is more yielded than the flanges. Since the matter in a beam profile is concentrated in the flanges and the axial stress is uniformly distributed in the cross-section, the web has less steel to support traction. So it will yield sooner.

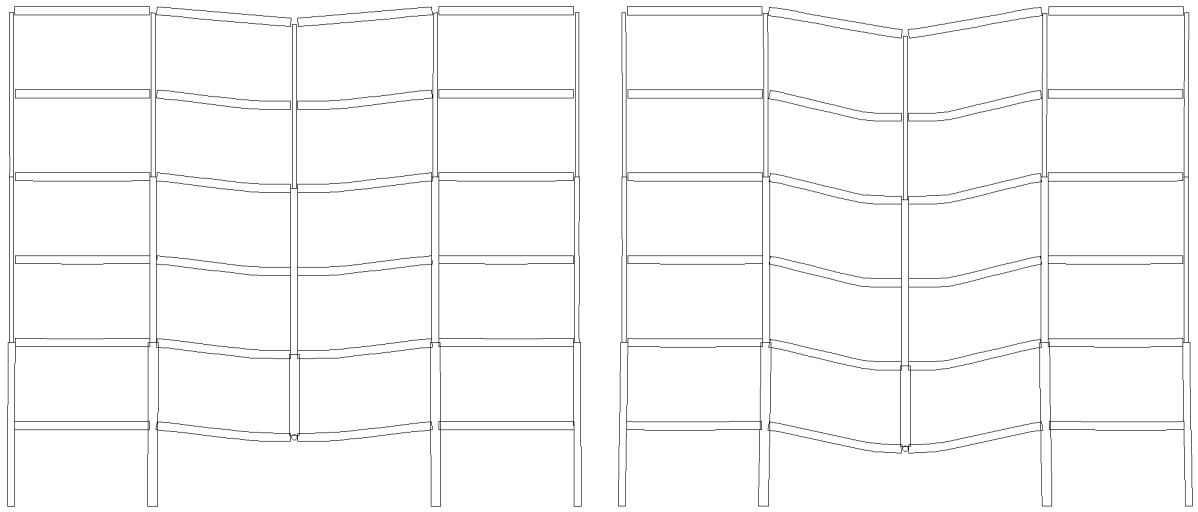

(a) Support Displacement of 50 cm (b) Support Displacement of 100 cm

Figure 5.3: Evolution of Displacement in Steel Frame

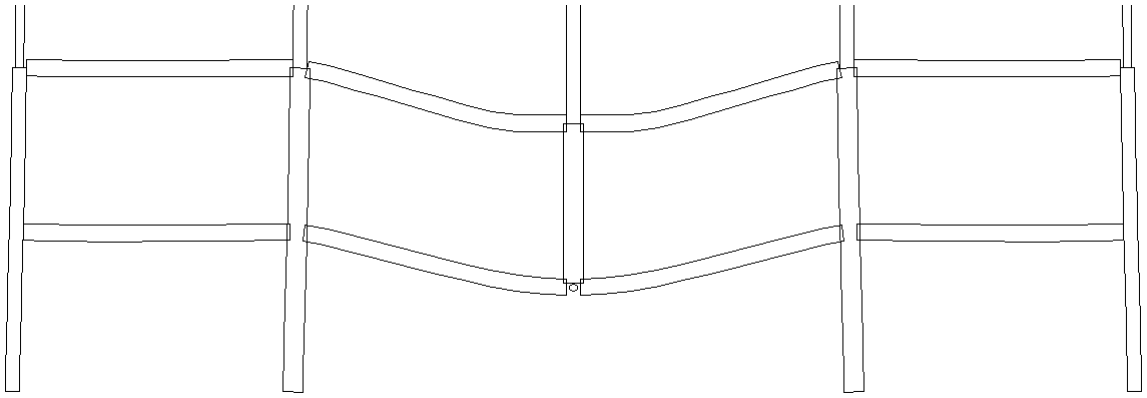

Figure 5.4: Steel Frame Deformation at Displacement of 120 cm

Another way to understand the activation of membrane effects is by studying the evolution of the normal force and the bending moment during the collapse of the frame. On Figure 5.5 representing the bending moment and the normal force, only half of the frame is drawn because of the symmetry of the case investigated. The bending moment is almost the same in all beams expected on the last floor. It is due to the thinner slab and the fact there is no crowd on the roof. The bending moment in the external columns is greater than in the internal ones because the eccentric loading results in flexural stresses. On normal force diagram, the internal columns are obviously more loaded than the external one.

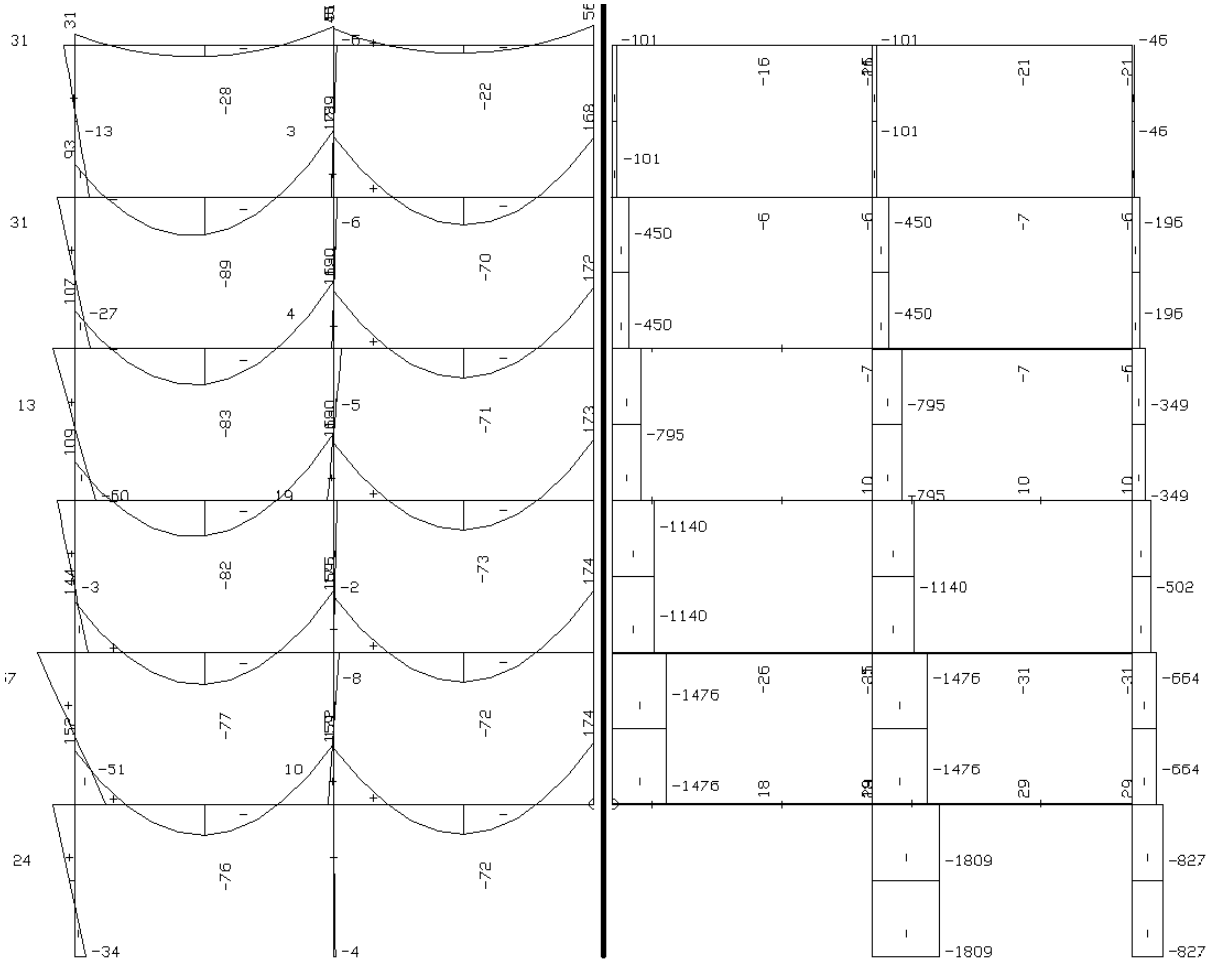

Figure 5.5: Bending Moment [kNm] (left) and Normal Force [kN] (right) with Column in place in Steel Frame

Right before the collapse, the normal force diagrams are completely different. On Figure 5.6, the compression in the central columns decreased while the compression inside the adjacent columns increased. The existence of compression in the central columns means that the structure is not robust since the support still needs to in place to sustain some loads. However, the compression decreasing proves all the interest of providing redundancy in the frame to promote alternative load paths. As an example, the compression rose from 1800 kN to 2400 kN in the lower column next to the removed column, equivalent to an increase of 33 % of the column compression. On the contrary, the external columns are too far away from the failure location to be really affected by the event. More surprising, the compression in this column even decreased by $\frac{-(749-827)}{827} = 9,4$ %. By being attracted inwardly, the lowest external column of the IAP tends to be lift up. This phenomenon does not take place in the columns above since the compression is slightly increased or not affected.

The right part of Figure 5.6 gives also information about the development of membrane effects. The axial force in beams was almost zero before the collapse since there were no horizontal loads acting on the frame. At the opposite, traction is higher than 500 kN in lowest central beam before the collapse. To sustain the central column failure, beams which are anchored in the IAP becomes in tension. This tension is transmitted to the adjacent beams in which the tension is higher than 200 kN. Therefore, a chain of tense beams is created.

The last floor is in compression because the indirectly affected parts rest on this beams. The frame does not collapse right after the panel mechanism. It provide additional strength and stiffness to the indirectly affected part.

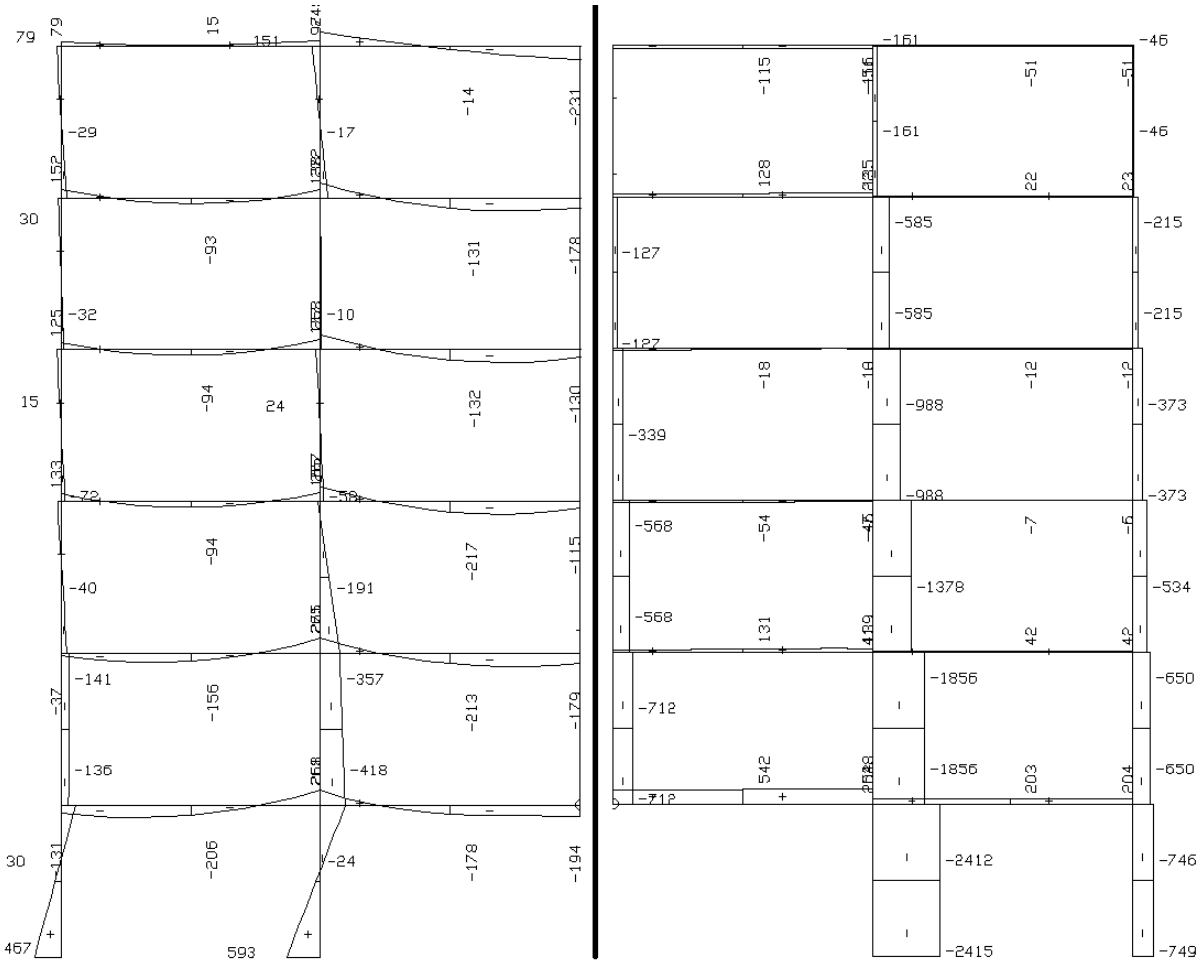

Figure 5.6: Bending Moment [kNm] (left) and Normal Force [kN] (right) at Displacement of 120 cm in Steel Frame

Let's finally discuss about the bending moment. The bending moment increased almost in all the beams comparing to the initial situation. In the catenary beams, the bending moment shape changed as long as the central support is moving down. This modification is explained by the Figure 5.7 above based on the work of L.N.N Hai and Clara Huvelle. Moreover, the bending moment in the central beam of the first floor starts to decrease because of M-N interaction. As normal stress is increasing in the beam due to catenary action, the area of steel allocated for flexural stress decreases. Whence a reduced bending moment. Otherwise, the bending moment would have a magnitude quite similar to the beam of the second and the third floors, in which there is lower tensile stress.

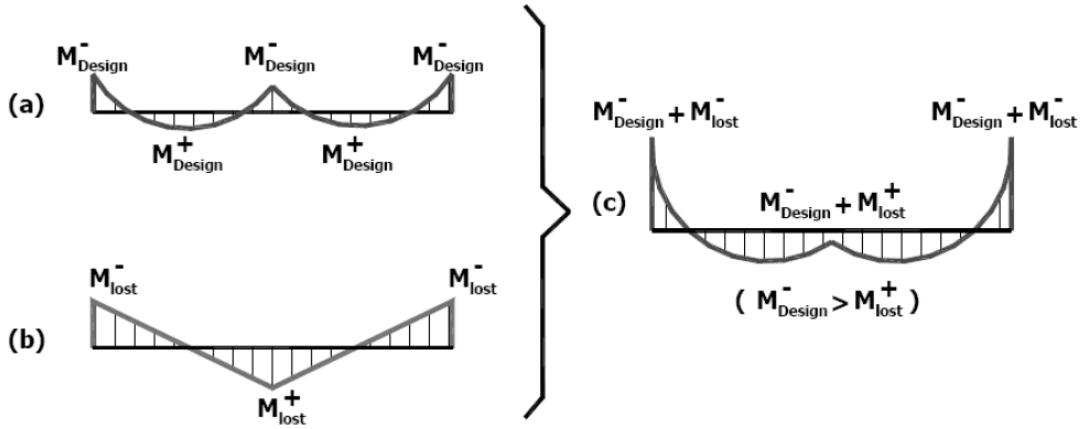

Figure 5.7: Addition of Bending Moment coming from the Initial Loading (a) and from the Column Loss (b) [18][19]

The bending moment evolution in the columns is also interesting to analyse. One can see on Figure 5.6 the bending moment reversal in the columns of the ground floor. Because the central beams are pulling the frame towards the inside, a horizontal force is applied at the top of the column. In her master's thesis dealing with the progressive plasticization of the part of the structure not directly affected by the exceptional event, Clara Huvelle explains this behaviour by comparing a frame under vertical dead load and a frame under a punctual horizontal load.

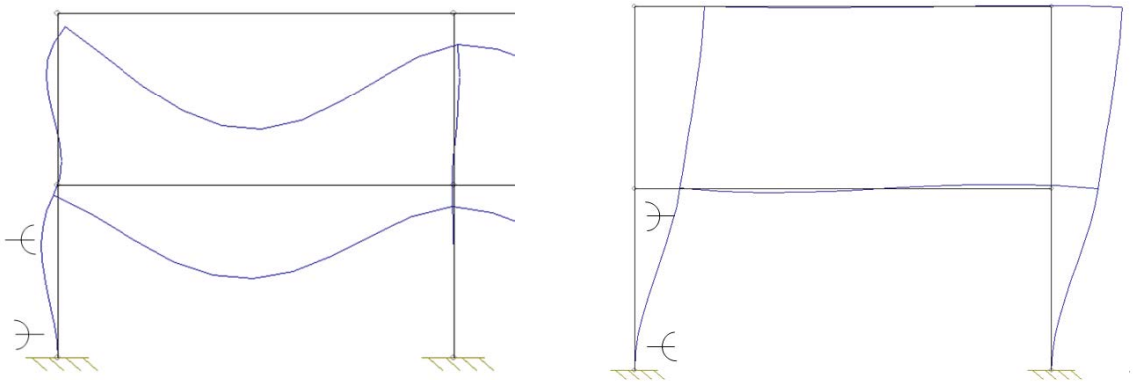

(a) Under Vertical Load

(b) Under Punctual Horizontal Load

Figure 5.8: Shape Deformation of the Frame under Vertical and Horizontal Loading [19]

5.1.2 Parametric Analysis

After apprehending the general behaviour of the steel under the accidental lost, it is gainful to determine what parameters can modify the building response during the column failure. This section will provide information about changes that can be made in the steel frame so that the structural integrity will be increase. More particularly, we will investigate the influence of the indirectly affected part, the steel grade, beams and columns profiles on the robustness of the steel frame.

Influence of Indirectly Affected Part Yielding

In this master's thesis work, Clara Huvelle described all the importance of the yielding of the indirectly affected part on the horizontal restrained. She investigated its integration in the analytical method currently developed by J.-F. Demonceau and L.L.N. Hai at the University of Liège.

In order to estimate the influence of the IAP yielding on the frame robustness, the idea is to consider the steel in the IAP as perfectly elastic. By doing so the external frame will never yielded, neither the column foundations. It will prevent the apparition of a panel mechanism in the IAP. To be consistent with the analytical model currently developed, the elastic IAP is defined as described on Figure 5.9.

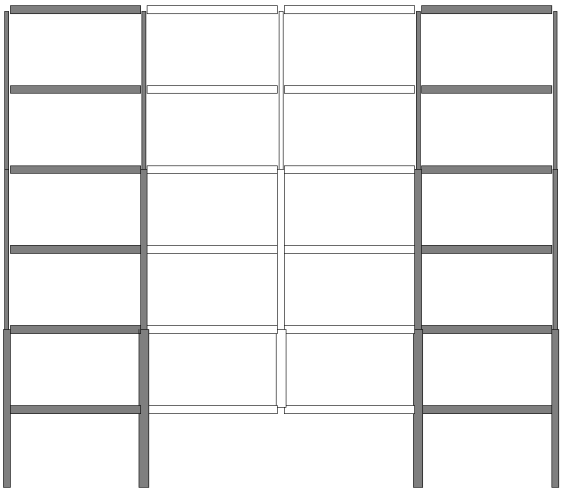

Figure 5.9: Elastic IAP Definition (Grey Elements)

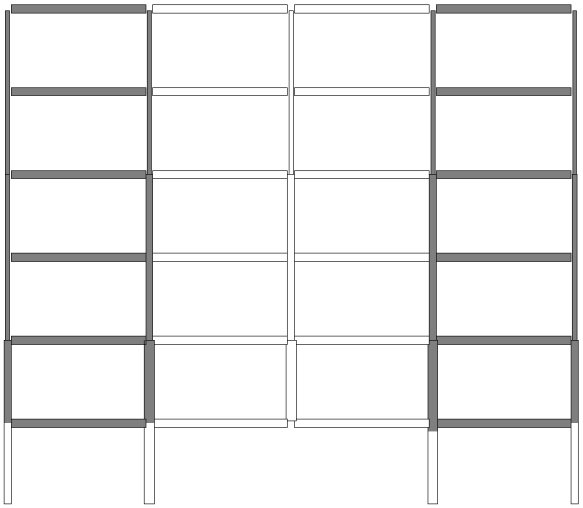

Figure 5.10: Elastic IAP with Ground Floor able to Yield

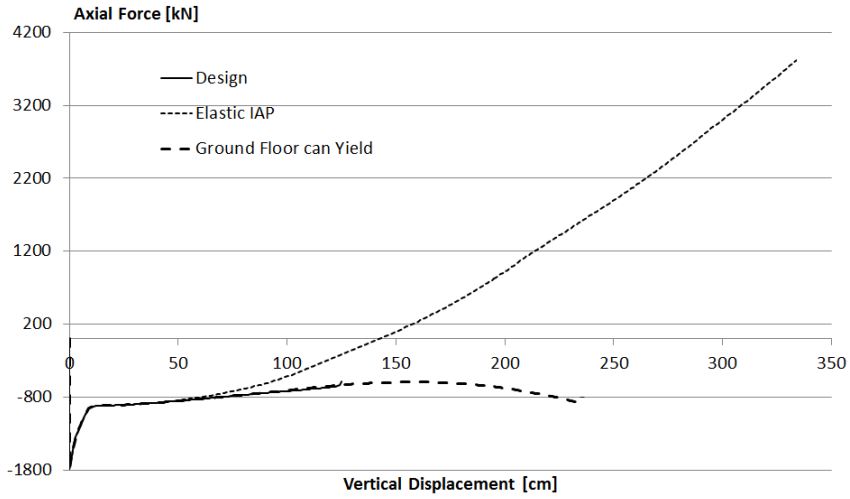

Figure 5.11: Full Development of Membrane Effects with Elastic IAP

As expected, the frame is know able to sustain the loading without the central column (with respect to our hypothesis) since the compression force in the central column falls down to zero

on Figure 5.12 at a displacement of 143 cm. Since there is no possibility to develop plastic hinges at the bottom of the columns, the plastic mechanism is no longer occurring. It results that the frame can sustain much more load by activating high membrane effects as evidenced by Figure **??**. To prove the critical effect of those plastic hinges on the robustness of the frame, let's focus on another simulation. If we now allow the ground floor to yield as described on Figure 5.10, the frame behaviour becomes again identical to the design case, in which every members of the frame can yielded.

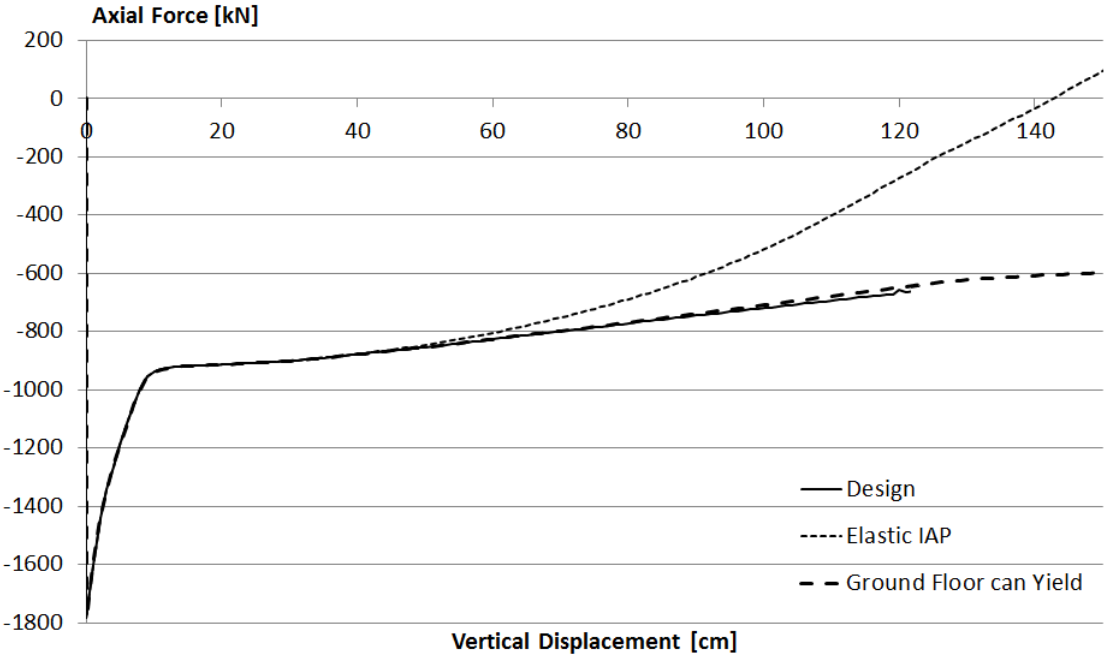

Figure 5.12: Influence of Indirectly Affected Part in Steel Frame

Influence of Bracing Systems

Instead of preventing the steel yielding in the IAP, we can restrain the horizontal displacement of the frame at the extremity of the directly affected part. Two simulations are run to measure the influence of this parameter. The first one includes a horizontal restraint on 1 side while the second simulation blocks the horizontal displacement of both sides.

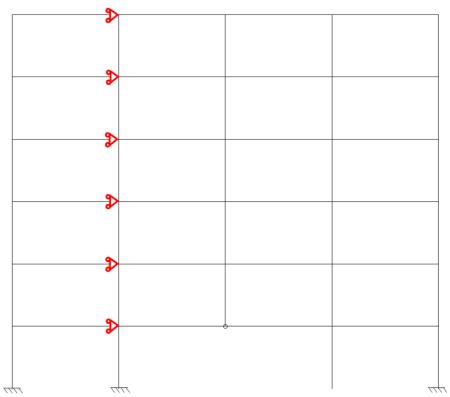

(a) Horizontal Displacement Restrained on One Side

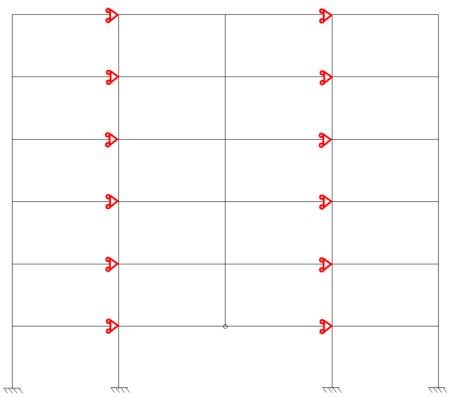

(b) Horizontal Displacement Restrained on Both Side

The results are presented on Figure 5.13. If the horizontal displacement is blocked only on 1 side, the collapse of the frame is led by the opposite side. Instead of having the two external frames moving inwardly, only the unrestrained side will be collapse towards the inside more significantly. In consequence, structural integrity is not improved. On the contrary, if both sides are horizontally maintained, the plastic mechanism leading to the collapse cannot occurs anymore. The beams being anchored at fixed nodes, they can develop full catenary action as shown on Figure 5.13.

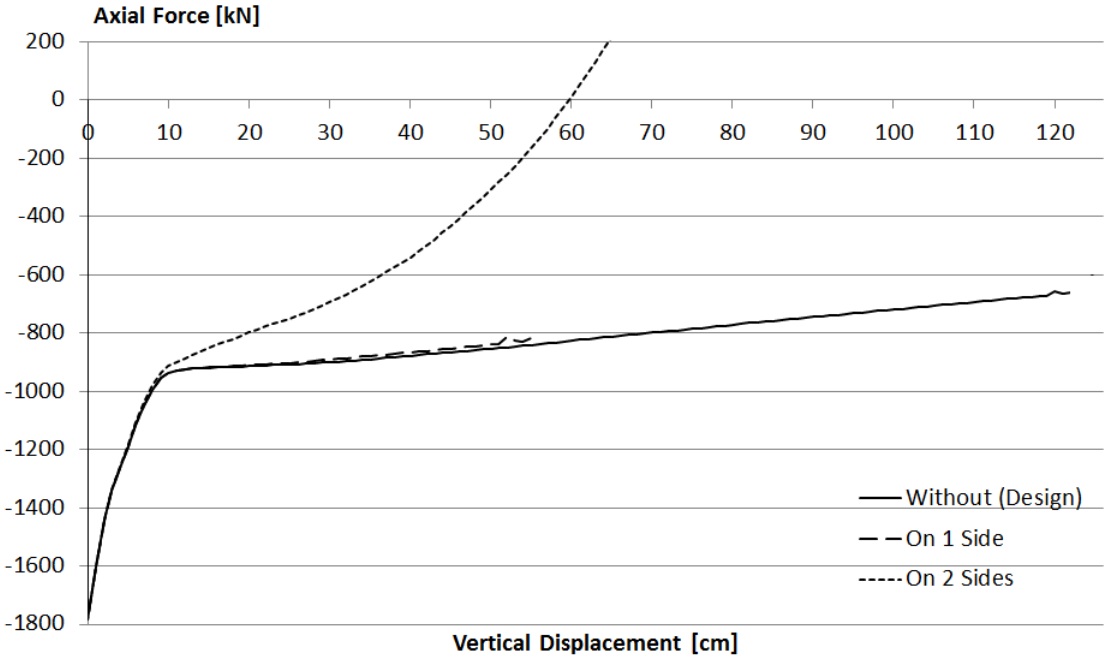

Figure 5.13: Normal Force Evolution according to Vertical Displacement of Central Support for Different Horizontal Restraints

The difference with the previous parameters comes from the displacement value for which the catenary action starts. In the case the frame is horizontally restrained, the beams can activate membrane effects, only after the plastic mechanism formation, a central deflection of only 7 cm because the fixed nodes provide immediately a infinitely rigid and undeformable anchorage.

At the opposite, keeping the IAP elastic still provide some flexibility to the external frames. The outer frames can move slightly towards the inside of the frame. However, at some point the horizontal force required to move the external frame inwardly will not be sufficient anymore to carry on the frame horizontal displacement. This restraint will provide a suitable anchorage for the central beams to activate membrane effects. In our particular case, the central columns have to fall from 40 cm to activate the catenary action. At this stage, the top of the ground columns has moved from $1,3$ cm (see Figure 5.45 in the comparison section).

Influence of Column Profile

In reality, it very difficult to realise a restraint so that there is no horizontal displacement. What can be done practically, by example, is to set up heavier columns. A heavier column profile will be stiffer, promoting therefore the development of catenary action. In the simulation, we will update the design by modifying the columns profile. On Figure 5.14, the legend contains 5

configuration summarised by the lighter profile set in place in the frame. As an example, the simulation HE 320 B means that all the columns in the initial design whose profiles are lower than HE 320 B have been changed to the latter. In the HE 400 B configuration, all the profiles are made of HE 400 B expected the three central columns (in red on Figure 3.4) because these profile are still heavier (HE 450 B). On the latest configuration HE 450 B, the entire frame is composed of HE 450 B columns.

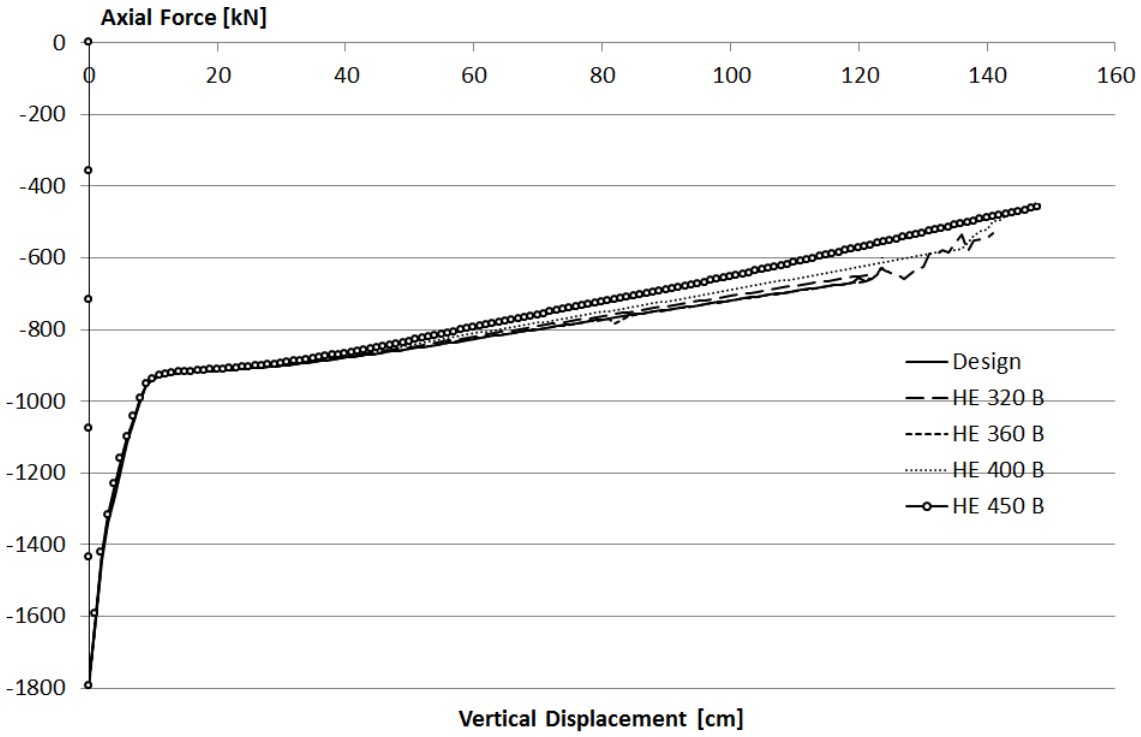

Figure 5.14: Normal Force Evolution according to Vertical Displacement of Central Support for Different Column Profiles

As can be seen on Figure 5.14 and in more detail on Figure 5.15, the results confirm the explanation here above. For an equivalent vertical displacement of the central span, the catenary action are greater, increasing the frame structural integrity and reducing the progressive collapse effect. At a displacement of 120 cm, the compression remaining in the initial design was -654 kN, while with the heaviest configuration it decreased to -572 kN. Knowing that the catenary phase started at the compression level of 925 kN, the benefit of heaviest columns on the last stage compared to the initial situation can be estimated to $30,2$ %. If we are interested in the total gain compared to the initial design, this benefit drops to $7,2$ %.

It is also interesting to note on bending moment diagrams on Figure 5.16 that the upper columns are more affected by the column loss. It justifies the interest in the establishment of an analytical model taking into account the coupling existing between the directly and indirectly affected parts. In the initial design depicted on Figure 5.6, only the first three floors were solicited. In addition, all the beams are subjected to some tension in this configuration (expected the last floor) since they can lean on stiffer columns.

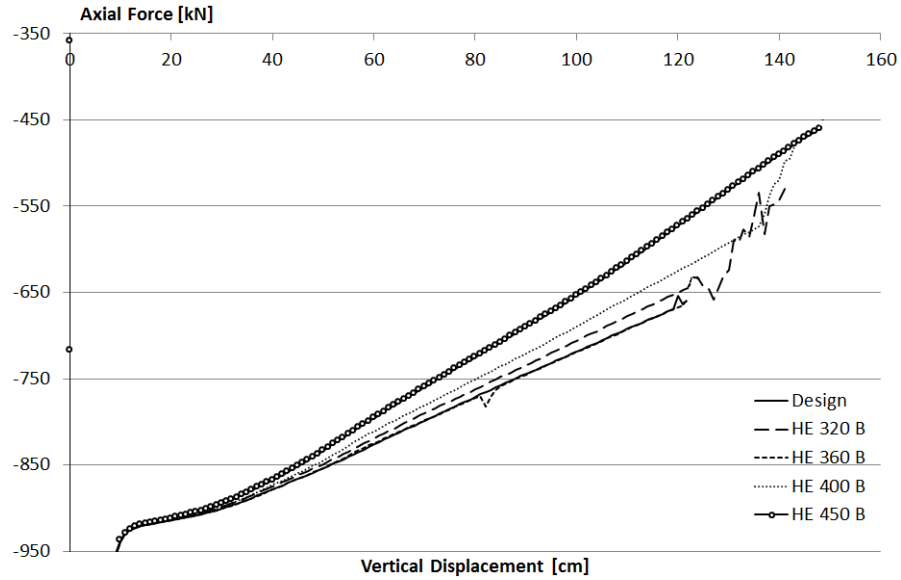

Figure 5.15: Membrane Effects Evolution according Vertical Displacement of Central Support for Column Profiles

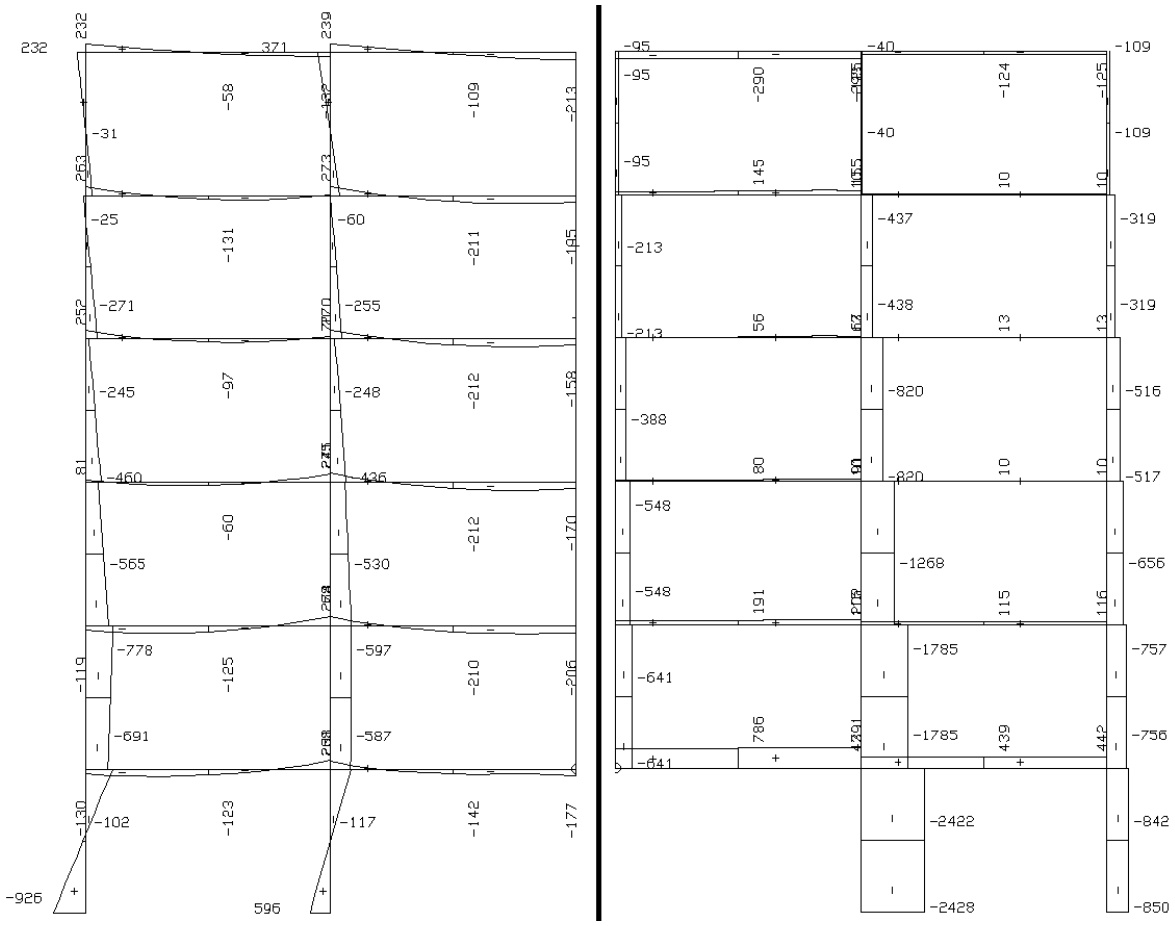

Figure 5.16: Bending Moment [kNm](left) and Normal Force [kN] (right) at Displacement of 120 cm in Steel Frame composed of HEB 450 Columns

Influence of Steel Grade

Modifying the yield strength affects the second part of the column loss, corresponding to the plastic mechanism formation in central frame. As can be seen on Figure 5.17, increasing the yielding limit enhances the frame structural integrity. With S235 mild steel, the beam mechanism is entirely achieved for a compression force in the central column of −940 kN. Only half of the compression in the central column is conveyed by the surrounding elements when the central part reaches the plastic mechanism. This means that the frame is not yet robust at this stage. Note that even by activating membrane effects, the frame is still not robust since the curve cannot reach an axial force of 0 kN.

On the contrary, S460 steel develops the complete plastic mechanism for a traction force of 316 kN. This means if the frame were made of S460 steel, it would have sustained the column loss without forming a complete plastic mechanism. Indeed, when the curve reached an axial force of 0 kN before the end of the second phase. In addition, the formation of the first plastic hinges can be detected. Around an axial force of −700 kN, the slope is changing.

If the frame were composed of S355 elements, it would have been robustness thanks to the development of catenary action. At a displacement of 120 cm, the curve intersect the abscissa axis.

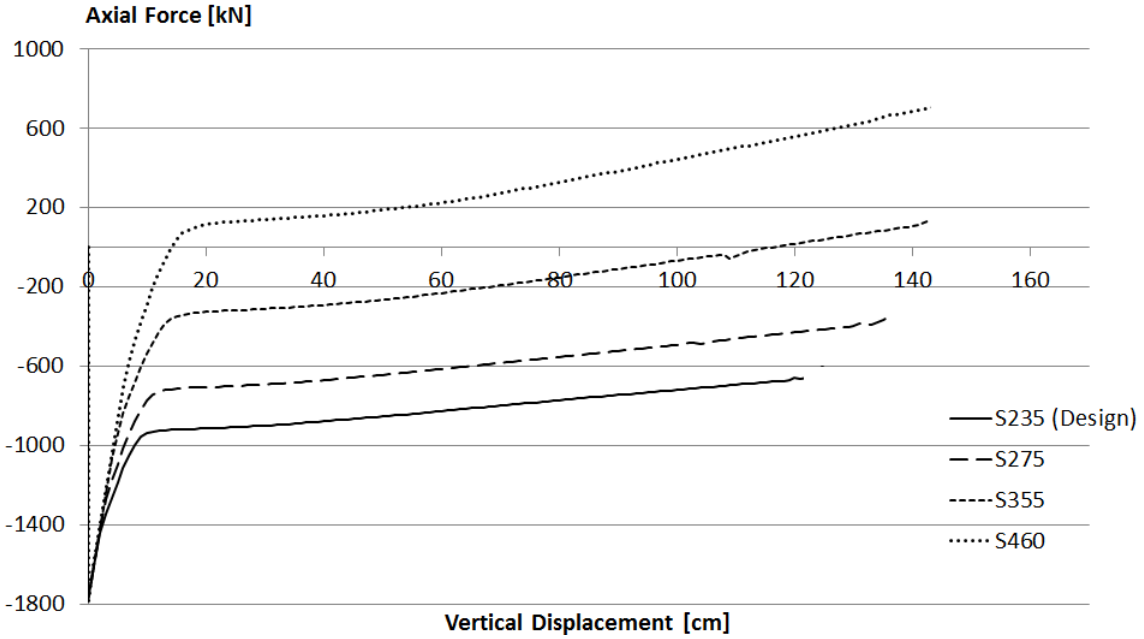

Figure 5.17: Normal Force Evolution according Vertical Displacement of Central Support for Different Steel Grade

Increasing the steel grade allows the frame central part of to transmit more loads to the surrounding part before the formation of the entire plastic mechanism. The central span deflection, when mechanism is formed, also raise with respect to the steel grade. The behaviour during the third phase, representing the activation of catenary action inside the frame, is also sensibly the same for all steel grade even if it can be noticed that the slope (i.e the rigidity) is slightly increased with the steel grade.

Influence of Beam Profile

Ordering heavier profiles will increase the frame bearing capacity and, in consequence it availability to the sustain the column lost. This conclusion is depicted on Figure 5.18. A greater beam profile will enable to transmit more load to the surrounding frame without yielding. By example, if beams were made of IPE 450, the frame could withstand the column loss thanks to the catenary action. Even more, frame made of IPE 500 profile can carry all the loading under the column loss without forming a plastic mechanism.

It can also be seen on Figure 5.18 that the displacement at the end of the second phase is nearly the same no matter what profile is. The second rigidity has also the same magnitude for each profile.

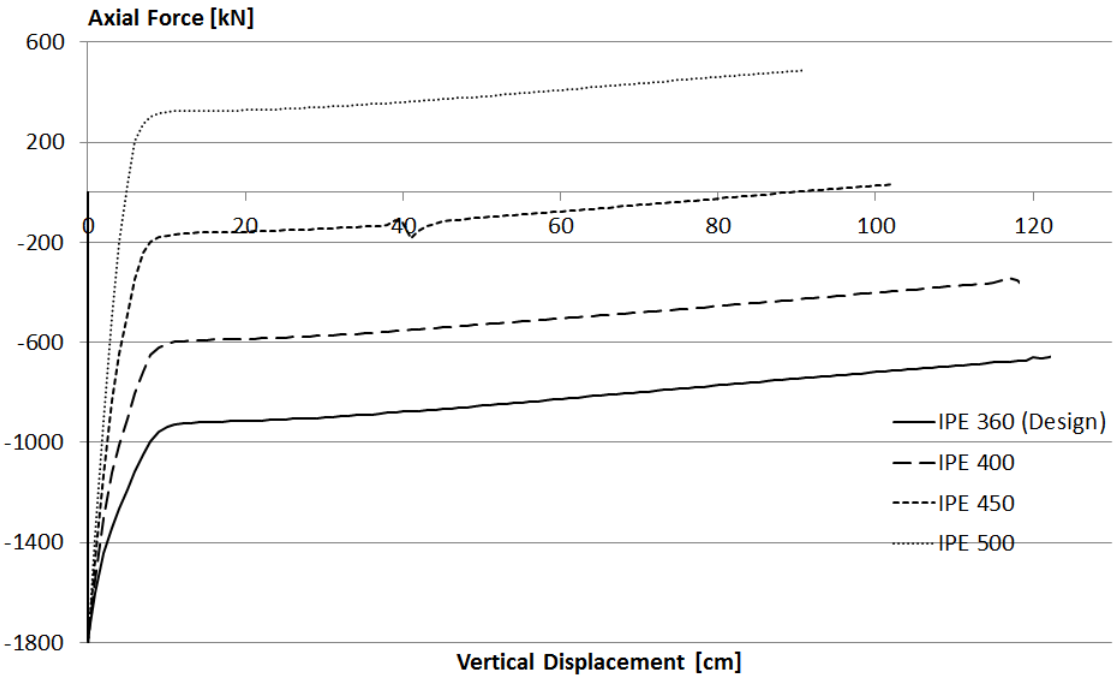

Figure 5.18: Normal Force Evolution according Vertical Displacement of Central Support for Different Beam Profiles

According Eurocodes EN 1991-1-7 recommendations for framed structures, the horizontal ties provided by the steel profile should be equal to :

$$T_i = 0,8\left(g_k + \Psi q_k\right) sL = 0,8\left((46,5 + 0,571) + 0,5 \cdot 18\right) 6 \cdot 6 = 1615 \text{ kN} \tag{5.1}$$

With profiles composed of S235 mild steel, the minimum reinforcement area $A_{s,min}$ should be equal to :

$$A_{s,min} = \frac{T_i}{f_{yd}} = \frac{1615 \times 10^3}{204} = 7917 \text{ mm}^2 \tag{5.2}$$

Compared to the design, it means that the cross-section area A_{ini} should be multiplied by :

$$\frac{A_{s,min}}{A_{s,ini}} = \frac{7917}{7270} = 1,08 \tag{5.3}$$

This means that the steel profile is almost sufficient to sustain the column loss according to Eurocodes (if the panel mechanism did not occur). However, Figure 5.12 and 5.13 prove that the reserve is large enough with IPE 360 beams. Eurocodes are very conservative in this case.

Changing the beam profile will also modify the localisation and the number of plastic hinges. As Ludivine Comeliau explained in this master's thesis, the number of hinges created during the plastic mechanism formation depends on the plastic moment M_{pl} of the beam, the beam length L and the uniformly distributed load p. A plastic mechanism composed of 3 hinges will be formed if the following expression is verified [11] :

$$p \leq 4\frac{M_{pl}}{L^2} = 4\frac{W_{pl}f_y}{L^2} = 4\frac{1019 \times 10^3 \cdot 235}{6000^2} = 26,6 \text{ kN/m} \tag{5.4}$$

This is not the case in this design since the uniformly distributed load applied on the beam is equal to $p = 46,5 + 9 + 0,571 = 56,1$ kN/m.

Increasing the beam profile will increase the plastic moment M_{pl}. With an IPE 500 beam, the uniformly distributed load p must be smaller than $57,3$ kN/m to form a plastic mechanism composed of three hinges. As can be seen Figure 5.20d, it is well the case.

On the other hand, we can remove the uniformly distributed load ($p = 0$ kN/m) to see if a three plastic hinges mechanism is recovered. As represented on Figure 5.19, a plastic mechanism composed of hinges at beam extremity is indeed created.

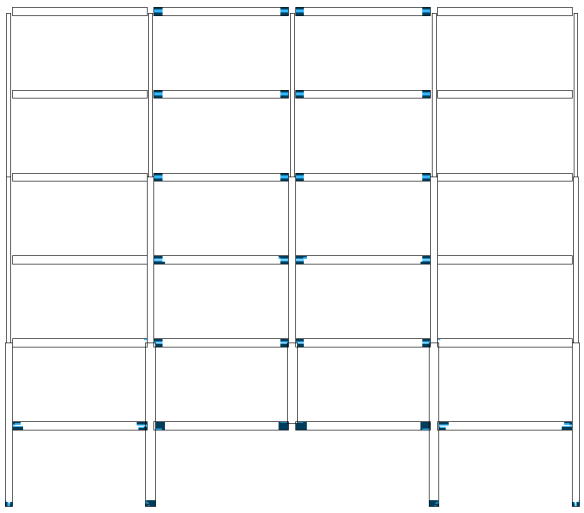

Figure 5.19: Plastic Hinges Localisation with IPE 360 but without Loading

Design a structure with two-way slabs reduces the beam profiled since the loading from the floor is supported by four spans instead of two. If one-way carrying slabs were considered in design, IPE 450 beams would have been necessary. Modifying thereby the plastic hinges localisation and the conclusion about the frame structural investigation.

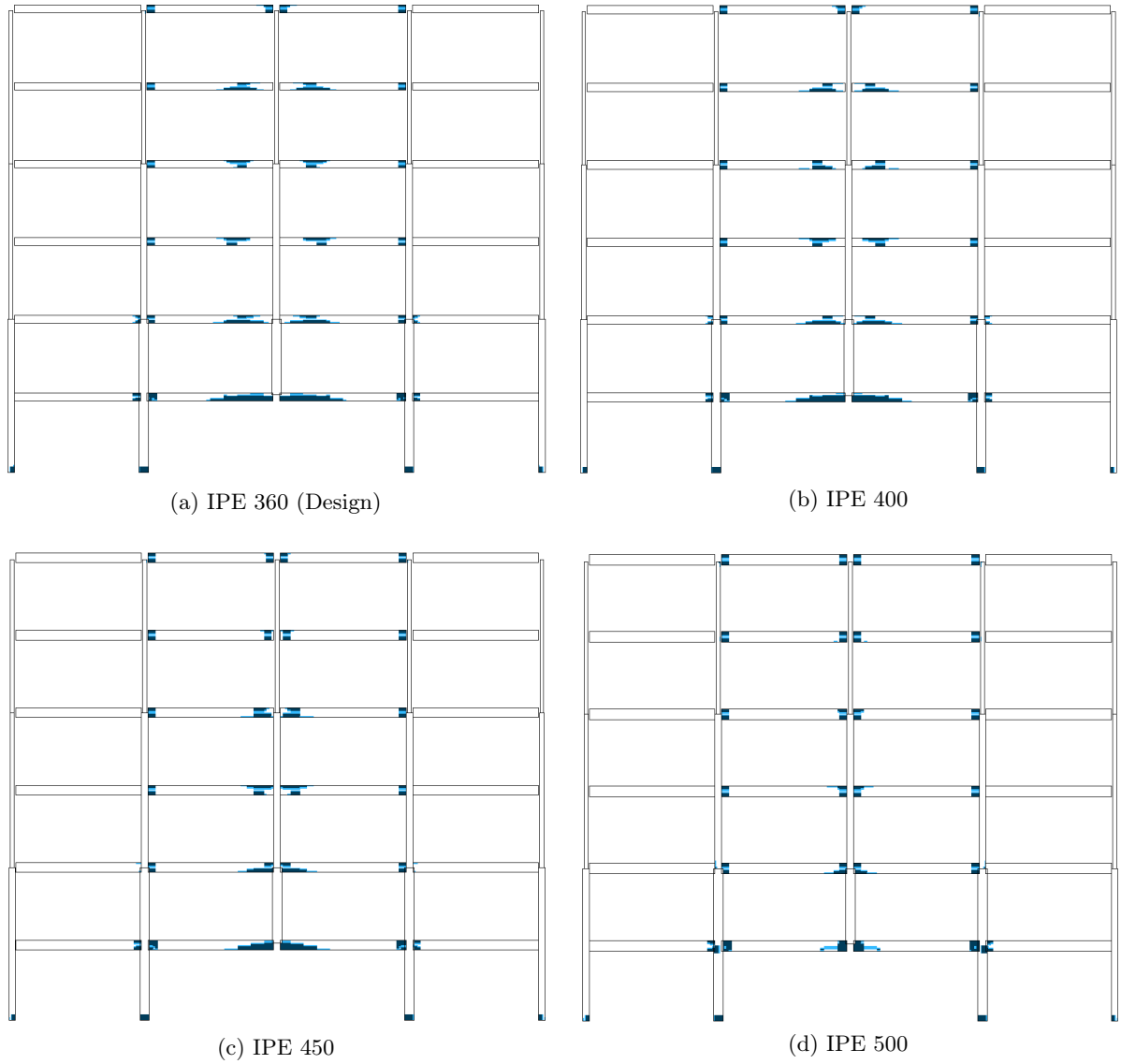

(a) IPE 360 (Design)

(b) IPE 400

(c) IPE 450

(d) IPE 500

Figure 5.20: Plastic Hinges Localization at Displacement of 80 cm according Beam Profile

5.1.3 Summarize Results

This section revealed the importance of beam extremities in the activation of catenary action. The more constrains the extremity is, the greater the membrane effect is. Nevertheless, the difficulty lies in design a suitable system able to restrain enough the beams.

As easier way to increase the general structural integrity of the frame is by using steel with higher limit strength. It has been shown it delays the plastic mechanism occurrence in the central frame and in the ground floor columns. It have been demonstrated that keeping the ground floor columns elastic confers to the frame the ability of activating high catenary effects. Again, all the difficulty is to find a realistic device able to prevent the formation of a plastic hinges in the ground columns.

Finally, another simple way to enhance the structural integrity of the frame is by setting up heavier beam profile. It allows the frame to withstand and transfer more loads before forming a

full plastic mechanism. But it does not use all the capacity of the element yet.

5.2 Reinforced Concrete Frame

After studying the behaviour of the steel frame under the column loss, we are interested in this section in the reinforced concrete frame response when one of its column failed. This section will ease the comparison between the two frames described in the following section 5.3 by understanding the respective structural response.

As for the steel frame investigation, this section is divided in three parts and is devoted to the ALS combination. The first part will talk about the evolution of the structural integrity during the column removal. Following this part, a parametric analysis will be made so that key parameters influencing the reinforced concrete robustness will be bring out. Finally, the last part of this section will summarize the interesting findings.

In order to avoid the repetition, the discussion will be more oriented to the reinforced concrete behaviour than on the explanation of general concept regarding catenary action and membrane effects. More detailed about this topic can be found in previous section 5.1.

5.2.1 Evolution of Column Loss

This part explains the establishment of membrane effects in the reinforced concrete according to the progression of vertical displacement of the central spans. To do so, we will compare three situations, each representing a key step during column failure. A good way to approach the behaviour of reinforced concrete is by interpreting the progression of the cracks within the structure and by following the evolution of the reinforcement rebars yielding.

The Figures 5.21a and 5.23a describes respectively the cracking and yielding states in the structures before the column failure. The Figures 5.21b and 5.23b represent the case before the development of significant membrane effects, but after the establishment of the plastic mechanism. Finally, Figures 5.20c and 5.22c depicts the situation right before the collapse.

On Figure 5.21a the cracks location is in accordance with the bending moment and the deformed shape. The beams are cracked at midspan on the bottom chord and on the top at connection with the columns. The external columns are cracked at the connection because of the rotation generated. The last floor is not cracked because of the lowest loading acting on the roof.

A vertical displacement of 40 cm as depicted on Figure 5.21b corresponds to a cracking situation before the development of membrane effects. The deflection at midspan increased, and so does the bending moment. So cracks in the bottom chord of concrete beams grew. However, cracks in the beam of the indirectly affected part seems not to be influenced yet. At this stage, the central beams are working as compressive arches which push on the IAP.

On the contrary, the top of the roof floor beams is cracked. Since the load on the roof is smaller, the bending moment due to the initial loading is lower too. So the negative bending moment M^{-}_{lost} on Figure 5.7 will lead to higher cracks in the upper part of the connection.

Furthermore, cracks in the external columns connections extended because of the higher rotation. At last, it can also be seen the apparition of cracks in the external foundation.

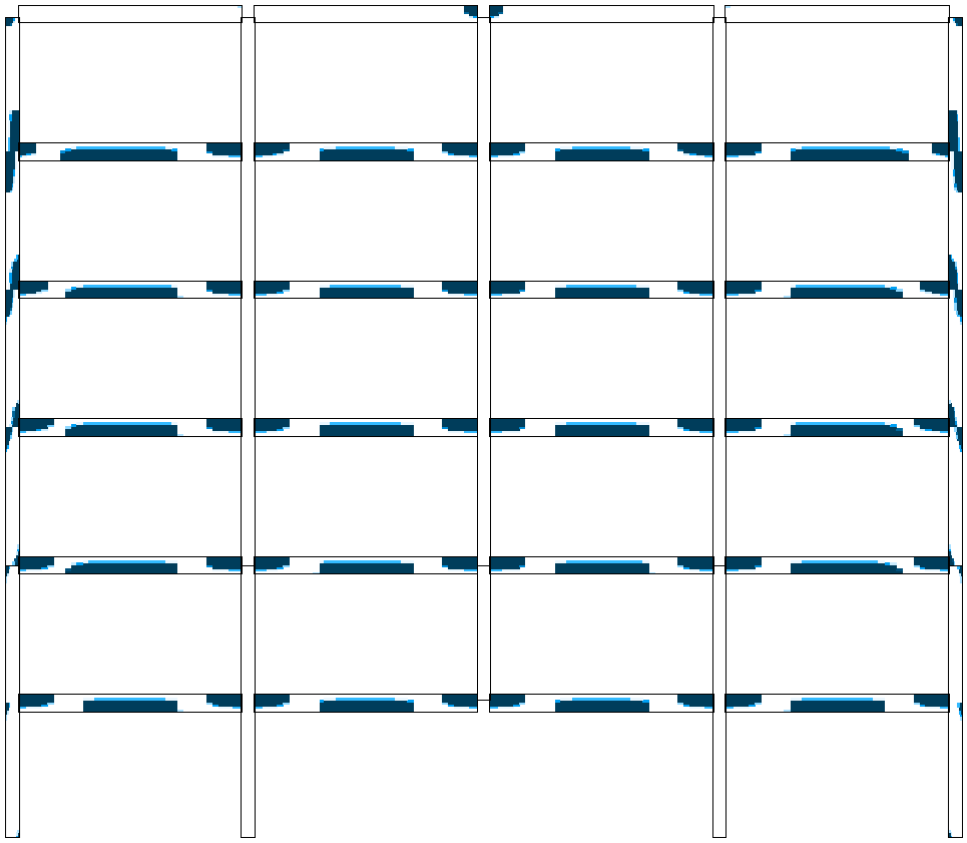

(a) Concrete Cracks with Central Column in place

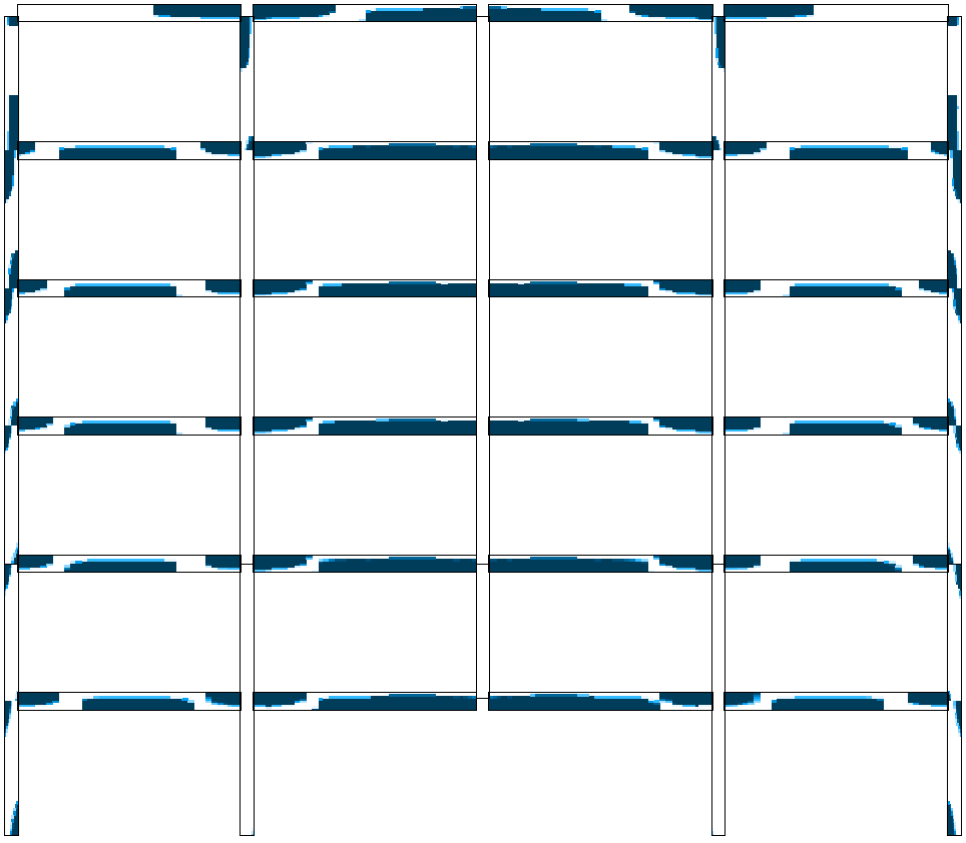

(b) Concrete Cracks at Displacement of 40 cm

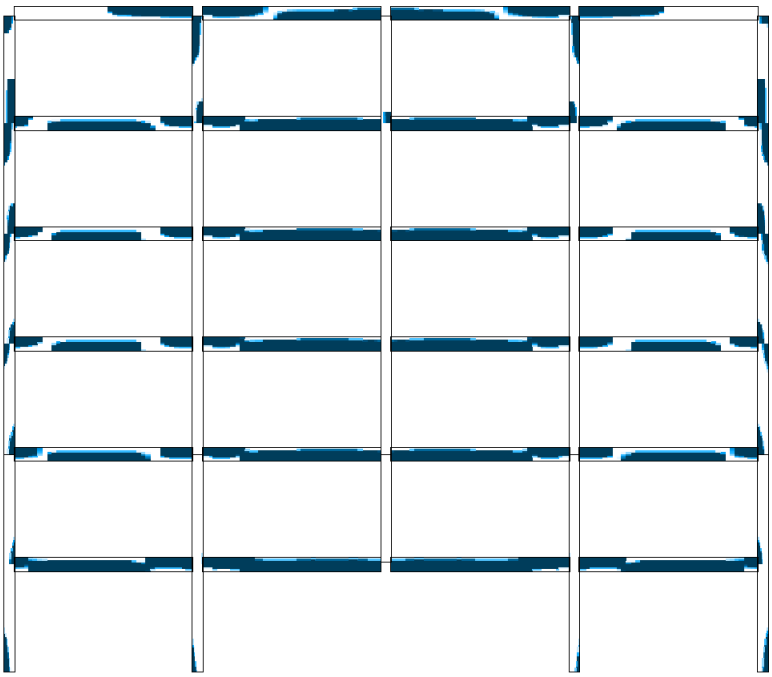

(c) Concrete Cracks at Displacement of 80 cm

Figure 5.20: Evolution of Cracks in Reinforced Concrete Frame

If we pursue the vertical displacement of the central support, reader can see on Figure 5.20c that the catenary beams are fully cracked because of the tension in the beams. Those cracks reveal the activation of membrane effect. A detailed representation of this cracking state is given on Figure 5.21. Moreover, cracks have now appeared in the all the frame foundations. Nevertheless, these cracks grew on the opposite side compared to the situation at a displacement of 40 cm. This effect is due to the bending moment reversal.

Note that FINElg is no more showing crack on the inner side of the column because the software plots the results at the current step. Even if in the computation FINElg takes into account the loading history, it does not represent the cracks on this side because the latter are subjected to compression stresses at this step. Actually, the inner cracks become tightened, but are still present.

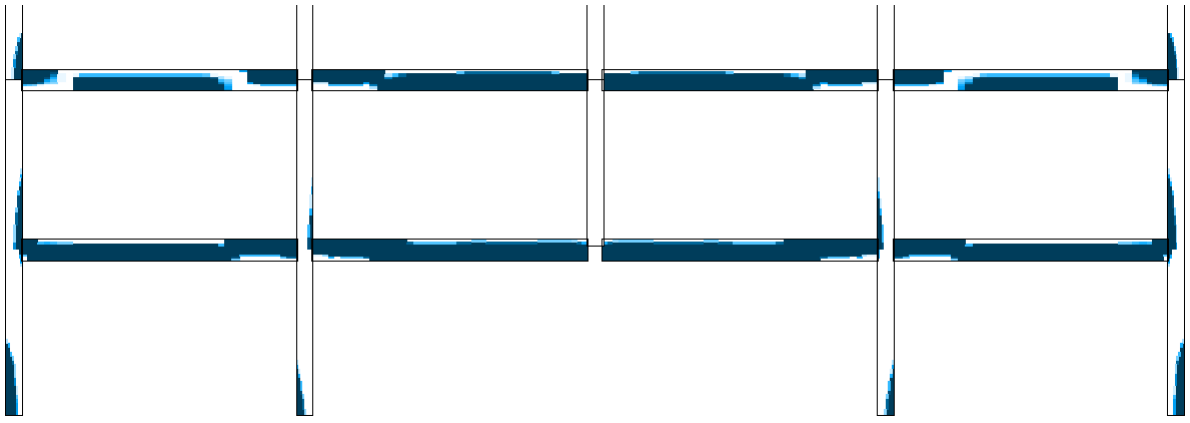

Figure 5.21: Concrete Cracks at Displacement of 90 cm

Since the concrete has nearly no resistance in tension, it means that only reinforcement rebars are working where the cross-section is crack. Thus it is interesting to study the evolution of the tension within the rebars.

The first situation in which the column is still in place is shown on Figure 5.23a. In accordance with the bending moment and the cracks, the rebars are tense at midspan at the bottom chord of the cross-section while there are in tension at the top of the cross-section around the columns connections.

As can be seen on the Figure 5.23b, both rebars layers at the outside extremity of the beam are yielded. However, they reaches a high level of stress for different reason. The top layer is yielded because of the tension in the rebars. On the contrary, the bottom layer is highly stress due to the compression. As can be seen on Figure 5.22 at a latter situation that the bottom corner of the beam is completely crushed.

We can also notice on Figure 5.23b, the bottom layer of reinforced concrete beams surrounding the central spans are highly stretched to sustain the loading. At the opposite, the top layer is not so solicited in tension due to the formation of a compressive arch within the beam.

At a displacement of 80 cm and 90 cm respectively plotted on Figure 5.22c and 5.22, the tension in the bottom reinforcement layer of central beams has increased, just as the tension at the top reinforcement layer at central beams extremity. Moreover, other interesting informations can be deduced from Figure 5.23 about the external beams of the first floor and about the foundations.

Regarding the first floor beams, it can be seen that the tension in the bottom reinforcement layer propagates outwardly towards the external columns as the vertical displacement of the supports increases. In fact, it indicates that the external beams are being hold by the external columns, promoting by the way the membrane effects. About the foundations, the rebars seems to be yielded in accordance with bending moment. Rebars on the inner side are in compression while the outer rebars are in tension.

In addition, it can be seen on Figure 5.22 that the additional compression due to the transmission of load coming from the central spans leads to high compression stress in reinforced concrete columns.

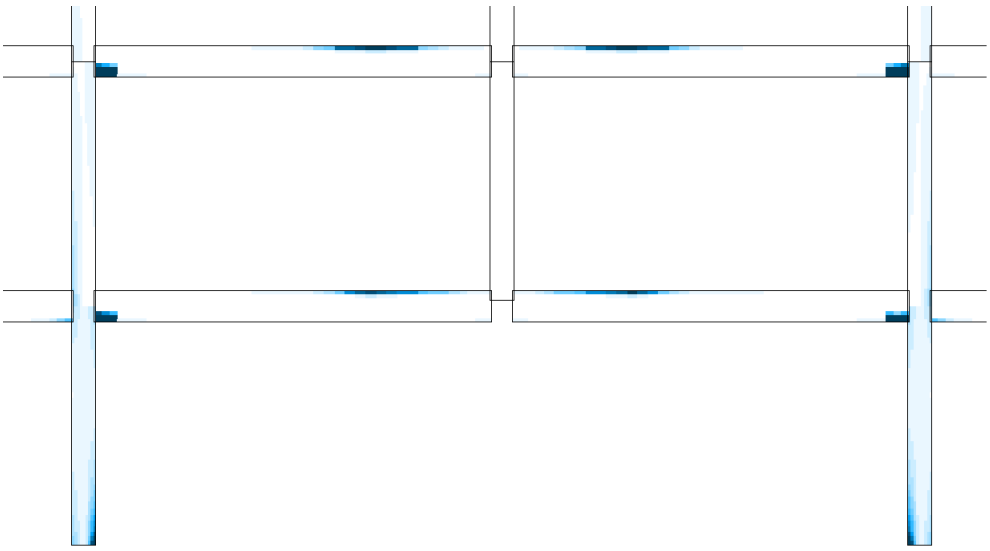

Figure 5.22: Concrete Crushing at Displacement of 90 cm

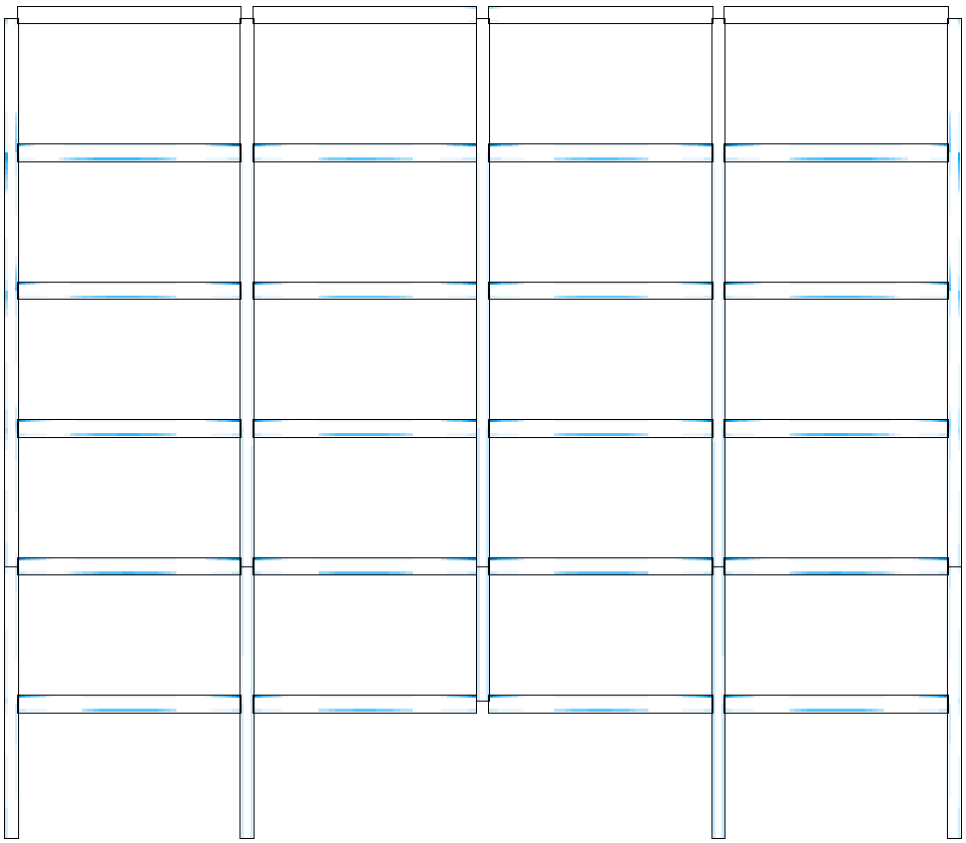

(a) Rebars Yielding with Central Column in place

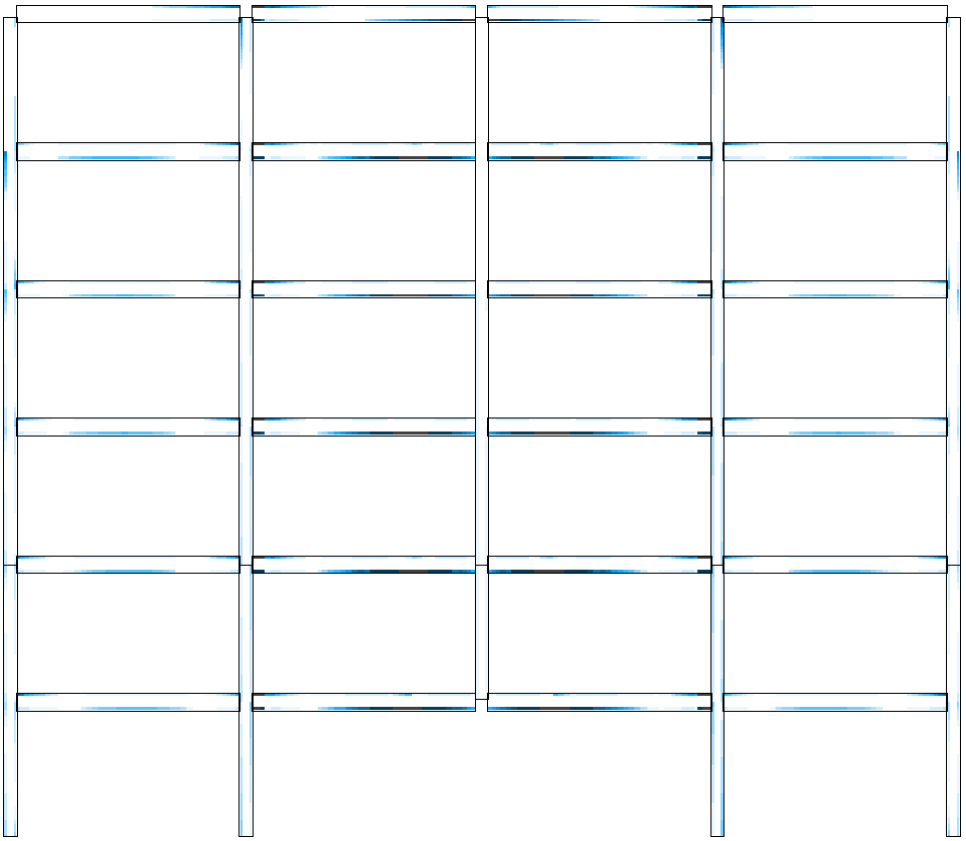

(b) Rebars Yielding at Displacement of 40 cm

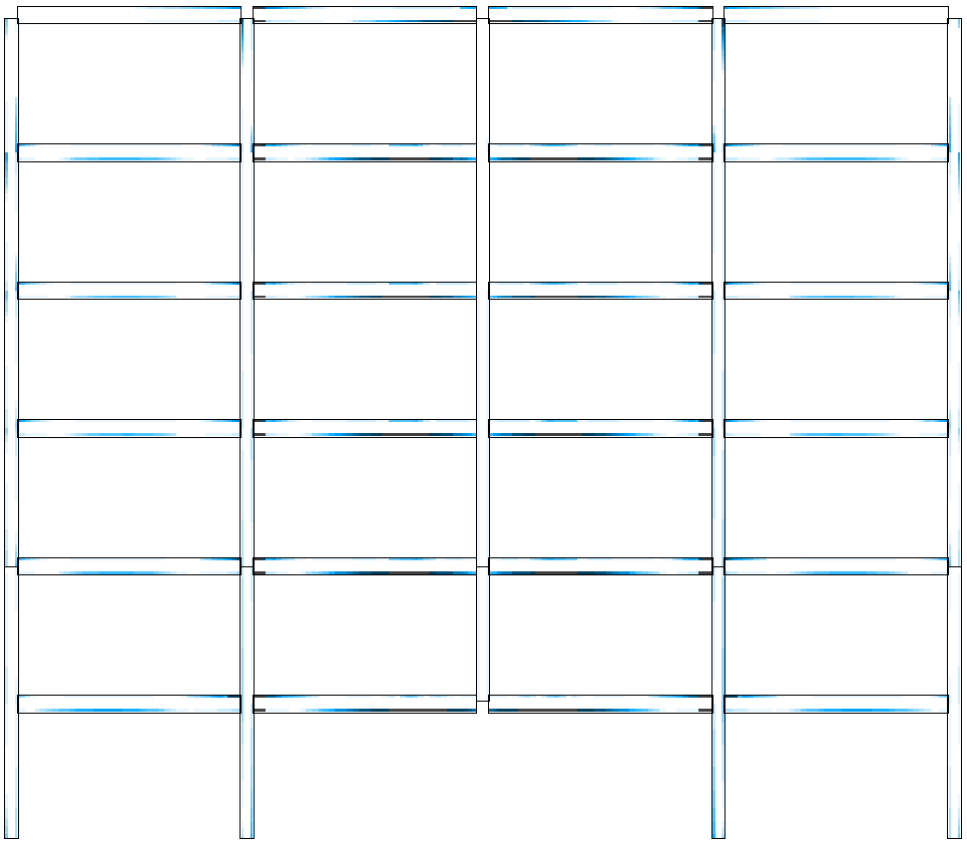

(c) Rebars Yielding at Displacement of 80 cm

Figure 5.22: Evolution of Rebars Yieling in Reinforced Concrete Frame

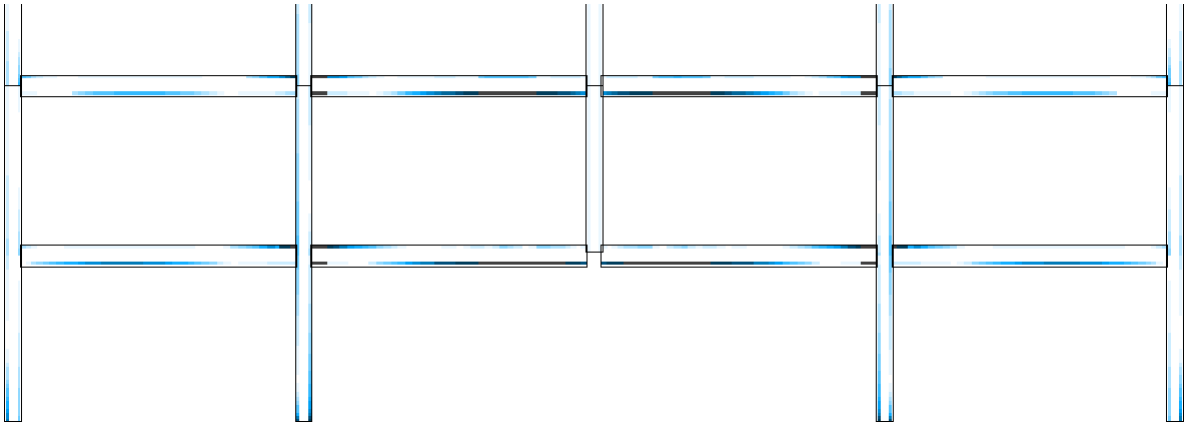

Figure 5.23: Rebars Yielding at Displacement of 90 cm

By investigating the internal forces diagrams, we will reach the same conclusion as the steel frame. The following Figure 5.24 and 5.25 are mainly given for informative purpose. Note that the slight variations are due to the self-weight. Through the bending moment diagram, it can be notice the moment reversal at the ground floor columns and the addition of bending moment of the column loss to the central bending moment.

Thanks to the normal force diagrams, we learn on Figure 5.25 that, at the last converged step,

the membrane effects is about 227 kN in the RC frame compared to 786 kN in the steel one. We can also notice the decompression in the lowest external columns. In addition, the displacement at the last step is about 90 cm. Since the compression is still present in the central beam, the reinforced concrete structure cannot sustain the column loss. Furthermore, the compression remaining is greater than in the steel frame which means that the reinforced concrete structure is less robust. More investigation are made in section 5.3 devoted to the structure comparison.

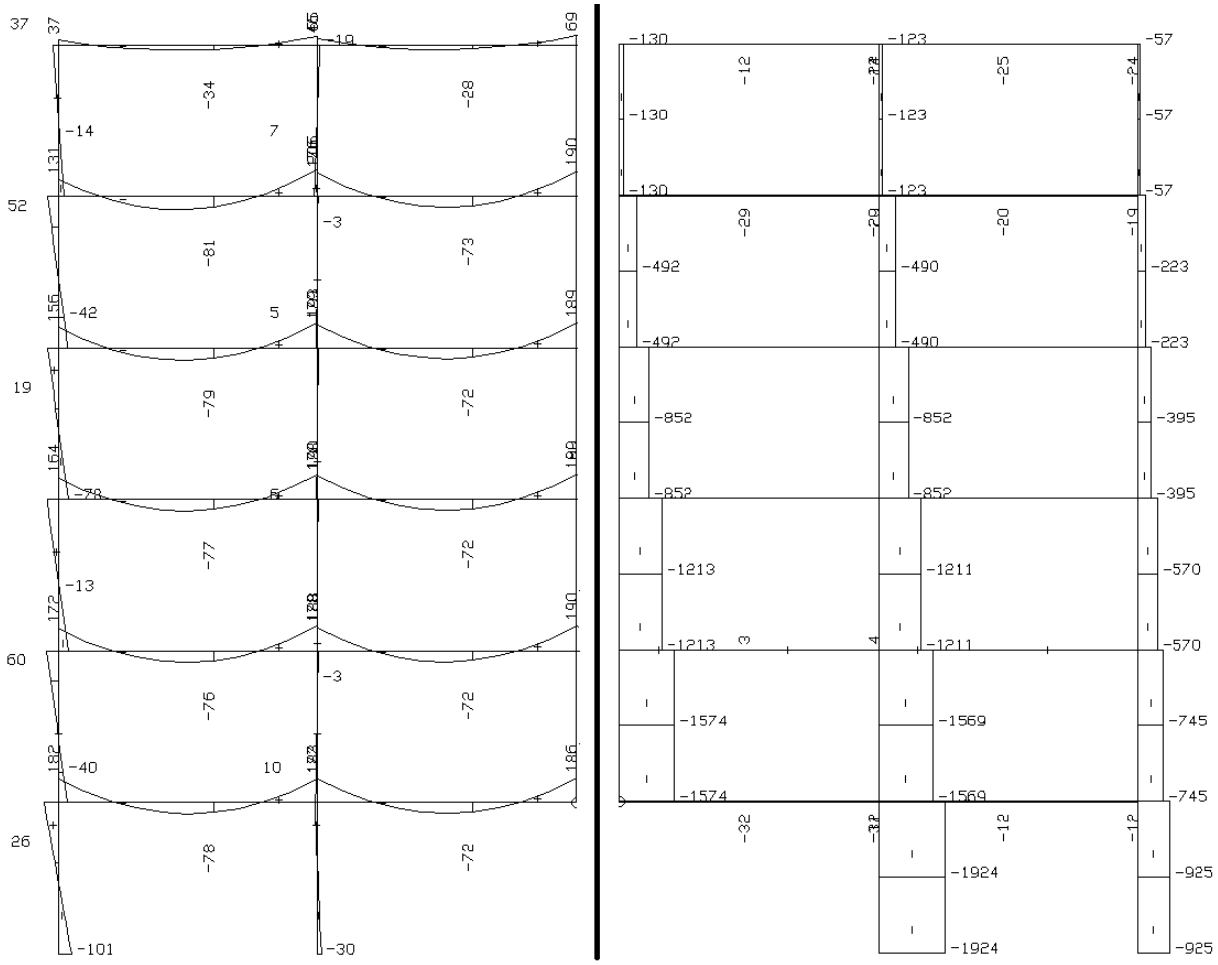

Figure 5.24: Bending Moment [kNm] (left) and Normal Force [kN] (right) with Column in place in RC Frame

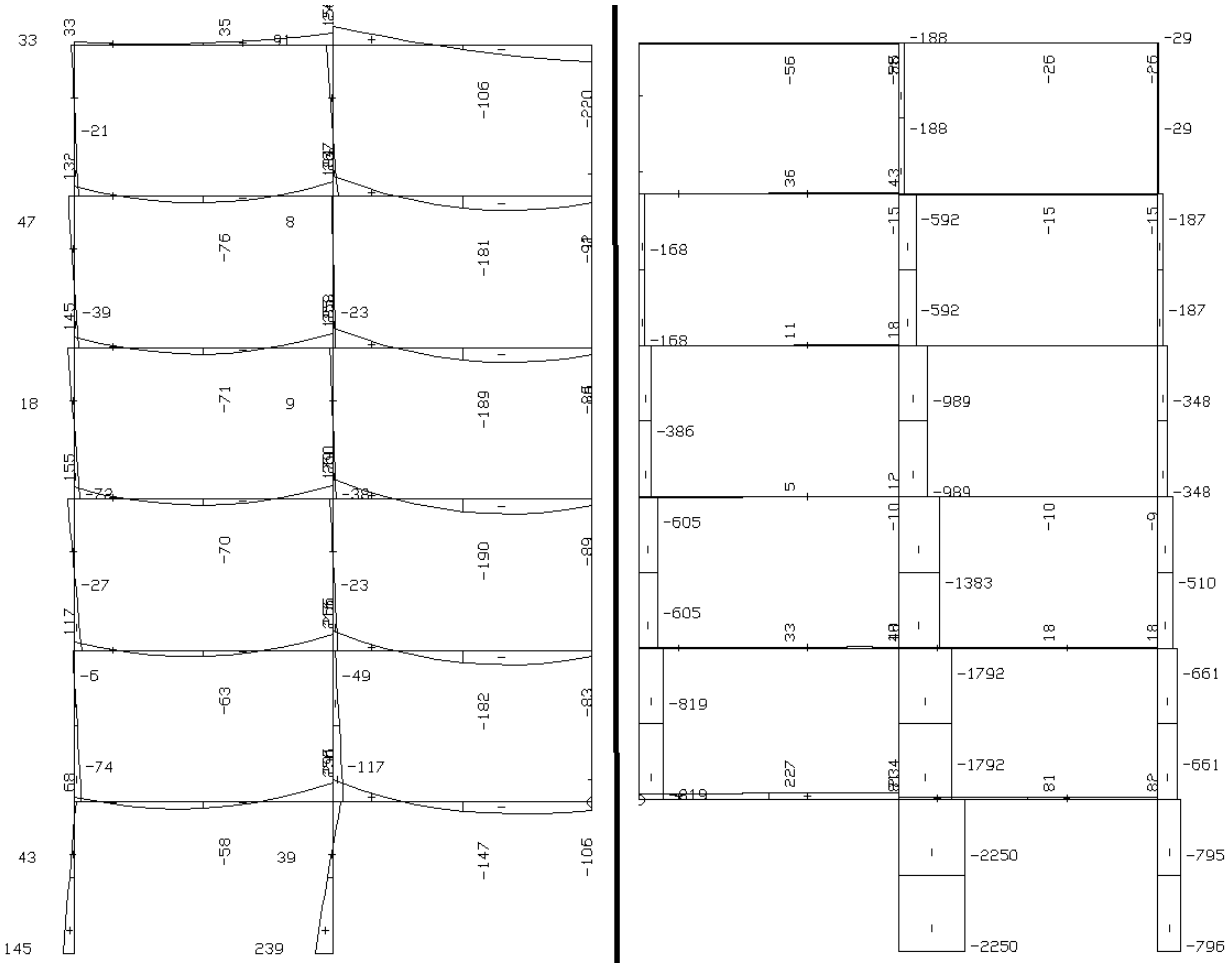

Figure 5.25: Bending Moment [kNm] (left) and Normal Force [kN] (right) at Displacement of 90 cm in RC Frame

5.2.2 Parametric Analysis

As for the steel structure, this section analyses the effects on the structural integrity of modifying one characteristic of the building at a time. The aim of this section is to determine the key parameters ruling the reinforced concrete structure behaviour. To reach this objective, several configuration will be study in which we will change by example the concrete class, the column width, the column reinforcement, the beam height, and so on.

Influence of Indirectly Affected Part

In the steel frame investigation, it have been discovered that the columns foundation yielding of leads to the collapse of the building. A plastic mechanism were created resulting in the formation of an unstable structure, no longer able to withstand the central frame. Hence we will also compare the influence of the IAP thanks to two configurations. In the first one, all the IAP is kept elastic which means that the steel rebarscannot yield and the concrete cannot crack or crush. The second configuration will keep the IAP elastic expected the ground floor columns.

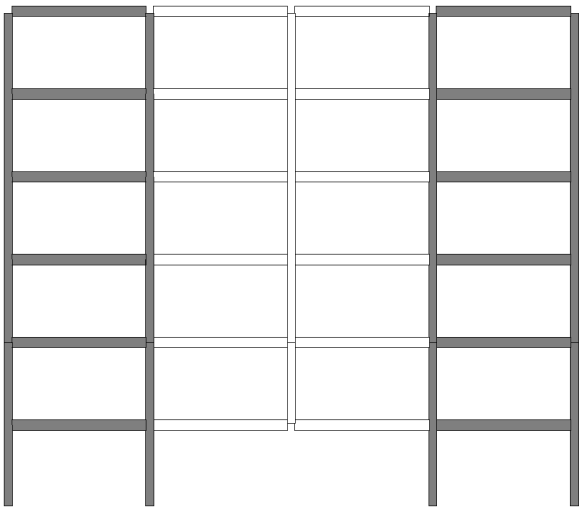

Figure 5.26: Elastic IAP Definition (Grey Elements)

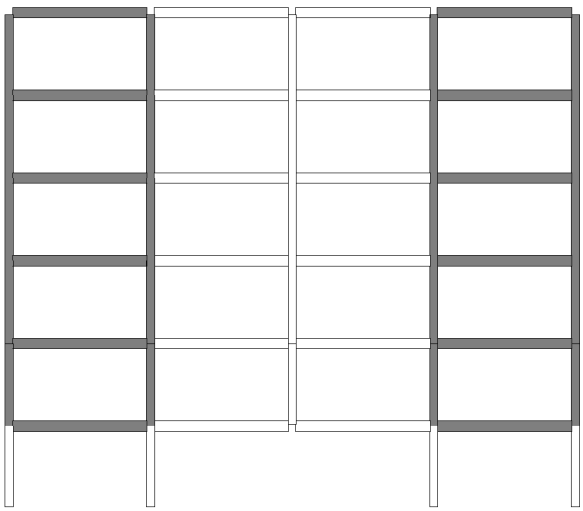

Figure 5.27: Elastic IAP with Ground Floor able to Crack

The results are quite similar to the steel frame. If the entire indirectly affected part is kept elastic, the membrane effects can completely be developed in the beams. The frame can withstand the column with a high level of safety. On the contrary, allowing the colmuns concrete to cracks and the reinforcement to yield will cause the premature rupture of the frame. The robustness reserve is also high with the elastic IAP.

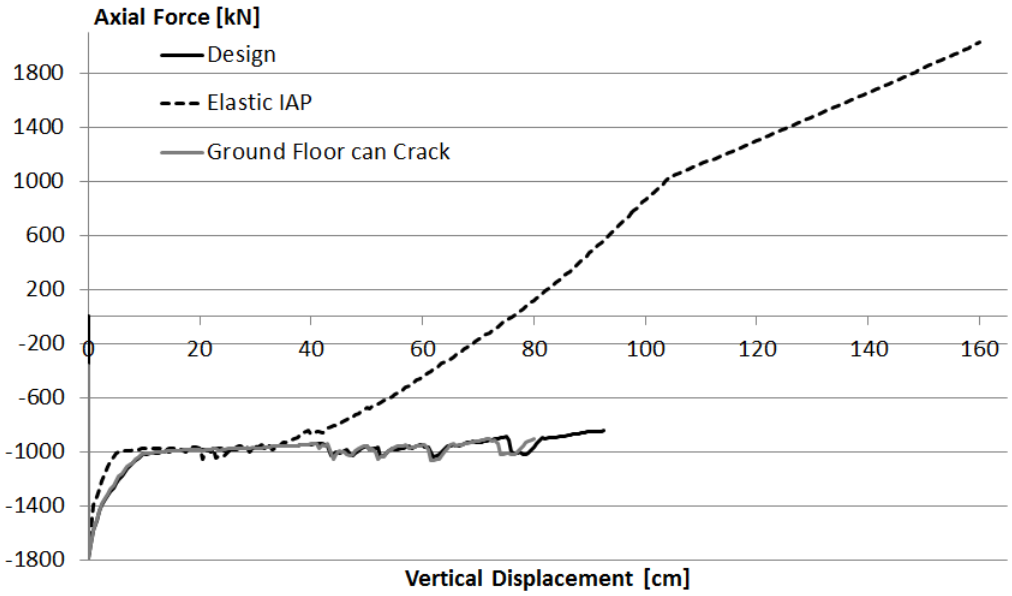

Figure 5.28: Membrane effects with Elastic IAP in RC Frame

When looking closer at the results on Figure 5.29, one can see the plastic hinges effects through the slope decrease in the second stage of the curve. Since the IAP is elastic, less plastic hinges are formed. In the same way, there are less cracks in the frame. The cracks are represented by the oscillations in the compression force. Nevertheless, a very low membrane effect can be

detected in the design situation as the general slope of the third phase is even though increasing.

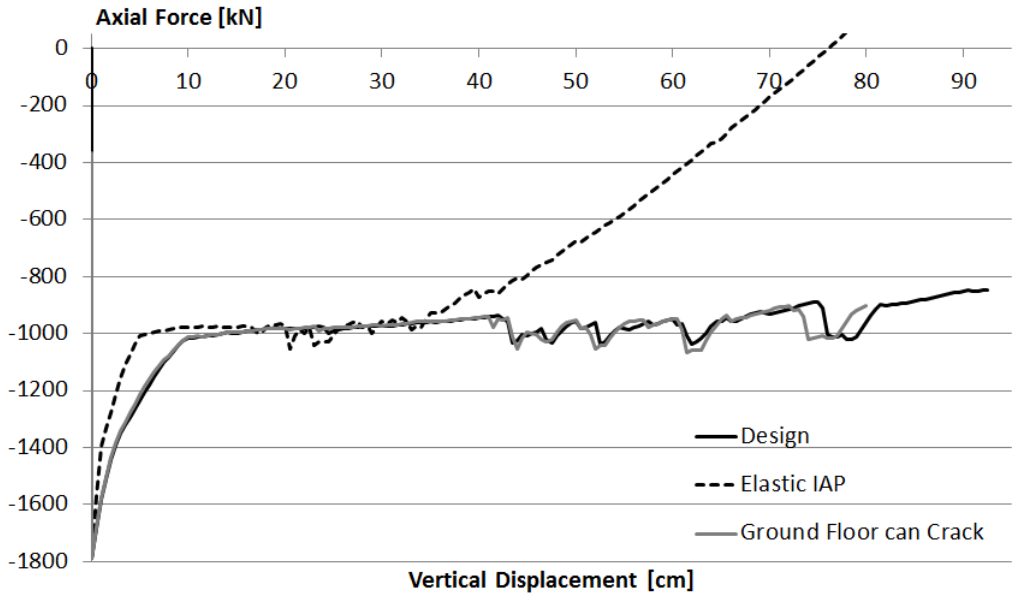

Figure 5.29: Influence of Indirectly Affected Part in Steel Frame

The Figures 5.30 described the benefit of keeping the IAp elastic. First of all, both reinforcement rebars can be stretched. It is confirmed by the fact that the entire cross-section is cracked. We are far beyond the compressive membrane action stage. All the beams are working in tension, not the lowest one. At the last floor, it can clearly be notice the compressive arch inside the central beams.

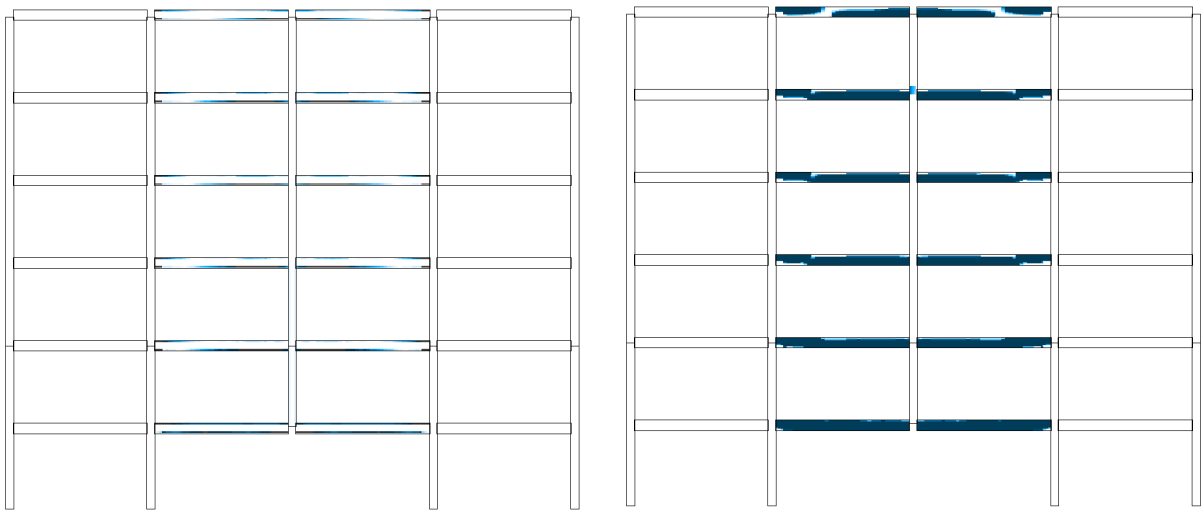

(a) Rebars Yielding at Displacement of 125 cm

(b) Deformation at Displacement of 125 cm

Figure 5.30: Positive Influence of Elastic Indirectly Affected Part in RC Frame

Influence of Bracing System

Instead of maintaining the IAP elastic, we can restrained the horizontal displacement at the beams extremity to hold the central part. Even if the situation tends to reduce the contribution of the indirectly affected part in the robustness, it is still an interesting case to study. Since the central lowest beam is restrained at both extremity, it will activate a compressive arch as depicted by the peak on Figure 5.32.

The displacement of the neutral axis due to cracking results in an in-plane expansion of the beam at its extremity. If the beam is restrained at its ends, by abutting as an example on a column, it will increase the strength of the beam. This phenomenon is called compressive membrane action or arching action and is schematically represented on Figure 5.31.

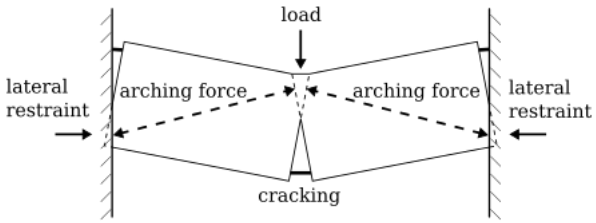

Figure 5.31: Basic Principle of Arching Action[35]

By pursing the vertical displacement of the central spans, we can go beyond this point. The strength of the beam decreases because the beams extremity starts to move inwardly. Therefore the compression in the column increase again. The frame needs back more the vertical support. Finally, the beam starts to develop a new rigidity since the rebars become in tension. In this case, the horizontal restraints make the structure robust since the curve reaches 0 kN.

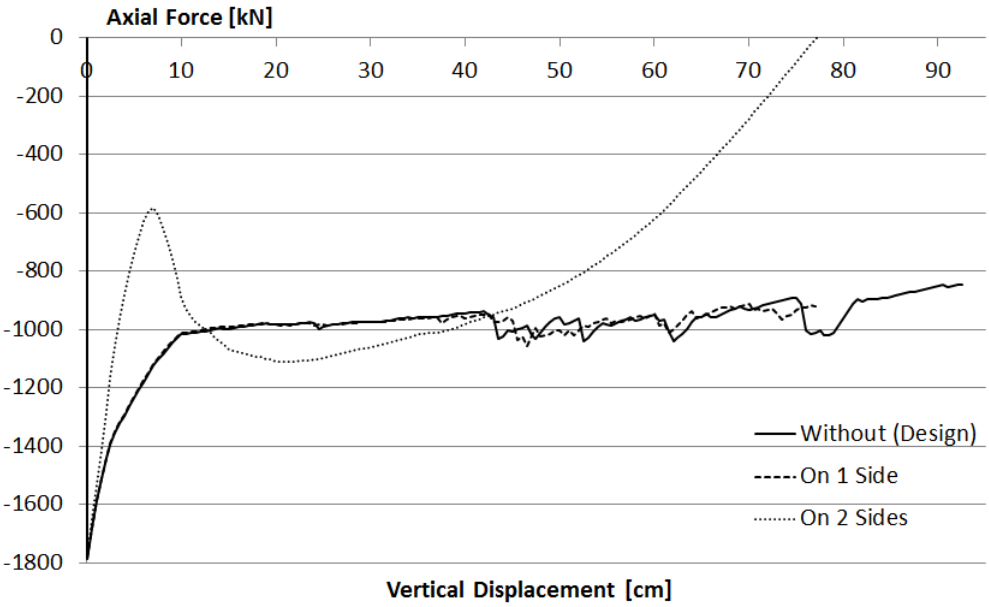

Figure 5.32: Normal Force Evolution according Vertical Displacement of Central Support for Different Horizontal Restraints

The compressive arch does not occur so obviously in the other configurations because the indirectly affected part is no stiff enough to constraint the beams.

Influence of Concrete Class

Some might think that ordering stronger concrete will enhance the structural integrity of the reinforced concrete building. In fact, a more resistant concrete will not change anything. In this case, the beams are not restrained enough to rely on the development of arch effects as explained in the previous section. Therefore, the only way to sustain the column lost in this building is by developing membrane effects. Since the catenary action is related to the traction force establishment within the beam, it will not affect the structural integrity of the frame to request a higher concrete class. It is proved by the Figure 5.33 hereafter.

All the concrete class has more or less the same path. This Figure 5.33 is also very interesting because it revealed that the reinforced concrete has two major behaviours. After investigation, it has been discovered that the reason lies in the meeting between the cracks developing in the beams. The cracks which originate from the upper part of the beam and localized near a column column meet the cracks created in the middle of the span, at the lower chord of the beam. The meeting of these two cracks suddenly decrease the rigidity of the elements in which it occurs. Before 40 cm, the behaviour of the concrete is smooth because each crack are growing independently. After a vertical displacement of 40 cm, the cracks starts to meet all over the frame. It also reveals the transition between the compressive action stage and membrane effect.

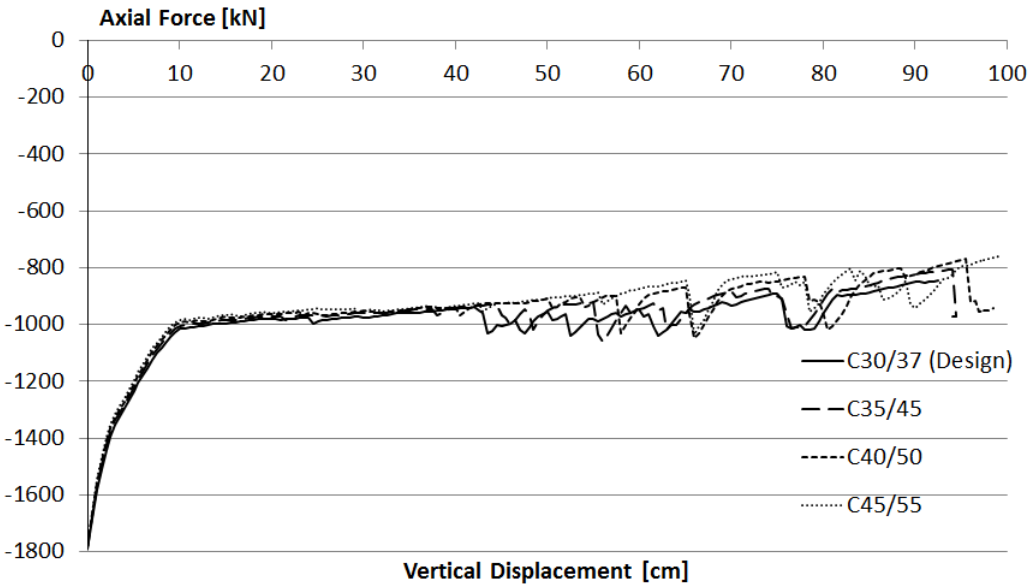

Figure 5.33: Normal Force Evolution according Vertical Displacement of Central Support for Different Concrete Class

Influence of Beam Reinforcement

Increasing the reinforcement inside the beams is the most obvious solution to consider. Indeed, it will postpone the rebars yield and so the plastic hinges formation. The influence of the reinforcement on the second phase of the curve is clearly shown on Figure 5.34. The more

reinforced the section is, the more straight the curve is and so the more elastic the response is during the second phase. For high reinforcement, the frame can sustain the column failure.

It can also be seen on Figure 5.34 that the oscillations due to cracking are lessened when the reinforcement quantity rises. A larger amount of steel will increase the inertia of the concrete beams when the cross-section becomes fully cracked. It will reduce the sudden decrease in strength when the top cracks coming from a support meet the bottom cracks from the midspan.

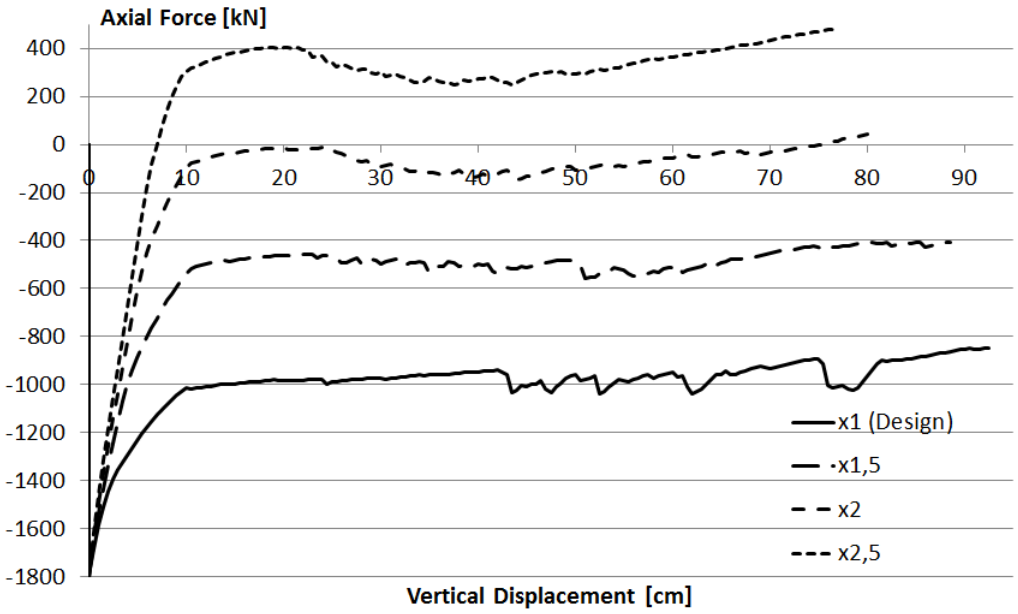

Figure 5.34: Normal Force Evolution according to Vertical Displacement of Central Support for Different Concrete Beam Reinforcements

The last phenomenon appearing when the reinforcement which changed is the arching action. As the reinforcement increases, it can be notice the development of a peak at the end if the second phase and before the third one. In this phase, the beams work as a tied-arch bridge. Since the steel quantity of the bottom reinforcement layer is enhanced, it will restrains the expansion of the beam outwardly. It requires a greater tensile force to stretched the rebars. Hence the compression can rely on this constraint and becomes greater. Small arching action therefore begins to take place in the reinforced concrete beams.

Note that to be able to increase the reinforcement, there must have space in the cross section. In this simulation, we did not take into account the available space. It is not always necessary the case. By the way, we assumed in the simulation that the reinforcement is situated on the top and bottom reinforcement. There is only two layers of reinforcement.

According Eurocodes EN 1991-1-7 recommendations for framed structures, the horizontal ties provided by the reinforcement should be equal to :

$$T_i = 0,8\left(g_k + \Psi q_k\right) sL = 0,8\left((46,5 + 3,94) + 0,5 \cdot 18\right) 6 \cdot 6 = 1712 \text{ kN} \tag{5.5}$$

With rebars composed of S500 steel grade, the minimum reinforcement area $A_{s,min}$ should be equal to :

$$A_{s,min} = \frac{T_i}{f_{yd}} = \frac{1712 \times 10^3}{435} = 3935 \text{ mm}^2 \tag{5.6}$$

Compared to the design, it means that the initial reinforcement area A_{ini} should be multiplied by :

$$\frac{A_{s,min}}{A_{s,ini}} = \frac{3935}{7\pi\frac{20^2}{4}} = \frac{3935}{2199} = 1,79 \tag{5.7}$$

This means that the reinforcement has to be increased to sustain the column loss according to Eurocodes (if the panel mechanism did not occur). However, Figure 5.28 and 5.32 prove that reserve is large enough with designed beams. As in the steel frame, Eurocodes are very safe in this case.

Influence of Beam Height

Figure 5.35 shows the influence of the beam height on the structural integrity of the frame. First of all, the higher height is advantageous during the second phase of the curve. Due to an increased level arm, the plastic moment is higher than in the design. So the formation of plastic hinges occurs latter and the central part can transmit more loads to the surrounding frame during the second phase.

Once the plastic moment is reached, all the configurations have the same behaviour. Especially at high displacement where the section is entirely cracked. Indeed, only the reinforcement plays a role in the absorption of the tension force.

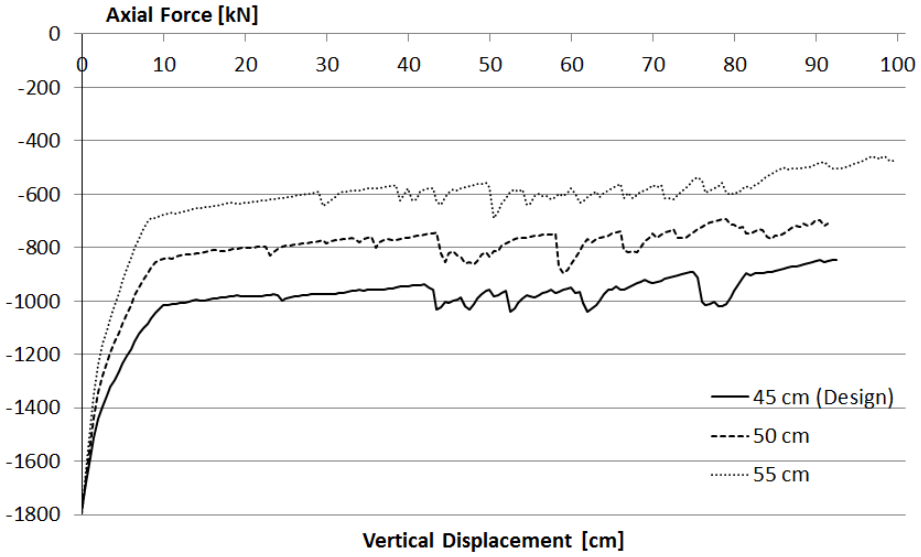

Figure 5.35: Normal Force Evolution according to Vertical Displacement of Central Support for Different Concrete Beam Heights

Influence of Column Width

Since the importance of restraining the beams extremity has been revealed at the beginning of this section, it might be interesting to focus on the influence of column width. However as indicated on Figure 5.36, the column width has no effect on the structural integrity.

Even if wider columns are less flexible and therefore can better restrain the beams, the foundation cracks exactly like in the design. The frame cannot take advantage of wider columns.

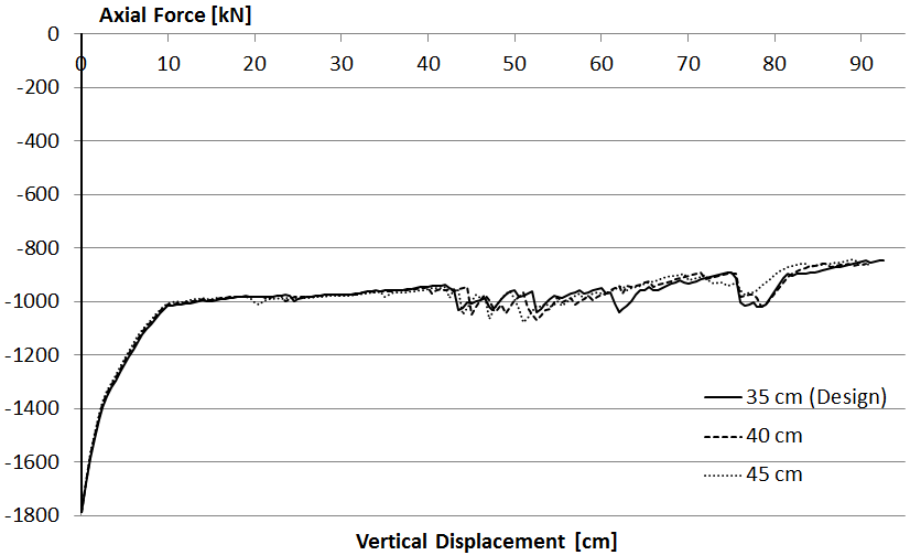

Figure 5.36: Normal Force Evolution according to Vertical Displacement of Central Support for Different Concrete Column Widths

Influence of Column Reinforcement

In the same vein, the designer might think that enhancing the column reinforcement will promote the stiffness and the resistance of the frame. It could have provide a better anchorage for the beams, resulting in an increase of the membrane effects that could have been activated as it was for the steel frame (see section 5.1.2).

However, contrary to steel results, there is no significant change. Since all curves overlap, it indicates a similar behaviour. Thus this is also probably due to the foundations cracking leading to a panel mechanism the frame like in the design case.

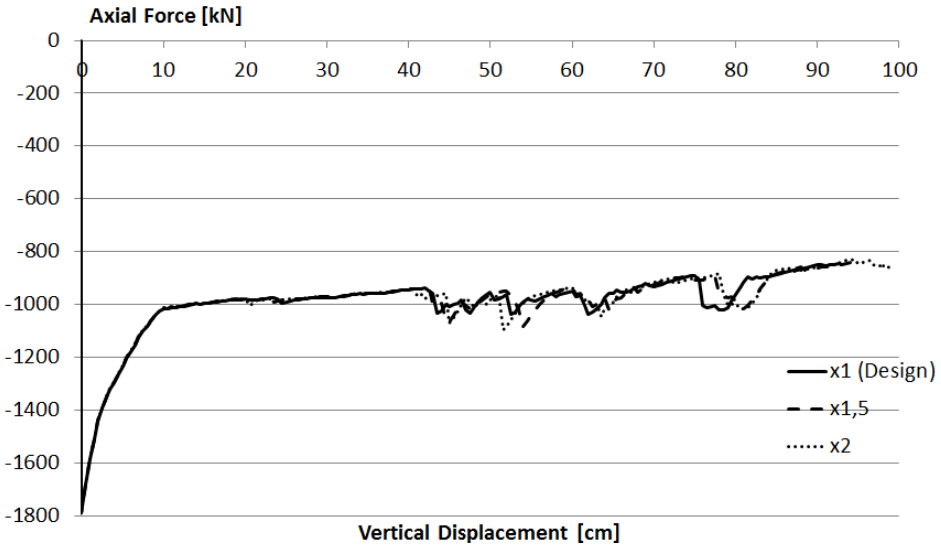

Figure 5.37: Normal Force Evolution according to Vertical Displacement of Central Support for Different Concrete Column Reinforcements

5.2.3 Summarize Results

From this parametric analyses, it has been demonstrated the importance of the indirectly affected part and especially the key role of the columns from the ground floor. Due to the foundations cracking and the yielding of the rebars at this location, a panel mechanism were formed within the frame. It resulted that the external frame were no longer able to sustain the central parts. If this panel mechanism can be avoid, we revealed that the frame can withstand the column lost with a high level of safety.

If we hold both beams extremity by restraining the horizontal displacement, high catenary action can be activated in the beams. Moreover, a compressive membrane arch occurs in the beams at first. In this case, the mechanism leading to the premature collapse of the frame was not occurring neither. Since we imposed the central beams external ends to be horizontal fixed, the frame was always supported.

Otherwise, the easiest solution was obviously to increase by more than the double the beams reinforcement. It was the only configuration able to sustain the central column failure. As a recall, the simulation does not taken into account the space available in cross-section.

Finally, it has be described that the concrete class or the columns have no influence of the frame structural integrity. Regarding the columns, it is mainly due to the cracking foundations.

5.3 Comparison of Steel and Reinforced Concrete Structures

The third section of this chapter is dedicated to the comparison of both structures under the accidental column lost. We will investigated in a more quantitative way the response of both frame. To do so we will study, among other thinks, the catenary beams rotation, the M-N interaction curves in the foundation and in the beams extremity, the horizontal displacement of the beams, etc.

Expected for the first part discussing about the loading combination, the study will mainly be focus on the data coming from the ALS combination obtained with the imposed displacement strategy.

5.3.1 Incremental Load Results

The first part focuses on the results given by the imposed load strategy. As explained in chapter 4, this strategy suits for any loading at the opposite of the imposed displacement. Nevertheless, this strategy is much less robust than the other. As a recall, a small increase in the loading can lead to a very high displacement. The new equilibrium states being so far away of the previous one, FINELg may not be able to catch it.

The results are presented on Figure 5.38. The ordinate axis represents the ratio between the reactions simulating the columns and the counteraction forces applies in order to model the progressive failure of the column. The three combinations defined in section 4.5 are plotted on the chart for each frame.

Contrary to the imposed displacement results presented in the following section, the imposed load strategy cannot catches the membrane effects for the reinforced concrete (see Chapter 4) . The results during the third phase cannot be reliable for the RC frame with this method. For the ALS combination, the computation breaks at 40 cm right before the development of membrane effects in the cross-section as it will be demonstrated hereafter.

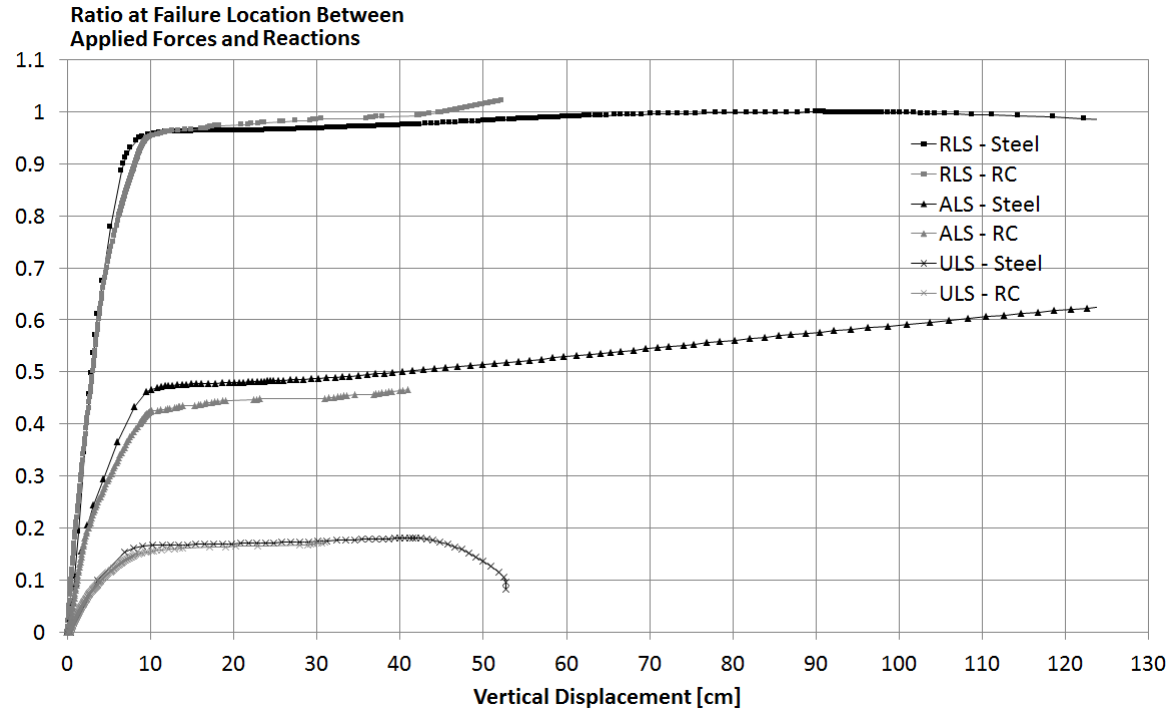

Figure 5.38: Comparison of Catenary action developed according Column Loss with Incremental Load

Some information can still be extracted from this chart. First of all, the designs are not sufficient to sustain the column failure at ULS or ALS. The ratio under ALS combination (0,43-0,47) is logically greater than under ULS combination (0,17) since the buildings are less loaded. However, a greater ratio does not necessarily means more loads can be transmit. In fact, this is the reactions that change the value of the ratio. The reactions are higher at ULS due to the greater loading. So for a same counteracting force applied, the ratio will be smaller at ULS than at ALS.

To reach a unitary ratio and therefore withstand the column loss, the loading in both structures has to be lowered. For the steel frame, only 40 % of the ULS loading was applied in the RLS combination while the coefficient $\gamma_R = \frac{1}{3}$ for the reinforced concrete structure.

It can also be seen that both structures has quite the same response during the formation of the plastic hinges. This means that the structures has been well designed since they starts to yield at the same level of load. The beams have more or less the same plastic moment. Note that the steel frame has a slightly better behaviour.

Thanks to the development of catenary action in the steel frame, the structure transmit 15 % more load at ALS. More that 60 % of the load initially acting in the column have been transmitted.

Finally, one can see that the central part of the steel frame move down further in the ALS and RLS combinations than in the ULS one. The heavy load in ULS precipitates the collapse that occurs already at 44 cm.

5.3.2 Incremental Displacement Results

Due to the limitation of the imposed displacement strategy (see section 4.4.3), only ALS combination will be discussed here. Note that the incremental displacement strategy is more appropriate to capture the reinforced concrete behaviour since we can reach a double displacement by comparison with the imposed load simulation.

The results on Figure 5.39 indicates that both frames has quite the same robustness. Nevertheless, the steel frame can sustain about 100 kN more at the end of the second phase. At the end of the third phase, the steel frame can bear 190 kN more, but for a higher vertical displacement of the support.

The catenary action in the steel frame starts to have a significant influence from 40 cm. The change of slope indicates the apparition of the second stiffness of steel beams. From Figure 5.39, it is more difficult to tell about the reinforced concrete frame when the membrane effect starts due to the cracking. The tension force and the cracking taking place inside the reinforced concrete beam are studied in more detail in the next section.

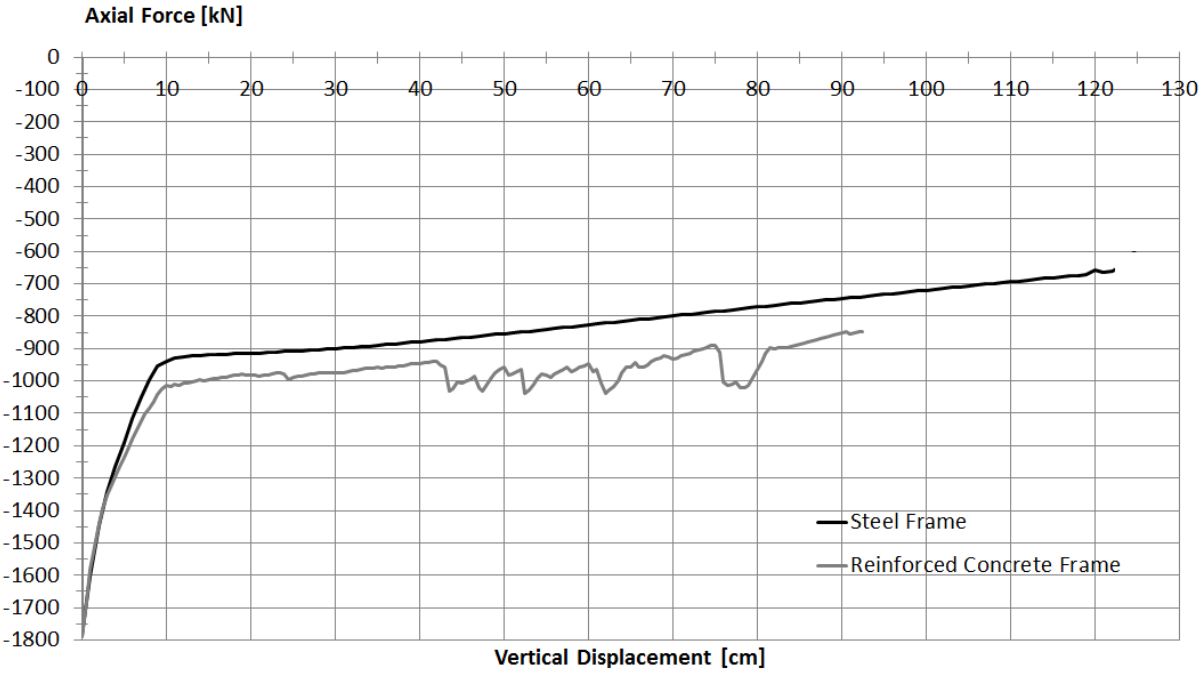

Figure 5.39: Comparison of Catenary action developed according Column Loss with Incremental Displacement

5.3.3 Evolution of Catenary Action and Membrane Effects

This section investigates the evolution of catenary action occurring in the beams supporting the first floor of the frame. The data were measured in the outside extremity of red elements represented on Figure 5.40, just next to the connection. The internal beams are the central beams which were directly connected the the removed column. The external beams are those situated in the indirectly affects part and connected to the external columns.

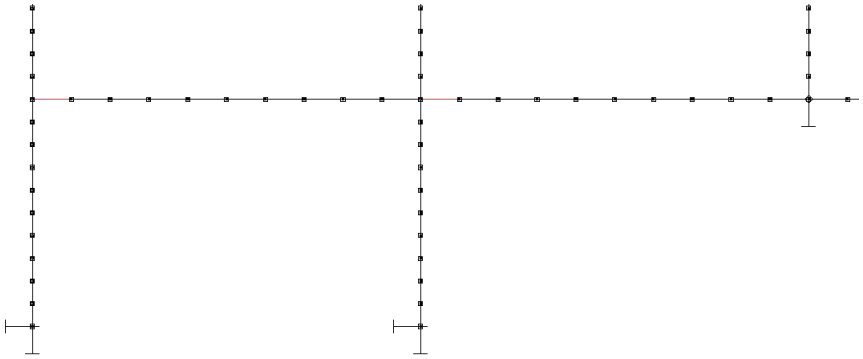

Figure 5.40: Beam Elements investigated

Figure 5.41 plots the normal forces evolution according to the vertical displacement at the support. The reader can see steel and RC beams have a very different behaviour at the beginning of the failure. The steel beams start directly to develop tension while the concrete beams have a compressive membrane action stage. This compressive arch almost reaches 150 kN in the internal RC beam. After a displacement of 50 cm, the compression becomes zero and the RC beams start to be in tension.

After 40 cm, the tension inside the internal steel profile begins to increase proportionally with the vertical displacement. Remember that on Figure 5.39, this displacement coincides with the development of the second stiffness of the beam. At the opposite, the external steel profile reaches a plateau around 65 cm for a load of 200 kN.

Meanwhile the bending moment on Figure 5.42 of external profiles changed sign and increased. The external central beam is pulling on the external column increasing the bending moment, but without modifying the normal force.

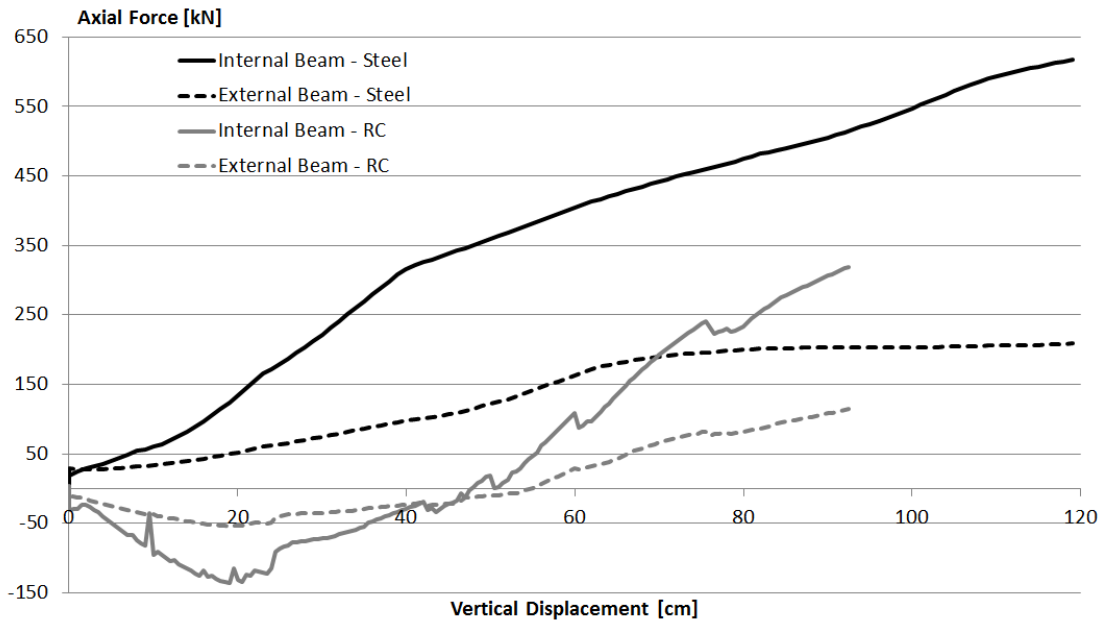

Figure 5.41: Comparison of Normal Force Evolution according to Vertical Displacement

Before the collapse, the magnitude of compression and tension develop inside the internal

beams are more than the double of the solicitation inside the external ones.

Thanks to Figure 5.42, the bending moment reversal occurring in the columns, and by continuity in the external beams investigated can be clearly notice. Indeed, the bending moment of the dotted curves first increase before decreasing as the axial load (i.e the pulling force) is getting higher. However, the reinforced concrete frame breaks before reaching the point of zero bending moment.

In addition, it is also confirm on Figure 5.42 that the oscillations present in Figure 5.39 on the RC curve are generated by the transition between the compressive membrane action and the catenary action. On the grey curve, one can see the scattered behaviour of the reinforced concrete when the compression decreases to switch to tension. During this time, the beam is able to reach and maintain the plastic moment of the cross-section. This behaviour change can also be notice on Figure 5.43 representing the moment rotation curve. While the compressive arch is occurring in the beam, the rotation tends to be directed upward to align the beam the with the compressive arch. This behaviour is described on Figure 5.44 representing the rotation evolution according the vertical displacement.

Then as we pursue the vertical displacement, the cracks from the upper corner and the bottom of midspan meet each others, causing the cracking of the entire cross-section. Therefore, the beam is no longer able to develop a compressive arch because the stiffness falls down and so begins to rotate downwardly to activate the membrane effects. After that, the extremity of the RC beam behaves like a plastic hinges.

The steel beams behaviour is smoother since there is no cracks. The external beam profile reaches the plastic moment and then start to form a plastic hinges as shown on Figure 5.42 and 5.43. Furthermore, after a axial force of 300 kN, the bending moment decreases as the normal force increases due to M-N interaction.

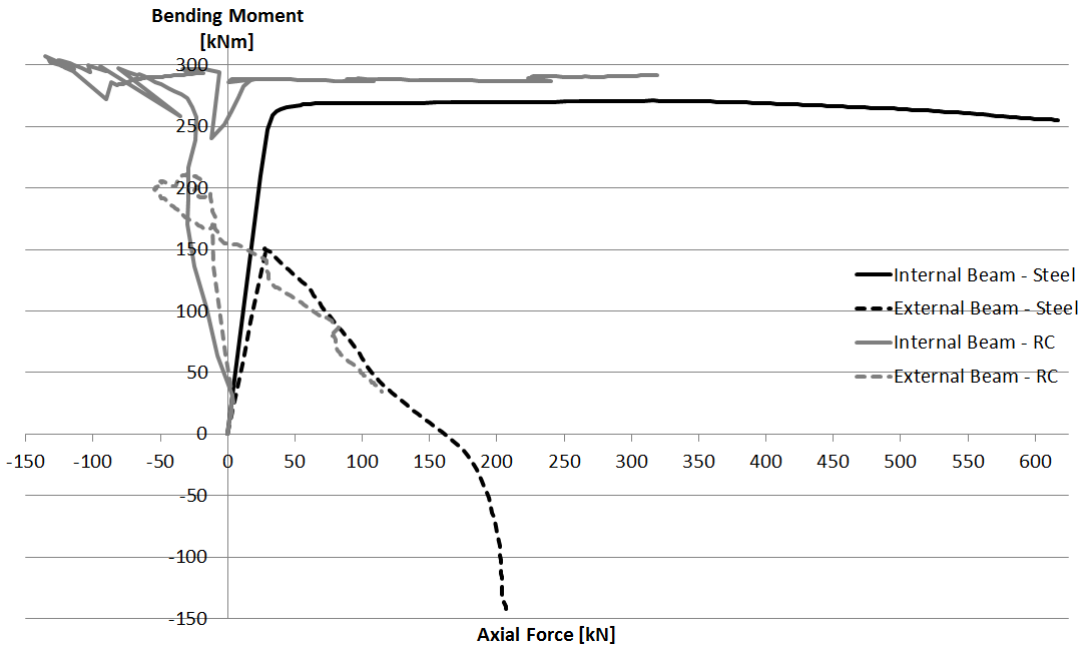

Figure 5.42: Comparison of M-N Interaction Diagrams according Vertical Displacement

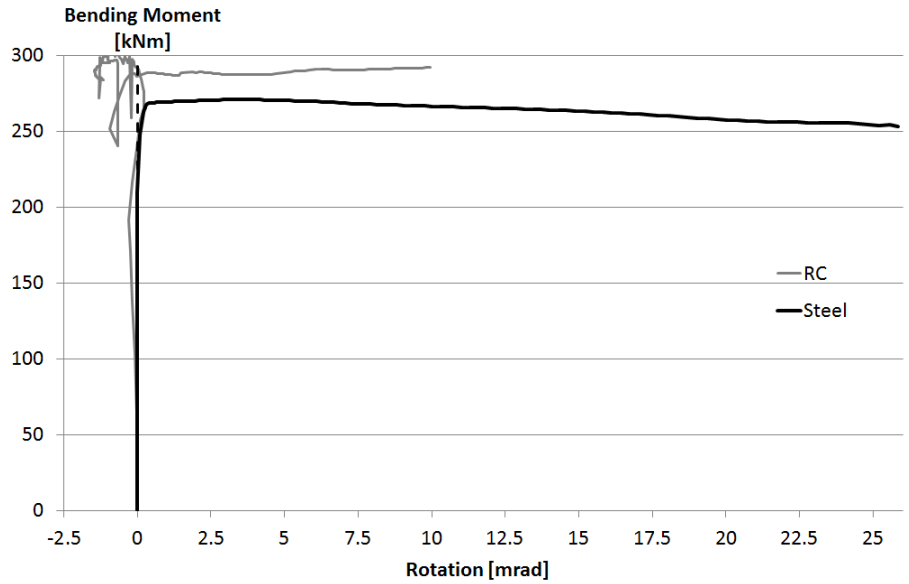

Figure 5.43: Comparison of Moment-Rotation Curve according Vertical Displacement

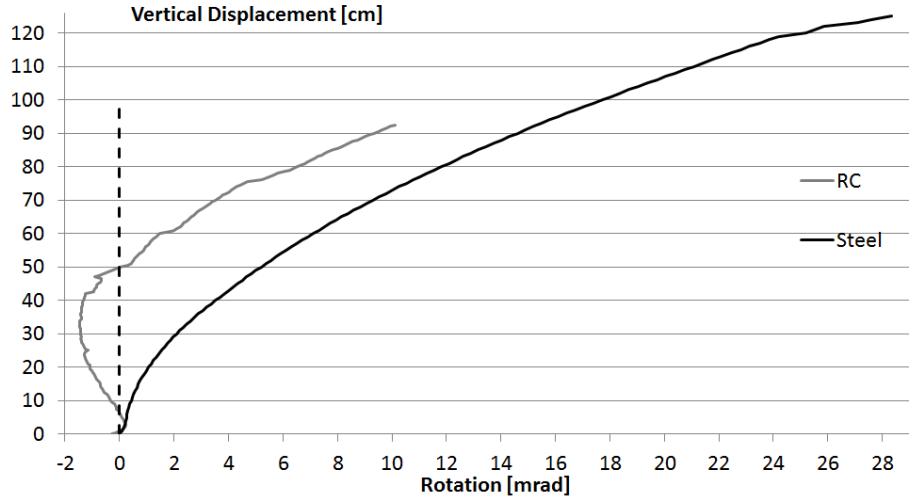

Figure 5.44: Rotation Evolution at Beams Extremity according Vertical Displacement

Figure 5.44 shows the rotation of the central catenary beams end. The compressive membrane occurs until a vertical displacement of 50 cm. Meanwhile, the tension force in the external steel beam is already higher than 350 kN (see Figure 5.41).

Studying the horizontal displacement of the central beams extremity on Figure 5.45 reveals the stiffness of the surrounding frames. As external frames get more flexible, the slope is decreasing. Both frames have the same rigidity since the curves are almost parallel. Yet the total horizontal inward displacement of the reinforced concrete frame is lower because of the compressive membrane action.

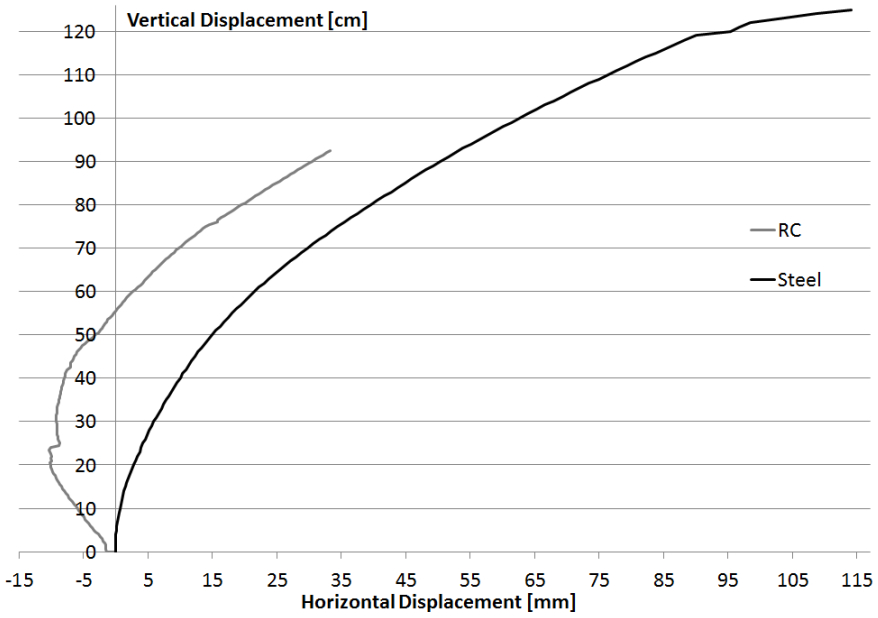

Figure 5.45: Horizontal Displacement Evolution at Beams Extremity according Vertical Displacement

Indeed, one can see the outward displacement created by the compressive membrane on Figure 5.45. As demonstrated in parametric analysis, restraining the horizontal displacement will enhance the arch compression. The total horizontal displacement of the catenary beam, or of top of the internal ground column, is more than 10 cm for the steel frame while it is only around 3 cm for the reinforced concrete frame before failure.

5.3.4 Evolution of Internal Forces in Foundations

Investigating the foundation level of stress will help to understand the development of the plastic mechanism leading to the premature collapse. As we mentioned in the parametric analysis, the frames cannot activate all catenary action potential because of the plastic hinges formation in the foundations. Moreover, studying the foundations will give information about the role played by the indirectly affected part in the structure under an accidental event.

Figure 5.46 plots the evolution of the shear force in both internal and external foundations while the Figure 5.47 represents the sum of these two, i.e. the total shear force developed in one indirectly affected frame foundations. These charts prove again the importance of the compressive arch in the reinforced concrete frame. A positive shear force means that the force is applied toward the outside.

In addition, trough the sign change, it can be seen the bending moment reversal. On Figure 5.47, the shear force when the columns are bent outwardly (see Figure 5.8a). The positive shear force is the reinforced concrete frame is more than three times higher than in the steel frame due to compression arch. At the opposite, the shear force went the columns are bent inwardly is three times bigger in the steel frame due to high horizontal displacement.

The higher shear force in the steel frame under large displacement is due to the higher traction force in the beams. These higher traction force is pulling horizontally on the top of the columns, resulting in the the bending moment and the shear force increasing.

It can be notice on Figure 5.47 for the steel frame that the increasing in attenuated when the catenary action takes place around 40 cm for the internal beam. It is due to the bending moment that starts to slightly decrease in the internal beams (see Figure 5.42).

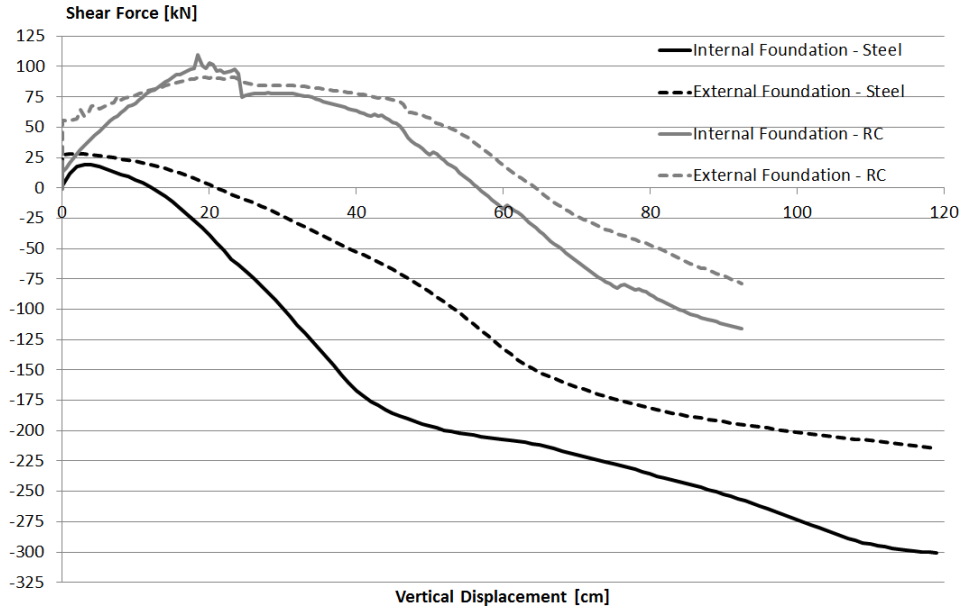

Figure 5.46: Shear Force Evolution in Foundations according Vertical Displacement

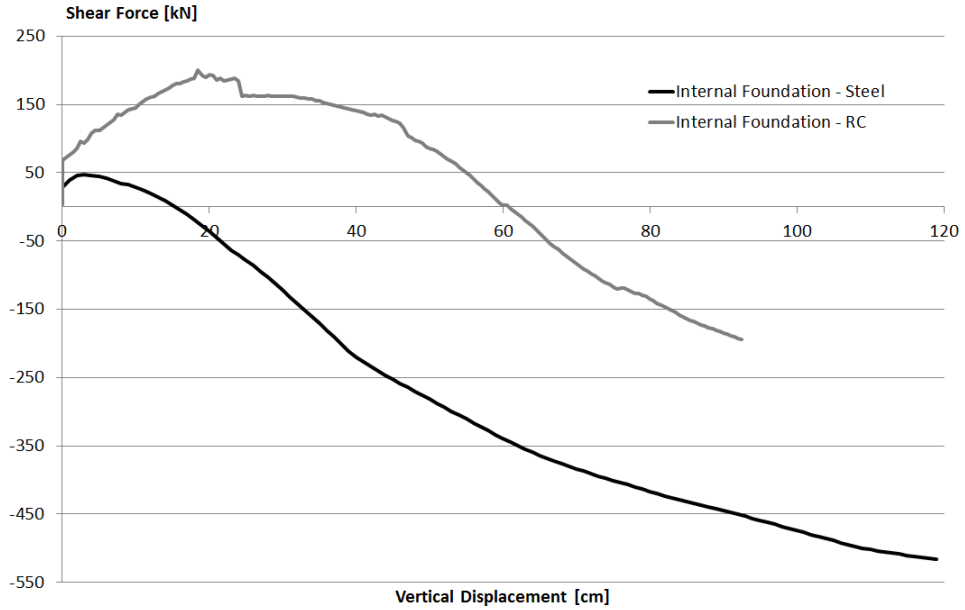

Figure 5.47: Total Shear Force Evolution in Foundations according Vertical Displacement

Studying the shear force evolution during the collapse confirms shear force can be neglected for columns. By example, before the collapse in steel frame the shear force in the internal foundation is equal to 300 kN. The internal column being a HEB 450 profile, the criteria is still

verified :

$$V_{Ed} = 300 \text{ kN} \leq 0,5V_{Pl,Rd} = 0,5\frac{A_v\frac{f_y}{\sqrt{3}}}{\gamma_{M0}} = 0,5\frac{7966\frac{235}{\sqrt{3}}}{1} = 540,4 \text{ kN} \tag{5.8}$$

Figure 5.48 describes the shear force before collapse. The right shear force diagram looks like a staircase waveform because of the discretization. Contrary to steel columns, shear force in catenary beams extremity seems to start to affects the beam resistance. Indeed, for the IPE 360 beam subjected to the highest shear forces, it comes :

$$V_{Ed} = 259 \text{ kN} \geq 0,5V_{Pl,Rd} = 0,5\frac{A_v\frac{f_y}{\sqrt{3}}}{\gamma_{M0}} = 0,5\frac{3510235\sqrt{3}}{1} = 239 \text{ kN} \tag{5.9}$$

At this point, it is wise to remember the initial design considers triangular load, while the investigation under accidental event assumes uniformly distributed load. So too light profiles have been set up compared to the investigation. The spans are more loading in the investigation than in the design. If the design was made with uniformly distributed load, IPE 450 beams would have been necessary. Making again shear force negligible.

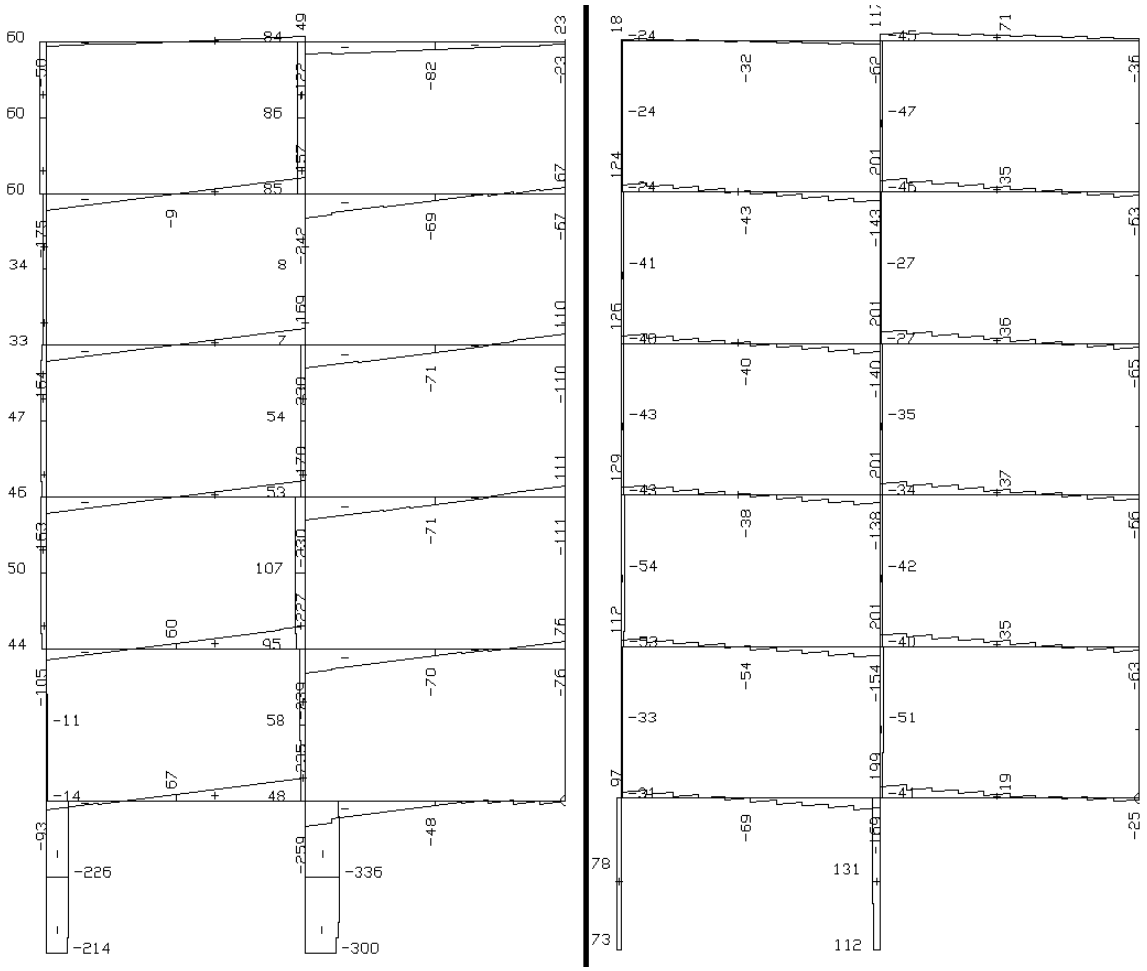

Figure 5.48: Shear Force [kN] in Steel (left) and RC (right) Frames before Collapse

Note that the shear force are defined within a constant in FINELg.

Finally the Figure 5.49 and 5.50 describes the formation of the plastic hinges in the foundation. On Figure 5.49, the straight lines of solid curve ranging from 0 kN to −1800 kN depict the M-N interaction with the column in place. These columns have been design to absorbed compression force. When the column starts to fail, the compression increase until −2250 kN. The bending moment also raises but at a significantly higher value for the RC frame since the compressive arch is pushing on the columns. On the contrary, the compression in the external columns slightly decrease from the initial situation due to a low uplift tendency.

After that, the bending moment reversal occurs. The load transmission in the central span is realized thanks to the tension in the beams. In consequence, the pulling force at the top of the column increase, and so does the bending moment in the foundation.

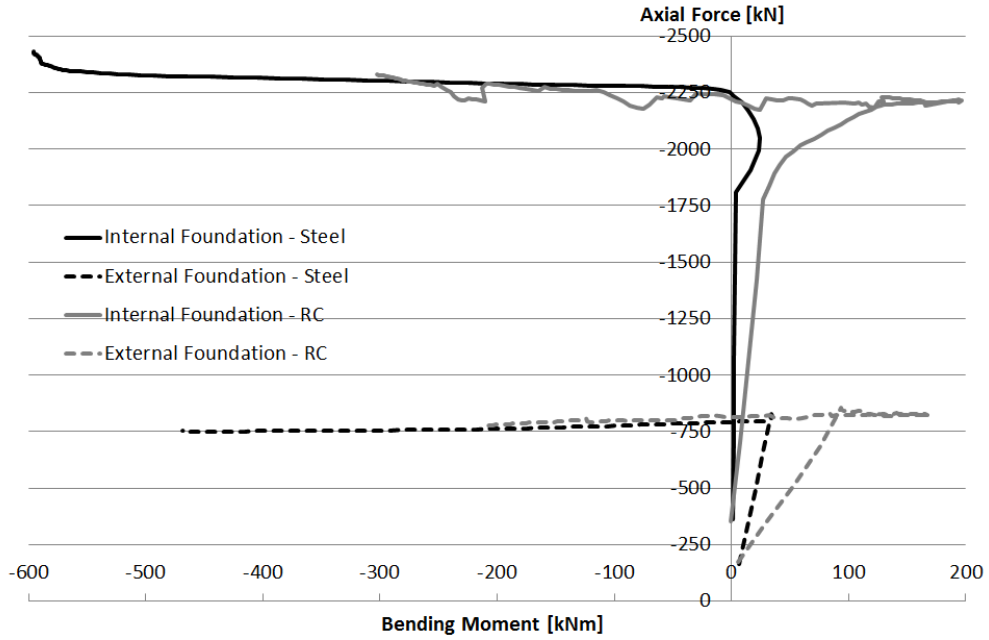

Figure 5.49: Comparison of M-N Interaction Diagrams in Foundations according Vertical Displacement

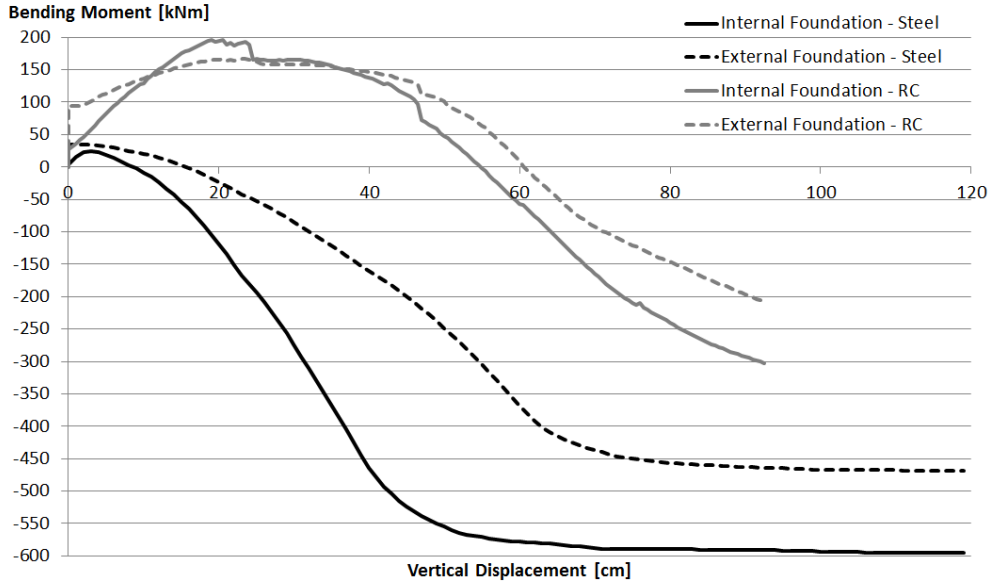

Figure 5.50: Comparison of Bending Moment in Foundations according Vertical Displacement

Following the bending moment reversal, the panel mechanism starts to shows up in steel frame. On Figure 5.50, plastic hinges formation can be noticed since the bending moment reaches a constant value. Figure 5.50 also indicates that the premature collapse of the reinforced concrete frame is due to a brittle failure in the column foundations.

5.4 Conclusion

From this comparison, it results the vertical displacement of steel frame is more important than the reinforced concrete one. The concrete frame collapse is due to a brittle failure following the plastic mechanism formation. Thanks to a higher ductility, the steel frame columns are able to provide more rotation. Increasing by the way the catenary action activated. About 10 % more of the column compression can be transmitted thanks to the steel frame.

In addition, it emerges that compressive arch in reinforced concrete beams takes an important part during the collapse.

Finally, we prove the shear force can effectively be neglected.

Conclusion

This master's thesis aimed to perform a comparative study between two identical structures under an accidental event, both structure differing only by the materials used. One was made of steel profiles while the other was made of reinforced concrete elements. In addition, the validation of FINELg reinforced concrete element was required before investigating the robustness analysis.

Through the slab strip experimental test simulation, it have been demonstrated that the finite element software FINELg was able to model the behaviour of a reinforced concrete beam in 2D. Both compressive membrane action and membrane effects have been activated in the plane beam element.

From the both numerical techniques implemented in the software, the incremental displacement method was more suitable to study the frame collapse, especially for the reinforced concrete frame. The main obstacle encountered in the reinforced concrete numerical models was the behaviour transition between compressive arch and the membrane effect in catenary beams. In addition, the proper simulations conduct is highly dependent of the incremental step due to the panel mechanism formation in the indirectly affected part.

In light of simulations, none of initial structures can be declared as robust according our hypothesis. The steel frame fails after a reduction of central column compression equal to 63 %. The reinforced frame for its part collapses when compression decrease of 53 %. The reason is the panel mechanism formation in the indirectly affected part. Despite the compression of roof beams, both frames cannot activate much more catenary action after the panel mechanism formation. Therefore the structures still collapse before all the loads from central spans have been transmitted to the surrounding frame.

Steel frame activated more catenary action thanks to a greater ductility of its elements. The central span vertical displacement reached 125 cm while reinforced concrete frame failed around 90 cm. Contrary to the steel frame, the reinforced concrete one was subjected to an important compressive membrane action.

5.1 Structural Requirements for Future Designs

Thanks to the parametric analyzes performed, several recommendations can be provided to design office to help them in future designs.

First of all, it have been discovered trough this case study that the structural integrity of both frame differs by 10 %. The steel structure stands out a little more than the reinforced concrete one. However, the main decision criterion to choice appropriate construction materials in structural integrity is the nature of the accidental event.

Reinforced concrete frame should be considered in case of fire since contrary to steel, it resists high temperature for a longer time. Note that fireproof coating exists to increase the

steel frame structural integrity. At the opposite, the inherent redundancy and higher ductility of steel frames make this material the ideal choice for blast conditions and in seismic zones.

Secondly, specific improvements can be made for each structure to increase structural integrity. According the parametric analyzes, it is much better to enhanced horizontal ties instead of the vertical tying. In addition, the major factor improving the robustness is the ability of holding columns in place. It has been evidenced restraining the catenary beams extremity (by maintaining the indirectly affected part in the elastic domain or by restraining the horizontal displacement of the frame) will increase the structural integrity.

The robustness in steel structures can also be greatly improved by ordering a higher steel grade or heavier beams profiles. To a lesser extent, heavier columns profiles slighty increase the structural integrity.

In concrete frames, changing the catenary beams reinforcement has proven to be really effective. Modifying the beams height is not sufficient to sustain the column loss. Furthermore, the columns specifications do not have a influence on reinforced concrete frame structural integrity because of foundations cracking.

5.2 Perspectives

All the investigations have been made according Eurocodes Limit State. It would have been interesting to compare the structural integrity under loading recommended by U.S standards. This would give information about which is the most unfavourable standards and how different the robustness level is in each design rules.

From a numerical view, it is crucial to developed the column loss simulation in FINELg. The incremental load strategy has shown some limitations for the reinforced concrete elements. On the contrary, the incremental displacement strategy implemented was only valid a symmetrical situation. Further developments should be made to implement the imposed displacement method to more general cases.

In the slab strip simulation, the next step is to introduce the heavy reinforced edges rigidity in order to perfectly match the experimental test performed by Ghent University.

If more time was available, it would have been wise to study the influence of the number of indirectly affected frame. More frames will confer more horizontal restraint to the central ones. In addition, it will influence the panel mechanism formation in the indirectly affected part.

Note that all this thesis is based on rigid and fully connections between. In reality, it may not be so simple to build a system able to reaches these characteristics. By example, it is difficult to transmit the traction force between two adjacent reinforced concrete beams. Reinforcement rebars must pass trough the columns without interfering columns reinforcement. Further technological investigation should be performed in this sense.

Finally, this master's thesis provide lots of results that could have been compared to the analytical model currently developed at University of Liège.

References

Bibliography

[1] EN 1990:2002. *Eurocode 0 : Basis of structural design.* European committe for standardization, June 2004.

[2] EN 1991-1-1. *Eurocode 1: Actions on structures - Part 1-1: General actions - Densities, self-weight, imposed loads for buildings.* European committe for standardization, April 2002.

[3] EN 1991-1-4. *Eurocode 1: Actions on structures - Part 1-4: General actions - Wind actions.* European committe for standardization, April 2005.

[4] EN 1991-1-7. *Eurocode 1 - Actions on structures - Part 1-7: General Actions - Accidental actions.* European committe for standardization, July 2004.

[5] EN 1993-1-1. *Eurocode 3: Design of steel structures - Part 1-1: General rules and rules for buildings.* European committe for standardization, May 2005.

[6] General Services Administration. *Progressive Collapse – Analysis and Design Guidelines for New Federal Office Buildings and Major Modernization Projects*, June 2003.

[7] EN 1991-1-3 ANB. *Eurocode 1 : Actions on structures - Part 1-3: General actions - Snow loads - National Annex.* European committe for standardization, February 2005.

[8] ArcelorMittal. *Gascogne Implementation Guide*, August 2007.

[9] Arval ArcelorMittal. *Le guide des systèmes thermiques et acoustiques*, May 2013.

[10] Simon Benson, Anuar AbuBakar, and Robert S. Dow. *A comparison of computational methods to predict the progressive collapse behaviour of a damaged box girder*, November 2012.

[11] Ludivine Comeliau. Effets du comportement dynamique des structures de bâtiments en acier suite à la ruine accidentelle de l'une des colonnes portantes. Master's thesis, Université de Liège, 2009.

[12] Jean-François Demonceau. *Steel and composite building frames: sway response under conventional loading and development of membrane effects in beams further to an expectional action.* PhD thesis, Université de Liège, 2008.

[13] Bureau d'études Greisch. *FINELg : Noninear Finite Element Analysis Program - User's Manual*, August 2003.

[14] Donald O. Dusenberry and Gunjeet Juneja. Review of existing guidelines and provisions related to progressive collapse. *Simpson Gumpertz & Heger Inc.*, 2003.

[15] Victor Gioncu, Marius Mosoarca, and Anthimos Anastasiadis. *Prediction of available rotation capacity and ductility of wide-flange beams: Part 1: DUCTROT-M computer program*, September 2011.

[16] Victor Gioncu, Marius Mosoarca, and Anthimos Anastasiadis. *Prediction of available rotation capacity and ductility of wide-flange beams: Part 2: Applications*, August 2011.

[17] Dirk Gouverneur, Robby Caspeele, and Luc Taerwe. Experimental investigation of the load-displacement behaviour under catenary action in a restrained reinforced concrete slab strip. *Elsevier – Engineering Structures*, 2013.

[18] L.N.N Hai. *Structural response of steel and composite building frames to an impact leading to the loss of a column.* PhD thesis, University of Liège, 2008.

[19] Clara Huvelle. Contribution à l'étude de la robustesse des structures de bâtiments prise en compte de la plastification progressive de la partie de la structure "non directement affectée" par l'événement exceptionnel considéré. Master's thesis, Université de Liège, 2011.

[20] Amin Khazaee. Nonlinear static and dynamic analysis for assessment of progressive collapse potential in intermediate rc frame structures. *International Journal of Advances in Engineering Sciences*, 2013.

[21] Kfir Menchel. *Progressive Collapse: Comparison of Main Standards, Formulation and Validation of New Computational Procedures.* PhD thesis, Université libre de Bruxelles, 2009.

[22] R Shankar Nair. Progressive collapse basics. *Modern steel construction*, 44(3):37–44, 2004.

[23] NIST : National Institute of Standards and U.S. Department of Commerce Technology, Technology Administration. *Best Practices for Reducing the Potential for Progressive Collapse in Buildings*, February 2007.

[24] Sivaraj Shyam-Sunder. *Federal Building and Fire Safety Investigation of the World Trade Center Disaster: Final Report of the National Construction Safety Team on the Collapses of the World Trade Center Tower (NIST NCSTAR 1)*, December 2005.

[25] Unified Facilities Criteria (UFC). Design of buildings to resist progressive collapse. *Department of Defense*, 2005.

Webgraphy

[26] http://www.fuenterrebollo.com/recuerdos/Windsor/torre-5.jpg, March 2014.

[27] http://mixstuff.ru/wp-content/uploads/2013/06/119.jpg, March 2014.

[28] http://s0.geograph.org.uk/geophotos/02/54/04/2540477_bcc5ce93.jpg, March 2014.

[29] http://theconstructor.org/building/robustness-of-buildings/7108/, March 2014.

[30] http://www.bollyn.com/public/wtc2collapse.jpg, March 2014.

[31] http://www.csi911.info/collapse_vlg.jpg, March 2014.

[32] http://www.mace.manchester.ac.uk/project/research/structures/strucfire/CaseStudy/HistoricFires/BuildingFires/default.htm, March 2014.

[33] Wikipedia. Progressive collapse — wikipedia, the free encyclopedia. http://en.wikipedia.org/w/index.php?title=Progressive_collapse&oldid=583992828. [13-March-2014].

[34] Wikipedia. Ronan point — wikipedia, the free encyclopedia. http://en.wikipedia.org/w/index.php?title=Ronan_Point&oldid=598163785, [13-March-2014].

[35] Wikipedia. Arching or compressive membrane action in reinforced concrete slabs — wikipedia, the free encyclopedia, 2013. [May-2014].